RECTANGULAR MICROSTRIP PATCH ANTENNA DESIGN FOR SATELLITE IMAGE VISION SYSTEM APPLICATION

A Thesis submitted to Gujarat Technological University

for the Award of

Doctor of Philosophy

in

Electronics & Communication Engineering

by

Ratansing N. Patel

129990911016

under supervision of

Dr. Vipul A. Shah

GUJARAT TECHNOLOGICAL UNIVERSITY

AHMEDABAD

June - 2019

DECLARATION

I declare that the thesis entitled "***Rectangular Microstrip Patch Antenna Design for Satellite Image Vision System Application***" submitted by me for the degree of Doctor of Philosophy is the record of research work carried out by me during the period from November, 2012 to June, 2019 under the supervision of **Dr. Vipul A. Shah** and this has not formed the basis for the award of any degree, diploma, associateship, fellowship, titles in this or any other University or other institution of higher learning.

I further declare that the material obtained from other sources has been duly acknowledged in the thesis. I shall be solely responsible for any plagiarism or other irregularities, if noticed in the thesis.

Signature of the Research Scholar: ..... Date: 15-06-2019

Name of Research Scholar: **Ratansing N. Patel**

Place: Ahmedabad

CERTIFICATE

I certify that the work incorporated in the thesis ***"Rectangular Microstrip Patch Antenna Design for Satellite Image Vision System Application"*** submitted by **Mr. Ratansing N. Patel** was carried out by the candidate under my supervision. To the best of my knowledge: (i) the candidate has not submitted the same research work to any other institution for any degree/ diploma, Associateship, Fellowship or other similar titles (ii) the thesis submitted is a record of original research work done by the Research Scholar during the period of study under my supervision, and (iii) the thesis represents independent research work on the part of the Research Scholar.

Signature of Supervisor: ..... Date: 15-06-2019

Name of Supervisor: **Dr. Vipul A. Shah**

Place: Ahmedabad

COURSE WORK COMPLETION CERTIFICATE

This is to certify that **Mr. Ratansing N. Patel**, Enrolment No. **129990911016** is a PhD scholar enrolled for PhD program in the branch **Electronics and Communication Engineering** of Gujarat Technological University, Ahmedabad.

(Please tick the relevant option(s))

☐ He/She has been exempted from the course-work (successfully completed during M.Phil Course)

☐ He/She has been exempted from Research Methodology Course only (successfully completed during M.Phil Course)

☑ He/She has successfully completed the PhD course work for the partial requirement for the award of PhD Degree.

His/ Her performance in the course work is as follows

Grade Obtained in Research Methodology (PH001)	Grade Obtained in Self Study Course (Core Subject) (PH002)
BC	AB

Supervisor's Sign

(Dr. Vipul A. Shah)

ORIGINALITY REPORT CERTIFICATE

It is certified that PhD Thesis titled ***"Rectangular Microstrip Patch Antenna Design for Satellite Image Vision System Application"*** by **Ratansing N. Patel** has been examined by us. We undertake the following:

a. Thesis has significant new work / knowledge as compared already published or are under consideration to be published elsewhere. No sentence, equation, diagram, Table, paragraph or section has been copied verbatim from previous work unless it is placed under quotation marks and duly referenced.

b. The work presented is original and own work of the author (i.e. there is no plagiarism). No ideas, processes, results, or words of others have been presented as an Author own work.

c. There is no fabrication of data or results which have been compiled / analyzed.

d. There is no falsification by manipulating research materials, equipment or processes, or changing or omitting data or results such that the research is not accurately represented in the research record.

e. The thesis has been checked using **Turnitin** (copy of originality report attached) and found within limits as per GTU Plagiarism Policy and instructions issued from time to time.

Signature of the Research Scholar: …… Date: 15-06-2019
Name of Research Scholar: **Ratansing N. Patel**
Place: Ahmedabad

Signature of Supervisor: …… Date: 15-06-2019
Name of Supervisor: **Dr. Vipul A. Shah**
Place: Ahmedabad

turnitin **Turnitin Originality Report**

Rectangular Microstrip Patch Antenna Design for Satellite Image vision System Application by Ratansing Patel

From Quick Submit (Quick Submit)

Processed on **29-May-2019** 15:00 IST
ID: 1047024233
Word Count: 28053

Similarity Index	Similarity by Source	
9 %	Internet Sources:	4 %
	Publications:	5 %
	Student Papers:	0 %

sources:

1 4% match (publications)
Lee, . "General Formulation of the Cavity Model", Microstrip Patch Antennas, 2010.

2 1% match (Internet from 20-Aug-2018)
http://shodhganga.inflibnet.ac.in/bitstream/10603/72833/9/09_chapter%202.pdf

3 1% match (Internet from 03-Apr-2012)
http://electro.zxq.net/projects/download/Patch-Antenna.pdf

4 1% match (Internet from 20-Jun-2017)
http://www.ee.cityu.edu.hk/~sklmw/apmtt/mat/Overview%20of%20Patch%20Antenna%20Part1.pdf

5 1% match (publications)
Choukiker, Yogesh Kumar, and Santanu Kumar Behera, "Modified Sierpinski square fractal antenna covering ultra-wide band application with band notch characteristics", IET Microwaves Antennas & Propagation, 2014.

6 1% match (Internet from 15-Sep-2017)
https://tel.archives-ouvertes.fr/tel-00499255/file/2009PEST1006_0_0.pdf

PhD THESIS Non-Exclusive License to GUJARAT TECHNOLOGICAL UNIVERSITY

In consideration of being a PhD Research Scholar at GTU and in the interests of the facilitation of research at GTU and elsewhere, I, **Ratansing N. Patel** having Enrolment No. **129990911016** hereby grant a non-exclusive, royalty free and perpetual license to GTU on the following terms:

a) GTU is permitted to archive, reproduce and distribute my thesis, in whole or in part, and/or my abstract, in whole or in part (referred to collectively as the Work") anywhere in the world, for non-commercial purposes, in all forms of media;

b) GTU is permitted to authorize, sub-lease, sub-contract or procure any of the acts mentioned in paragraph (a);

c) GTU is authorized to submit the Work at any National / International Library, under the authority of their "Thesis Non-Exclusive License";

d) The Universal Copyright Notice (©) shall appear on all copies made under the authority of this license;

e) I undertake to submit my thesis, through my University, to any Library and Archives. Any abstract submitted with the thesis will be considered to form part of the thesis.

f) I represent that my thesis is my original work, does not infringe any rights of others, including privacy rights, and that I have the right to make the grant conferred by this non-exclusive license.

g) If third party copyrighted material was included in my thesis for which, under the terms of the Copyright Act, written permission from the copyright owners is required, I have obtained such permission from the copyright owners to do the acts mentioned in paragraph (a) above for the full term of copyright protection.

h) I retain copyright ownership and moral rights in my thesis, and may deal with the copyright in my thesis, in any way consistent with rights granted by me to my University in this non-exclusive license.

i) I further promise to inform any person to whom I may hereafter assign or license my copyright in my thesis of the rights granted by me to my University in this non-exclusive license.

j) I am aware of and agree to accept the conditions and regulations of PhD including all policy matters related to authorship and plagiarism.

Signature of the Research Scholar: …… Date: 15-06-2019
Name of Research Scholar: **Ratansing N. Patel**
Place: Ahmedabad

Signature of Supervisor: …… Date: 15-06-2019
Name of Supervisor: **Dr. Vipul A. Shah**
Place: Ahmedabad

THESIS APPROVAL FORM

The viva-voce of the PhD Thesis submitted by Mr**. Ratansing N. Patel** (Enrolment No. **129990911016**) entitled **"Rectangular Microstrip Patch Antenna Design for Satellite Image Vision System Application"** was conducted on **15th June, 2019** at Gujarat Technological University.

(Please tick any one of the following options)

☐ The performance of the candidate was satisfactory. We recommend that he/she be awarded the Ph.D. Degree.

☐ Any further modifications in research work recommended by the panel after 3 months from the date of first viva-voce upon request of the Supervisor after which viva-voce can be re-conducted by the same panel again.

(Briefly specify the modification suggested by the panel)

☐ The performance of the candidate was unsatisfactory. We recommend that he/she should not be awarded the Ph.D. Degree.

(The panel must give justifications for rejecting the research work)

Name and Signature of Supervisor with Seal

1) External Examiner 1 Name and Signature

2) External Examiner 2 Name and Signature

3) External Examiner 3 Name and Signature

ABSTRACT

Emerging advantages of Microstrip patch antennas make them solid aspirant for the field of communication in Satellite application. Thesis comprises Microstrip patch antennas with entire arithmetical calculations, model results, measurement results and the appropriate antenna applications on the working frequencies. These novel designs have frequency ranges from 6 GHz to 15 GHz. These antenna simulations performed by using Ansoft HFSS and fabricated. Rectangular tree fractal antenna measured by Vector network analyzer (VNA). It presents simulation and measured results in provisions of Bandwidth, Return loss and VSWR. Microstrip patch antennas have wide range of applications, however here in this thesis they present WiMAX, WiBRO, RLAN and LMS Satellite Communication applications.

By adopting the tree fractal concept the issues of edge radiation, capacitive and inductive effect on radiation cab be resolve. To address RTFA structure with 4 level iterations in *L* shape and 3 level iterations in *U* shale also improved impedance matching and return loss. The concept of tree fractal including number of iterations supports multiband frequency operation and wide band application and it can be preferred for 6 GHz to 15 GHz frequency band and also improved bandwidth.

A RTFA novel structure with L = 30 mm and W = 23 mm along the square patch yielded a triple notch band characteristics at resonant frequency of 7.4 GHz, 10.7 GHz and 13 GHz, as well as an improved resonant return loss (-28.85 dB) and VSWR (1.07) and also bandwidth is enhance upto 19.23%.

The experimental results have some deviations compared to the simulation results due to machining error and welding error. The result shows operating bandwidth of the proposed rectangle tree fractal antenna (RTFA) covers the entire frequency band from 6 GHz to 15 GHz, and including notch bands of 5.92 GHz – 8.45 GHz for WiMAX, WiBRO, 8.5 GHz – 10.55 GHz for RLAN and 12.75 GHz – 14.5 GHz for LMS is achieved by using defected ground structure (DGS) on the ground plane to improve the impedance characteristics between adjacent resonant frequencies and triple band notch characteristics is proposed by three U-slots on the tree fractal path and effectively suppress the interferences..

ACKNOWLEDGEMENT

I wish to express my sincere appreciation to those who have contributed to this thesis and supported me in one way or the other during this amazing journey.

First, I am extremely grateful to my supervisor, ***Dr. Vipul A. Shah***, Professor and Head, Instrument and Control Engineering Department, Dharmsinh Desai University, Nadiad, Gujarat for his guidance and all the useful discussions and brainstorming sessions, especially during the difficult conceptual development and decision stage. His deep insights helped me at various phases of my research. His invaluable suggestions and constructive criticisms from time to time enabled me to maintain my enthusiasm to complete my work successfully.

The completion of this work would not have been possible without, the Doctorate Progress Committee (DPC) members: ***Dr. Vishvjit K. Thakar***, Professor, Information and Communication Technology Department, Sankalchand Patel University, Visnagar, Gujarat and ***Dr. Rutvij C. Joshi,*** Associate Professor, Electronics and Communication Engineering Department, A.D. Patel Institute Technology, Valabhvidhyanagar, Gujarat. I am thankful for their rigorous examinations and precious suggestions during my research.

My gratitude goes out to the assistance and support of ***Dr. Akshai Agrawal***, Ex. Vice Chancellor, ***Dr. Navin Sheth,*** Vice Chancellor, ***Shri S.D. Panchal***, Registrar, Data Entry Operator and other staff members of PhD Section, GTU.

At this stage, I would also like to acknowledge the support provided by my institute and faculty members of ***Government Polytechnic, Palanpur***. I would also like to acknowledge my ***family members*** for their helping hands and patience as and when required.

Ratansing N. Patel

Table of Contents

List of Abbreviation

AR	Axial Ratio
BW	Bandwidth
CP	Circular Polarization
DGS	Defected Ground Structure
FDTD	Finite Difference Time Domain Method
FEM	Finite Element Method
GPS	Global Positioning Satellite
HFSS	High Frequency Structural Simulator
IFS	Integrated Function System
LHCP	Left Handed Circular Polarization
LMS	Land Mobile Satellite and Radio Navigation
LP	Linear Polarization
MEMS	Micro-electro Mechanical Systems
MIC	Microwave Integrated Circuit
MNM	Multiport network model
MoM	Method of Moments
MPA	Microstrip Patch Antenna
MSA	Microstrip Antenna
PCB	Printed circuit board
PTFE	Poly Tera Fluoro Ethylene
RLAN	Radio location and Aeronautical/Maritine radio navigation
RMPA	Rectangular Microstrip Patch Antenna
RMS	Rectangular Microstrip Antenna
RTFA	Rectangular Tree Fractal Microstrip Patch Antenna
SDT	Spectral Domain Technique
SWR	Standing Wave Ratio
UWB	Ultra Wide Band
VNA	Vector Network Analyser
VSWR	Voltage Standing Wave Ratio
WiBRO	Wireless Broadband
WiMAX	Worldwide Interoperability for Microwave Access
WLAN	Wireless Local Area Network

List of Figures

List of Tables

CHAPTER 1

Introduction

The Concept of the Microstrip Antennas (MSA) was proposed first time in 1953 (Deschamps, G. A., 1953) on the other hand practical antennas were developed by (Munson, R. E., 1973 and 1974) and (Howell, J. Q., 1975) in the 1970s. The abundant advantages of MSA, such as its low weight, compact size, and ease of fabrication using printed-circuit technology, led to the design of several configurations for various applications (Bahl, I. J., and P. Bhartia, 1980), (Carver, K. R., and J. W. Mink, 1981), (Mailloux, R. J., 1981), (James, J. R., 1981) and (James, J. R., and P. S. Hall, 1989). With increasing requirements for personal and mobile communications, the demand for smaller and low-profile antennas has brought the MSA to the forefront.

Microstrip antennas (often called patch antennas) are widely used in the microwave frequency region because of their simplicity and compatibility with printed circuit technology, making them easy to manufacture either as stand-alone elements or as elements of arrays. In its simplest form a microstrip antenna consists of a patch of metal, usually rectangular or circular on top of a grounded substrate, as shown in Figure 1.1.

An MSA in its simplest form consists of a radiating patch on one side of a dielectric substrate and a ground plane on the other side. The top and side views of a rectangular MSA (RMSA) are shown in Figure 1.2. However, other shapes, such as the square, circular, triangular, semicircular, sectoral, and annular ring shapes shown in Figure 1.3 are also used.

Radiation from the MSA can occur from the fringing fields between the periphery of the patch and the ground plane. The length L of the rectangular patch

for the fundamental TM_{10} mode excitation is slightly smaller than $\lambda/2$, where λ is the wavelength in the dielectric medium, which in terms of free-space wavelength λ_0 is given as $\lambda_0/\sqrt{\varepsilon_e}$, where ε_e is the effective dielectric constant of a microstrip line of width W. The value of ε_e is slightly less than the dielectric constant ε_r of the substrate because the fringing fields from the patch to the ground plane are not confined in the dielectric only, but are also spread in the air. To enhance the fringing fields from the patch, which account for the radiation, the width W of the patch is increased.

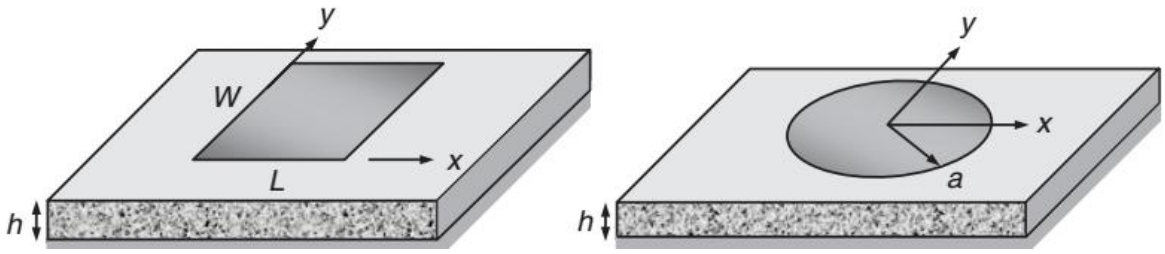

(a) (b)

FIGURE 1.1 (a) Rectangular microstrip patch and (b) Circular microstrip patch

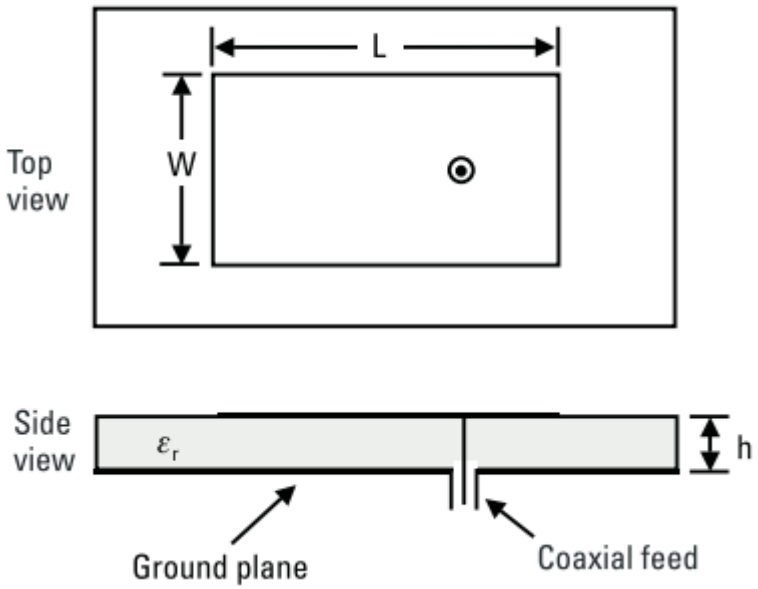

FIGURE 1.2 MSA configurations

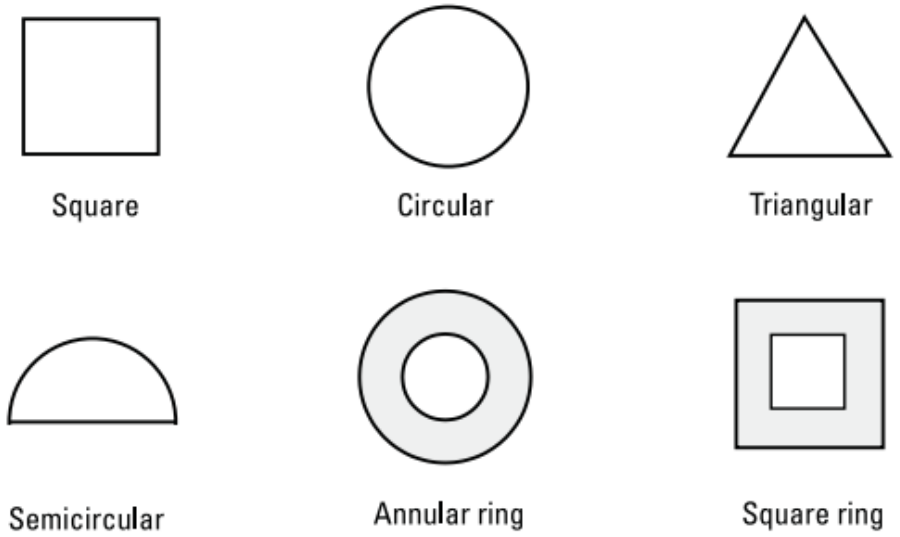

FIGURE 1.3 Different shapes of microstrip patch

The fringing fields are also enhanced by decreasing ε_r or by increasing the substrate thickness h. Therefore, unlike the microwave integrated circuit (MIC) applications, MSA uses microstrip patches with larger width and substrates with lower ε_r and higher h.

For MSA applications in the microwave frequency band, generally h is taken greater than or equal to 0.159 cm [2]. MSAs have several advantages compared to the conventional microwave antennas.

The main advantages of MSAs are listed as follows:

- They are lightweight and have a small volume and a low profile planar configuration.
- They can be made conformal to the host surface.
- Their ease of mass production using printed-circuit technology leads to a low fabrication cost.
- They are easier to integrate with other MICs on the same substrate.
- They allow both linear polarization and CP.
- They can be made compact for use in personal mobile communication.
- They allow for dual- and triple-frequency operations.

1.1 Feed Method

Various methods may be used to feed the microstrip antenna, as shown in Figure 1.4 for the rectangular patch. The coaxial probe feed shown in Figure 1.4(a) is one of the most common feeds for a stand-alone element. The inset feed in Figure 1.4(b) is common for array applications. The proximity-coupled feed in Figure 1.4(c) requires multilayer fabrication but reduces spurious radiation from the feed line. The aperture coupled feed shown in Figure 1.4(d) has the advantage of eliminating feed-line radiation at the expense of some back radiation from the aperture and also allows for relatively thick substrates, since probe reactance is not an issue.

1.1.1 Radiation Efficiency and Bandwidth

Radiation efficiency depends largely on the substrate permittivity and thickness. A substrate that has a higher permittivity or that is thicker will suffer from increased surface wave excitation, which will lower the efficiency. Using a foam substrate is a simple way to eliminate surface-wave excitation. Removing the substrate outside of the patch cavity will also eliminate surface-wave excitation. On the other hand, if the substrate is too thin, the efficiency will be low due to conductive and dielectric losses. Assuming a typical Teflon substrate (ε_r = 2.2 with a loss tangent of 0.001) and copper for the patch and ground plane with a conductivity of 3.0×10^7 S/m, the radiation efficiency is maximum for a substrate thickness of about $0.02\lambda_0$, reaching about 90 percent. When using a foam substrate, the efficiency continuously increases with increasing substrate thickness, approaching 100 percent for thicker substrates.

The bandwidth increases with the substrate thickness and inversely with the substrate permittivity, so bandwidth is made larger by using thicker low-permittivity substrates (e.g., a thicker foam substrate) at the expense of increased lateral size and vertical thickness. For a coaxially fed microstrip antenna, the substrate thickness is limited by the inductance of the feeding coaxial probe, which increases directly with increasing substrate thickness. For a typical substrate material such as Teflon and a 50 Ω coaxial feed cable the probe reactance will become sufficiently large when the substrate thickness is about $0.018\lambda_0$ to render the antenna non resonant unless a matching element is used. This limits the achievable bandwidth of a simple coaxially fed microstrip antenna.

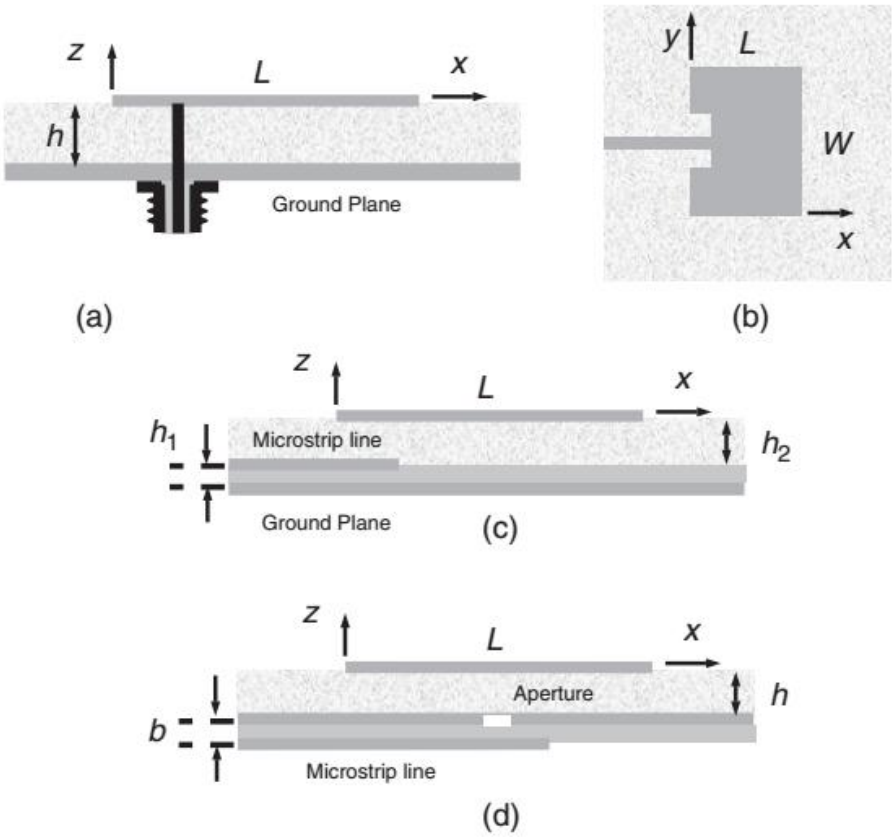

FIGURE 1.4 Feeding methods for a microstrip antenna (a) coaxial feed, (b) inset feed, (c) proximity coupled feed, and (d) aperture coupled feed

Many specialized techniques have been developed to increase the bandwidth of a microstrip antenna. These include either using thick foam substrates along with aperture coupled feeds to avoid the probe reactance limitation, or using capacitive elements to compensate for the probe inductance.

It may be achieved by using configurations that exhibit dual or multiple resonances, including stacked resonators or antennas surrounded by parasitically coupled elements. Antennas that have special geometries may also be used to greatly increase the bandwidth. By using these techniques, bandwidths exceeding 100 percent have been achieved.

For a Teflon substrate and copper conductors, the maximum bandwidth (VSWR < 2) of a rectangular microstrip antenna having a typical width/length (W/L) ratio of 1.5 will be about 2.5 percent, reached when the substrate thickness is about $0.025\lambda_0$. For a typical substrate thickness of $0.01\lambda_0$, the bandwidth is about 1.5 percent. Typical substrate materials and dielectric constants are listed in Table 1.1.

TABLE 1.1 Typical dielectric constant and loss for different materials

Dielectric Material	Dielectric Constant (ε_r)	Dielectric Loss Tangent
AIR	1	0.03
FR4 (EPOXY)	4.3	0.025
PAPER	2.31	0.0025
Bakelite	4.82	0.0020
Teflon (PTFE)	2.1	0.0002
Rogers RT/Duroid 5870	2.33	0.0012

Considering the trade off between the antenna dimensions and its performance, it was found suitable to select a thin dielectric substrate with low dielectric constant. The length of the antenna is responsible for determining the resonant frequency and the inductance of the antenna increases as the length increases. Typical frequency band of various wireless communication applications are listed in Table 1.2. The dimension of the antenna is important parameter to determining the resonant frequency and it is also affect capacitive and inductive effect at the time of radiation.

Two important antenna parameters are the gain and the impedance bandwidth. The gain describes the directional property of an antenna while the impedance bandwidth describes the range of frequencies within which the voltage standing wave ratio is below a certain value. This value is usually taken as 2 in academia and 1.5 in industry. Both will be used in this book. Table 1.2 shows the typical frequency range for different applications. The bandwidth of an antenna is the range of frequencies within which the performance of the antenna, with respect to some characteristic, conforms to a specified standard.

TABLE 1.2 Typical frequencies of various wireless communication applications

Applications	Frequency Band
Global Positioning Satellite (GPS)	1575 MHz and 1227 MHz
Cellular Phone	900 MHz (GSM) and 1800 MHz CDMA)
Personal Communication System	1.85-1.99 GHz and 2.18-2.20 GHz
Satellite Applications	7 -9 GHz
Wireless Local Area Networks	2.40-2.48 GHz and 5.4 GHz
Cellular Video	28 GHz
Direct Broadcast Satellite	11.7-12.5 GHz
Automatic Toll Collection	905 MHz and 5-6 GHz
Collision Avoidance Radar	60 GHz, 77 GHz, and 94 GHz
Wide Area Computer Networks	60 GHz

In the case of the microstrip patch antenna which is basically a strongly resonant device, it is usually the variation of impedance, rather than pattern, which limits the standard of performance. If the antenna impedance is matched to the transmission line at resonance, the mismatch off resonance is related to the voltage standing wave ratio (denoted by VSWR or SWR). The value of VSWR which can be tolerated then defines the bandwidth of the antenna. If this value is to be less than S, the usable bandwidth of the antenna is related to the total Q factor by

$$B = \frac{S - 1}{Q\sqrt{S}} \tag{1.1}$$

where

B = Bandwidth,

S = Voltage standing wave ratio

Q = Quality factor

To derive Equation 1.1, consider the transmission line of characteristic resistance R_o terminated in the microstrip patch antenna, which has input impedance Z_{in}, as illustrated in Figure 1.5. Consider the antenna as a resonant circuit. From elementary circuit theory, the input impedance of the resonant circuit can be written in term of the Q of the circuit and the frequency deviation from resonance, Δ

$$Z_{in} = R_{in}(1 + j2Q\Delta) \tag{1.2}$$

where

Z_{in} = Input impedance

R_{in} = Input resistance

Δ = Frequency deviation

$$\Delta = \frac{f - f_r}{f_r} \tag{1.3}$$

The voltage reflection coefficient Γ and the standing wave ratio S are given by

$$\Gamma = \frac{Z_{in} - R_0}{Z_{in} + R_0} \tag{1.4}$$

$$S = \frac{1 + |\Gamma|}{1 - |\Gamma|} \tag{1.5}$$

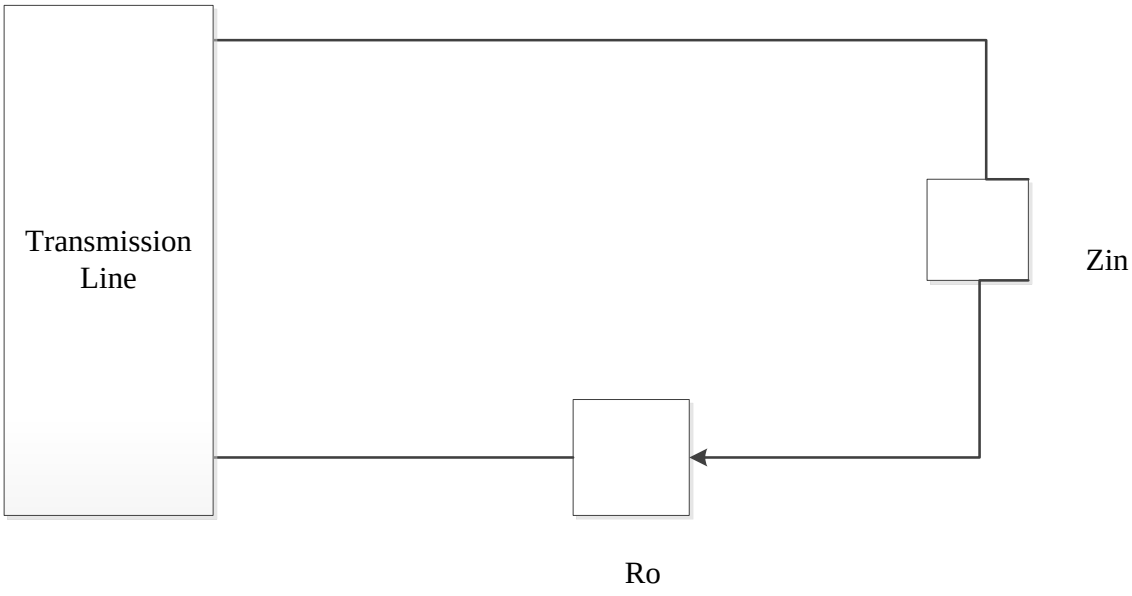

FIGURE 1.5 Equivalent models for impedance matching

Thus

$$\frac{S-1}{S+1} = |\Gamma| = \left|\frac{Z_{in} - R_0}{Z_{in} + R_0}\right| \tag{1.6}$$

where

Γ = Reflection coefficient

R_o = Output resistance

Using equation 1.2, we have

$$\frac{S-1}{S+1} = \frac{|1 + j2Q\Delta - R_0/R_{in}|}{|1 + j2Q\Delta + R_0/R_{in}|} \tag{1.7}$$

On letting $T = \frac{Ro}{Rin}$, we obtain

where

T = Resistor transfer ratio

$$\frac{(1-T)^2 + 4Q^2\Delta^2}{(1+T)^2 + 4Q^2\Delta^2} = (\frac{S-1}{S+1})^2 \tag{1.8}$$

The solution for Δ^2 is:

$$\Delta^2 = \frac{1}{4Q^2}\left[\frac{(TS-1)(S-T)}{S}\right] \tag{1.9}$$

Referring to Figure 1.6, let f_2 and f_1 respectively be the frequencies above and below resonance at which the voltage standing wave ratio equals *S*. The fractional bandwidth is corresponding to the value of *S*.

$$B = \frac{f_2 - f_1}{f_r} = 2\Delta \tag{1.10}$$

where

f_2 = Higher cut-off frequency

f_1 = Lower cut-off frequency

f_r = Resonance frequency

Thus

$$\frac{B^2}{4} = \frac{1}{4Q^2}\left[\frac{(TS-1)(S-T)}{S}\right] \tag{1.11}$$

$$B = \frac{1}{Q}\sqrt{\frac{(TS-1)(S-1)}{S}} \tag{1.12}$$

If the antenna is matched at the frequency f_r, $R_{in} = R_o$ and $T = 1$ and we obtain equation 1.1

In the literature, S is usually chosen to be 2 for defining the VSWR and BW. In industry, the more stringent standard $S = 1.5$ is used.

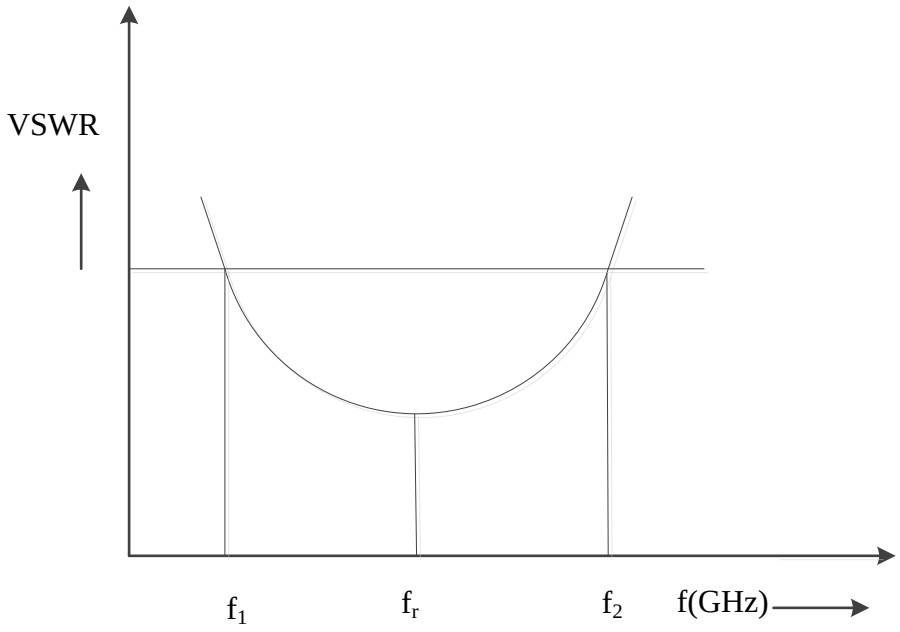

FIGURE 1.6 Illustration of VSWR against frequency plot

1.2 Motivation

Based on the above mentioned challenges, the characteristics of Microstrip patch antenna can be summarized by the following:

- Infinite number of resonant modes, each characterized by a resonant frequency.
- Dimension factors vary from patch to patch.
- Radiation pattern characteristics.
- Half-power beam width.
- Directional characteristics.
- Feeding technique and feed position.
- Input resistance variation at resonance with feed position.
- Bandwidth and impedance matching.
- Return loss and VSWR.
- Substrate material selection and dielectric loss.

1.3 Research Objectives

The main research objectives are:

- To study the MPA design structure, substrate material characteristics, and feeding techniques with different patch structure.
- To study the MPA design structure, substrate material characteristics, and feeding techniques with different design parameters.
- Using structural simulator, suggest an approach to address some of the challenges regarding BW enhancement, S_{11}, and VSWR.
- To address the impedance matching and reactance variation issues as it occurs in case of most of antenna design structures.
- To implement the idea which optimize existing methods to improve the performance and propose the new design structure which include edge slit/slot at a different angle by applying rectangular tree fractal concept.
- To fabricate simulated design with proper dimension, substrate suitable material with as much as number of iteration
- Testing of RTFA using Vector network Analyser (VNA).
- Comparison and analysis of RTFA testing and simulation results.

1.4 Contribution

The original contribution of the thesis is in terms of modifications suggested in rectangular microstrip patch antenna structure for bandwidth enhancement with multi-band supporting frequency operation and VSWR improvement for satellite communication application. By introducing tree fractal concept resolve the issues of edge radiation, capacitive and inductive effect on radiation. To address RTFA structure with 4 level iterations in *L* shape and 3 level iterations in *U* shape also improved impedance matching and return loss. The concept of tree fractal including number of iterations supports multiband frequency operation and wide band application and it can be preferred only for 6 GHz to 15 GHz frequency band and also improved bandwidth.

1.5 Organization of the Thesis

In rest of the thesis, chapter 2 covers related literature reviews which include an overview of fractal antenna engineering research, various feeding techniques, bandwidth enhacement method, VSWR improvement methods, resonant behavior of fractal, novel ultra-wideband fractal tree-shape antenna, frequency dependent behaviour of microstrip, printed UWB vivaldi antenna using stepped connection structure between slot line and tapered patches. Chapter 3 is on microstrip patch antenna, where different material consideration and feeding techniques mathematical analysis and also losses are presented. It is followed by microstrip feed line with FR4 material based approach for MPA design. Chapter 4 and chapter 5 are for rectangular microstrip strip antenna design and also tree fractal concept is introduced for design consideration**.** In chapter 4, the work focuses on rectangular microstrip patch antenna design steps and parameters and also introduced number of slits/slots in RMPA with different shapes, while chapter 5 is for the work on tree fractal rectangular microstrip patch antenna design. The chapters 4 and 5 are also cover the simulation/measured results and discussion. Conclusion and future work is presented in chapter 6.

CHAPTER 2

Literature Review

2.1 Overview

This chapter represents the survey of microstrip patch antenna design structure including different feeding technique, substrate material, input and output parameters at suitable centre frequency for different communication application. The survey will cover the basic concept, overall structure, selected modified technique with variation of BW and frequency band etc. General text books on microstrip patch antenna and antenna design handbook are (Girish Kumar, K. P. Ray, 2003) and (David R. Jackson, 2007).

The origin of microstrip antennas apparently dates back to 1953, when Deschamps proposed the use of microstrip feed lines to feed an array of printed antenna elements (G. Deschamps and W. Sichak, 1953). The printed antenna elements introduced there were not microstrip patches, but flared planar horns. The microstrip patch antenna was first introduced by Munson in a symposium paper in 1972 which was followed by a journal paper in 1974. These papers discussed both the wraparound microstrip antenna and the rectangular patch. Shortly after Munson's symposium paper, Howell also discussed rectangular patch antennas in another symposium paper in which he credits Munson with the basic idea by referencing a private communication. In a later journal paper, Howell introduced the circular patch as well as the circularly polarized patch antenna. Soon after the introduction of the microstrip antenna, papers appeared describing methods of analysis for these antennas, including the transmission line model (A. G. Derneryd, 1976) the cavity model, and the spectral-domain method. A good review of the early history of microstrip antennas is provided in the article by Carver and Mink. A discussion of microstrip antennas may be found in a variety of books devoted to this type of antenna as well as in more general antenna books and handbooks.

The simple model of rectangular microstrip antenna excited by a coaxial line with and without air gaps in terms of input impedance developed by (F. Abboud, J.P. Damiano, A. Papiernik, 1962). Estimation of radiation loss and design implications by introducing different feed appears to be little scope for significantly reducing the radiation loss, both in view of the limited types of connectors commercially available and the fundamental radiation mechanism (A. Henderson and Prof. J.R. James, 1981). New Procedure for Design of Microstrip Patch Antennas Using Method of Moments discussed by (R A Abd-Alhameed, N J McEwan,P S Excell, M M Ibrahim, *Z* M Hejazi and M Musa, 1997). The concept of the fractal, review the progress in fractal antenna study and implementation, compare different types of fractal antenna elements and arrays and discuss the challenge and future of this new type of antenna by (Tian Tiehong, Zhou Zheng, 2003). By introduction of the 3D microstrip-line fed of the rectangular slot, a broadband impedance matching of the rectangular slot over a large frequency band can be achieved. In addition, by adjusting the tuning structure of microstrip-line-fed near the side perpendicular to microstrip line, A very broadband operation of triangular slot antenna can be obtained (Wen-Shan Chen and Chin-Hsin Kao, 2005). The open condition is a significant new concept in the design of high-gain antennas and must be applied in designing high-gain antennas on non-negligible bandwidth, making it possible to use a practical dielectric cover of moderate thickness (Chi Sang You and Woonbong Hwang, 2005).

A novel reconfigurable microstrip patch antenna is presented that is monolithically integrated with RF micro electro mechanical systems (MEMS) capacitors for tuning the resonant frequency and also discussed CPW method by (Emre Erdil, Kagan Topalli, Mehmet Unlu, Ozlem Aydin Civi, and Tayfun Akin, 2007). Wideband Microstrip Patch Antenna with U-Shaped Parasitic Elements proposed by (Sang-Hyuk Wi, Yong-Shik Lee, and Jong-Gwan Yook, 2007) and also achieve wide bandwidth with relatively small size. An ultra wideband antenna mounted on two vertical planes has been designed for microwave imaging arrays, the selected application being breast cancer detection. The antenna has shown good impedance matching over the whole required bandwidth show excellent performance in the input impedance and radiation pattern over the target range from 4 GHz to 8 GHz. The 4 GHz to 8GHz frequency band for microwave imaging perform better in comparison with other microwave frequencies. (S.Adnan, R.A. Abd-Alhameed, H.I.Hraga, I.T.E.Elfergani and M.B.Child, 2010).

Microstrip antennas are excited for radiation modes using different techniques which lead to best impedance matching between the feed line and the patch. The proposed rectangular patch antenna is designed at 2.4 GHz and fed by coaxial line and microstrip line. (Aditi Mandal, Antara Ghosal, Anurima Majumdar, 2012). Two different designs of multi-band microstrip patch antenna and their parameters are discussed and compared. The proposed slotted dual-band antenna has a very simple structure, which makes the design simpler and fabrications easier, and is very suitable for applications in the access points of wireless communications (Meriem Harbadji, Amel Boufrioua, 2014). An effective approach to reduce the patch size in rectangular patch microstrip antennas has been proposed. The approach is based on inductively loading the patch using a cuboid ridge. The cuboid ridge is included in the transmission line model of the patch antenna and a theoretical background of the approach has been explained (Alireza Motevasselian1, William G. Whittow,2015). A broadband slot antenna with narrow slits and a small conductor strip has been proposed so that the undesired frequencies could be rejected, resulting in EMI mitigation (Pichet Moeikham, Prayoot Akkaraekthalin, 2015). The proposed structure showed promising results in perspective of return loss, gain, efficiency and directivity for the applications wireless communication system including IEEE 802.11a WLANs application that allocate channels between 5.15 to 5.825 GHz base on effect of Different Slots in a Design of Microstrip Antennas (Bappadittya Roy, Ankan Bhattacharya, A.K.Bhattacharjee, S.K.Chowdhury, 2015). On the basis of all three parameter rectangular patch shows better results than triangular and circular patch with FR-4 dielectric at 2.4 GHz frequency (Rajan Fotedar, Pankaj Singh Garia, Rahul Saini, A. Vidyarthi, R. Gowri, 2015).

The rectangular slot antenna with rectangular stub for a wide impedance bandwidth is proposed and in addition, the interference frequency band has been rejected by placing the folded parasitic line surrounding the rectangular stub of the presented antenna (Chatree mahatthanajatuphat, narintra srisoontorn, thanakarn suangun, Prayoot akkaraekthalin, 2016). A novel rectangle tree fractal antenna (RTFA) for ultra-wideband (UWB) application with dual band notch characteristics is proposed by (Zhangfang Hu, Yinping Hu, Yuan Luo, and Wei Xin, 2016).

For any microstrip patch antenna design structure, the objective is to improve directional characteristics and enhance BW, VSWR and gain with reduction of edge unwanted

radiation. Depending on the applications, the specific objectives may cover one or more of the following.

- Improving the directional characteristics and gain
- Refining the geometric parameters to better structure for impedance matching
- Improving the accuracy of the out parameters as per requirement of the application at hand
- Increasing the bandwidth and VSWR and multiband notch characteristics
- Managing the simulated and fabricate results

In general, majority of the researchers have contributed to one or more of the basic structure for design approach by some modifications to the components or suggesting alternative method to the component/s. So knowledge of related basics, principles and their combinations can easily help for establishing a new patch structure design technique. According to the major surveys, microstrip patch antenna design structure consists of the following main elements.

- Various design dimensions that will be considered in terms of edge, corner, slot, length and width
- Modified structure that will include impedance matching, bandwidth enhancement and gain improvement with appropriate dimension and size
- Similarity (or dissimilarity) measure that gives the merit of slotted patch features, by maximising (or minimising) it; this is also termed as multiband frequency operation
- Optimization method used to find the optimal geometric structure include number of slot by applying concept of tree fractal by maximising (or minimising) the iteration

As discussed in the previous chapter, microstrip patch antenna can be design according to structural geometry and dimensions based on different method of analysis. Design structure consist three layers top substrate and bottom layer which is named by ground plane. Top and bottom layers made by metal like copper and substrate made by dielectric materials. Selection of dielectric materials based on availability and loss tangent which listed in Table 1.1. Structure geometry and dimension are selected based on resonant frequency.

2.2 Methods of Analysis

The Microstrip Antenna (MSA) has a two-dimensional radiating patch on a thin dielectric substrate and therefore may be categorized as a two-dimensional planar component for analysis purposes. The analysis methods for MSAs can be broadly divided into two groups. In the first group, the methods are based on equivalent magnetic current distribution around the patch edges (similar to slot antennas). There are three popular analytical techniques:

- The transmission line model
- The cavity model
- The multiport network model

In the second group, the methods are based on the electric current distribution on the patch conductor and the ground plane (similar to dipole antennas, used in conjunction with full wave simulation/numerical analysis methods). Some of the numerical methods for analyzing MSAs are listed as follows:

- The method of moments (MoM)
- The finite element method (FEM)
- The spectral domain technique (SDT)
- The finite difference time domain method (FDTD)

This section briefly describes these methods.

2.2.1 Transmission Line Model

The transmission line model is very simple and helpful in understanding the basic performance of a MSA. The microstrip radiator element is viewed as a transmission line resonator with no transverse field variations (the field only varies along the length), and the radiation occurs mainly from the fringing fields at the open circuited ends. The patch is represented by two slots that are spaced by the length of the resonator. This model was originally developed for rectangular patches but has been extended for generalized patch shapes. Many variations of this method have been used to analyze the MSA (James, J. R., and P. S. Hall, 1989), (Bhatacharya, A. K., and R. Garg, 1985) and (Dubost, G., and G. Beauquet, 1986). Although the transmission line model is easy to use, all types of

configurations cannot be analyzed using this model since it does not take care of variation of field in the orthogonal direction to the direction of propagation.

2.2.2 Cavity Model

In the cavity model, the region between the patch and the ground plane is treated as a cavity that is surrounded by magnetic walls around the periphery and by electric walls from the top and bottom sides. Since thin substrates are used, the field inside the cavity is uniform along the thickness of the substrate (Lo, Y. T., D. Solomon, and W. F. Richards, 1979), (Richards, W. F., Y. T. Lo, and D. D. Harrison, 1981) and (Lo, T., and S. W. Lee, 1988). The fields underneath the patch for regular shapes such as rectangular, circular, triangular, and sectoral shapes can be expressed as a summation of the various resonant modes of the two-dimensional resonator.

The fringing fields around the periphery are taken care of by extending the patch boundary outward so that the effective dimensions are larger than the physical dimensions of the patch. The effect of the radiation from the antenna and the conductor loss are accounted for by adding these losses to the loss tangent of the dielectric substrate. The far field and radiated power are computed from the equivalent magnetic current around the periphery.

An alternate way of incorporating the radiation effect in the cavity model is by introducing an impedance boundary condition at the walls of the cavity. The fringing fields and the radiated power are not included inside the cavity but are localized at the edges of the cavity. However, the solution for the far field, with admittance walls is difficult to evaluate (Lo, Y. T., D. Solomon, and W. F. Richards, 1979).

2.2.3 Multiport Network Model (MNM)

The MNM for analyzing the MSA is an extension of the cavity model (Lo, Y. T., D. Solomon, and W. F. Richards, 1979), (Okoshi, T., and T. Miyoshi, 1972) and (Gupta, K. C., and P. C. Sharma, 1981).In this method, the electromagnetic fields underneath the patch and outside the patch are modeled separately. The patch is analyzed as a two dimensional planar network, with a multiple number of ports located around the periphery. The multiport impedance matrix of the patch is obtained from its two-dimensional Green's function. The fringing fields along the periphery and the radiated fields are incorporated by

adding an equivalent edge admittance network. The segmentation method is then used to find the overall impedance matrix. The radiated fields are obtained from the voltage distribution around the periphery.

The above three analytical methods offer both simplicity and physical insight. In the latter two methods, the radiation from the MSA is calculated from the equivalent magnetic current distribution around the periphery of the radiating patch, which is obtained from the corresponding voltage distribution. Thus, the MSA analysis problem reduces to that of finding the edge voltage distribution for a given excitation and for a specified mode. These methods are accurate for regular patch geometries, but except for MNM with contour integration techniques they are not suited for arbitrary shaped patch configurations. For complex geometries, the numerical techniques described below are employed (Lo, Y. T., D. Solomon, and W. F. Richards, 1979).

2.2.4 The Method of Moments (MoM)

In the MoM, the surface currents are used to model the microstrip patch, and volume polarization currents in the dielectric slab are used to model the fields in the dielectric slab. An integral equation is formulated for the unknown currents on the microstrip patches and the feed lines and their images in the ground plane (Newman, E. H., and P. Tulyathan, 1981). The integral equations are transformed into algebraic equations that can be easily solved using a computer. This method takes into account the fringing fields outside the physical boundary of the two-dimensional patch, thus providing a more exact solution.

2.2.5 The Finite Element Method (FEM)

The FEM, unlike the MoM, is suitable for volumetric configurations. In this method, the region of interest is divided into any number of finite surfaces or volume elements depending upon the planar or volumetric structures to be analyzed (Silvester, P., 1973). These discredited units, generally referred to as finite elements, can be any well-defined geometrical shapes such as triangular elements for planar configurations and tetrahedral and prismatic elements for three-dimensional configurations, which are suitable even for curved geometry. It involves the integration of certain basic functions over the entire conducting patch, which is divided into a number of subsections. The problem of solving wave equations with inhomogeneous boundary conditions is tackled by decomposing

it into two boundary value problems, one with Laplace's equation with an inhomogeneous boundary and the other corresponding to an inhomogeneous wave equation with a homogeneous boundary condition (Lee, H. F., and W. Chen, 1997).

2.2.6 The Spectral Domain Technique (SDT)

In the SDT, a two-dimensional Fourier transform along the two orthogonal directions of the patch in the plane of substrate is employed. Boundary conditions are applied in Fourier transform plane. The current distribution on the conducting patch is expanded in terms of chosen basis functions, and the resulting matrix equation is solved to evaluate the electric current distribution on the conducting patch and the equivalent magnetic current distribution on the surrounding substrate surface. The various parameters of the antennas are then evaluated (Itoh, T., and W. Menzel, 1981).

2.2.7 The Finite Difference Time Domain Method (FDTD)

The FDTD method is well-suited for MSAs, as it can conveniently model numerous structural inhomogenities encountered in these configurations (Lee, H. F., and W. Chen, 1997). It can also predict the response of the MSA over the wide BW with a single simulation. In this technique, spatial as well as time grid for the electric and magnetic fields are generated over which the solution is required. The spatial discretizations along three Cartesian coordinates are taken to be same. The E cell edges are aligned with the boundary of the configuration and H fields are assumed to be located at the center of each E cell. Each cell contains information about material characteristics. The cells containing the sources are excited with a suitable excitation function, which propagates along the structure. The discredited time variations of the fields are determined at desired locations. Using a line integral of the electric field, the voltage across the two locations can be obtained. The current is computed by a loop integral of the magnetic field surrounding the conductor, where the Fourier transform yields a frequency response. The above numerical techniques, which are based on the electric current distribution on the patch conductor and the ground plane, give results for any arbitrarily shaped antenna with good accuracy, but they are time consuming. These methods can be used to plot current distributions on patches but otherwise provide little of the physical insight required for antenna design.

2.3 RMSAs with a U-Slot

A very promising configuration that yields broad BW is a RMSA with a U-shaped slot (Huynh, T., and K. F. Lee, 1995). A resonant U-slot is cut symmetrically around the center of the patch. When slot cut is inside the patch the resonance frequency of the patch change slightly in comparison with the resonance frequency of the slot. Accordingly, the dimensions of the slot are chosen such that its resonance frequency is close to that of the rectangular patch with a slot (Lee, H. F., and W. Chen, 1997). A thick foam substrate of thickness h = 2.7 cm, which corresponds to 0.08λ at 0.9 GHz, is used to obtain a broad BW. The resonance frequency of the RMSA with a U-slot is primarily determined by the length of the patch, and the position of the loop in the impedance plot primarily depends upon the total length of the U-slot. The loop in the lower frequency region is due to the resonance of the U-slot. On the other hand, for the RMSA without a U slot, there would be large inductive reactance in the input impedance of the patch, because the substrate is electrically thick and even if the feed point is shifted to the edge of the patch, it is not possible to achieve impedance matching. So, a U-slot adds a capacitive component in the input impedance that compensates for the inductive component of the coaxial probe. Instead of cutting a U-shaped slot in the rectangular patch, it can be cut inside the circular patch is fabricated on the low-cost printed circuit board (PCB) substrate in the inverted suspended configuration (Lee, K. F., et al., 1997).

It is observed that by cutting a slot inside or along the periphery of the RMSA, various compact configurations are realized with a reduced BW. If the resonance frequencies of the slot and the patch are close to each other, then broad BW could be obtained. However, care must be taken so that the polarization of the radiated field of the slot and the patch are similar, so that the pattern remains stable over the VSWR BW (Clenet, M., and L. Shafai, 1999) and (Tong, K. F., et al., 2000).

2.4 Square MSA with Modified Edges

Instead of using a nearly square MSA to generate CP, the edges of the square MSA can be modified by adding stubs or by cutting notches. By adding only one stub or by cutting one notch, CP can also be obtained, but then the configuration is not symmetrical. However, as long as the total effective areas of these perturbations are of the same order, the performance of one edge modified is similar to that of a two edge modified square

MSA. The area of the stub or the notch is very critical to yield a lower AR value, just as in the case of a nearly square MSA, where L_1/L_2 ratio is very critical to yield CP. The advantage of these configurations is that the fine-tuning can be easily done by trimming the dimensions of the stub or notch.

2.5 Square MSA with Modified Corners

CP can also be obtained by modifying corners of the square MSA. Small isosceles right angle triangular patches or small square patches are removed from the diagonally opposite corners of the square patch. Chopping off two diagonally opposite corners makes the resonance frequency of the mode along this diagonal to be higher than that for the mode along the un chopped diagonal. The patch is fed along the central axis so that the orthogonal modes are generated. Instead of chopping the corners, small square patches could be added at the corners to obtain CP. In this case, the resonance frequency and AR BW are slightly smaller than that of the corner-chopped cases because of its larger patch area.

2.6 Modified Square MSA with Slits at the Edges

A compact CP MSA is also realized by cutting two pairs of slits of unequal lengths L_1 and L_2 of narrow width W ($W << L_1, L_2$), at the four edges of the square patch For the feed point location, RHCP is obtained when $L_1 > L_2$, and LHCP is obtained when $L < L_2$. With an increase in L_1 and L_2, the resonance frequency of the antenna decreases with a corresponding decrease in the BW. The gain of this compact CP MSA can be increased by placing a λ/4 thick substrate of a high dielectric constant on top of the patch, which is known as the superstreet (Reddy, K. T. V., and G. Kumar, 2000). A compact CP configuration could be realized by cutting four equal slits of length L at the edges of nearly square MSA. By varying the length L, the resonance frequency can be tuned. Instead of nearly square, any other single-feed CP MSA configuration could be used with similar performance.

2.7 State of the Art in Rectangular Microstrip Patch Antenna

In (R A Abd-Alhameed, N J McEwan,P S Excell, M M Ibrahim, *Z* M Hejazi and M Musa, 1997) author discussed New Procedure for Design of Microstrip Patch Antennas Using Method of Moments. Review the progress in fractal antenna study and implementation is

also included and compare different types of fractal antenna elements and arrays. In (Tian Tiehong, Zhou Zheng, 2003) author discusses the challenge and future of this new type of antenna by introduction of the 3D microstrip-line fed of the rectangular slot, a broadband impedance matching of the rectangular slot over a large frequency band.

In (Wen-Shan Chen and Chin-Hsin Kao, 2005) author discussed adjustment of tuning structure of microstrip-line-fed near the side perpendicular to microstrip line, A very broadband operation of triangular slot antenna can be obtained. In (Chi Sang You and Woonbong Hwang, 2005) author proposed new concept in the design of high-gain antennas and applied in designing high-gain antennas on non-negligible bandwidth, making it possible to use a practical dielectric cover of moderate thickness.

In (Emre Erdil, Kagan Topalli, Mehmet Unlu, Ozlem Aydin Civi, and Tayfun Akin, 2007) author proposed a novel reconfigurable microstrip patch antenna that is monolithically integrated with RF micro electro mechanical systems (MEMS) capacitors for tuning the resonant frequency and also discussed CPW method. In (Sang-Hyuk Wi, Yong-Shik Lee, and Jong-Gwan Yook, 2007) Wideband Microstrip Patch Antenna with U-Shaped Parasitic Elements proposed by author and also achieve wide bandwidth with relatively small size. In (S.Adnan, R.A.Abd-Alhameed, H.I.Hraga, I.T.E.Elfergani and M.B.Child, 2010) an ultra wideband antenna mounted on two vertical planes has been designed by author for microwave imaging arrays, the selected application being breast cancer detection. It showed good impedance matching over the whole required bandwidth and also shows excellent performance in the input impedance and radiation pattern over the target range from 4 GHz to 8 GHz. The 4 GHz to 8 GHz frequency band for microwave imaging perform better in comparison with other microwave frequencies.

In (Aditi Mandal, Antara Ghosal, Anurima Majumdar, 2012) author propose new design of microstrip antennas which are excited for radiation modes using different techniques which lead to best impedance matching between the feed line and the patch. The proposed rectangular patch antenna is designed at 2.4 GHz and fed by coaxial line and microstrip line. Two different designs of multi-band microstrip patch antenna and their parameters are discussed and compared. In (Meriem Harbadji, Amel Boufrioua, 2014) author proposed slotted dual-band antenna which has a very simple structure, which makes the design simpler and fabrications easier, and is very suitable for applications in the access points of wireless communications.

In (Alireza Motevasselian, William G. Whittow, 2015) author proposed an effective approach to reduce the patch size in rectangular patch microstrip antennas. The approach is based on inductively loading the patch using a cuboid ridge. The cuboid ridge is included in the transmission line model of the patch antenna and a theoretical background of the approach has been explained. In (Pichet Moeikham, Prayoot Akkaraekthalin, 2015) a broadband slot antenna with narrow slits and a small conductor strip has been proposed by author and in results are excellent so that the undesired frequencies could be rejected, resulting in EMI mitigation. In (Bappadittya Roy, Ankan Bhattacharya, A.K.Bhattacharjee, S.K.Chowdhury, 2015) author proposed new structure and promising results in perspective of return loss, gain, efficiency and directivity for the applications wireless communication system including IEEE 802.11a WLANs application that allocate channels between 5.15 to 5.825 GHz base on effect of Different slots. On the basis of all three parameter rectangular patch shows better results than triangular and circular patch with FR-4 dielectric at 2.4 GHz frequency.

In (Chatree mahatthanajatuphat, narintra srisoontorn, thanakarn suangun, Prayoot akkaraekthalin, 2016) author design the rectangular slot antenna with rectangular stub for a wide impedance bandwidth and in addition, the interference frequency band has been rejected by placing the folded parasitic line surrounding the rectangular stub of the presented antenna. In (Zhangfang Hu, Yinping Hu, Yuan Luo, and Wei Xin, 2016) author proposed a novel rectangle tree fractal antenna (RTFA) for ultra-wideband (UWB) application with dual band notch characteristics. The result of multiband operation is compare with single band. 3 - 5 GHz and 6 - 9 GHz band notch band results are improved the bandwidth and VSWR for multiband frequency.

2.8 Problem Statement

After over all survey of literature from many research journal papers it is observed that the proposed novel RFTA antenna characteristic to some other antennas presented in (Sengupta, K. and K. J. Vinoy, 2006 and S. Ramo, J. R. Whinnery, 1944), (Werner, D. H. and S. Ganguly, 2003 and Choukiker, Y. K. and S. K. Behera, 2014) and (Zhao, X. Y., H. G. Zang, and G. L. Zhang, 2015). It is clear that the proposed RTFA is smaller. Some of the other antennas are large in size, have no notch band or cannot cover the whole band of UWB and also limited upto dual notch band characteristics.

This thesis proposed a novel rectangle tree fractal antenna (RTFA) for ultra-wideband (UWB) and LMS application with triple band notch characteristics with improvement of BW and VSWR. The radiating path is the tree fractal structure which is formed by the superposition of a number of rectangular patches, and multi-frequency resonance characteristics are obtained by only increasing the tree fractal iterations. The proposed RTFA covers the entire frequency band from 6 to 15 GHz, and including notch bands of 5.92 GHz – 8.45 GHz for WiMAX, WiBRO, 8.5 GHz – 10.55 GHz for RLAN and 12.75 GHz – 14.5 GHz for LMS is achieved by using defected ground structure (DGS) on the ground plane to improve the impedance characteristics between adjacent resonant frequencies. The triple notch bands characteristics are realized by three U-slots on the tree fractal path and effectively suppress the interferences. The measurement and simulation results have an acceptable agreement, and indicate that the antenna is suitable for WiMAX, WiBRO, RLAN and LMS applications.

CHAPTER 3

Microstrip Patch Antenna

3.1 Overview

I review some antennas that are commonly used before the advent of microstrip patch antennas. They will be referred to as conventional antennas. The simplest and most widely used antenna element is the half wave dipole, which consists of two linear conductors about a quarter waves long, driven by a source at the center. An antenna consisting of a driver, a reflecting element, and one or more directing elements is called an Uda-Yagi array or a Yagi for short. Other traditional antenna elements are the loop antenna, the horn antenna, and the helical antenna.

The loop antenna is used extensively in TV reception and as directional finders. By flaring the aperture of an open-ended waveguide, a horn antenna is obtained. The horn antenna is used extensively at microwave frequencies, both as feed antennas for parabolic reflectors and as the standard calibration antenna for gain. For communication with satellites and space vehicles, electromagnetic wave with circular polarization (CP) is preferred over linear polarization (LP). The helical antenna is a popular CP antenna and was the antenna brought to the moon by the astronauts in the late 1960 and early 1970.

Two important antenna parameters are the gain and the impedance bandwidth. The gain describes the directional property of an antenna while the impedance bandwidth describes the range of frequencies within which the voltage standing wave ratio is below a certain value. This value is usually taken as 2 in academia and 1.5 in industry. Table 3.1 shows the typical values of these two parameters for the conventional antenna elements described above.

TABLE 3.1 Typical gain and bandwidth of conventional antenna

Element	Typical gain	Typical Bandwidth
Half-wave dipole/Folded dipole	2 dB	8 - 16%
One wavelength loop	4 dB	10%
Yagi	12 dB	5%
Helical antenna	16 dB	70%
Horn antenna	20 dB	20%

Several undesirable features of the conventional antennas can be noted. They are bulky and they protrude from a surface. Moreover, it is difficult to design conventional antennas to perform more than one function, such as dual frequency and dual-polarization.

3.2 Geometries of the Basic Microstrip Patch Antenna

The idea of microstrip patch antennas arose from utilizing printed circuit technology not only for the circuit components and transmission lines but also for the radiating elements of an electronic system. It was first proposed by Deschamps. However, little attention was paid to his idea until the 1970's. Since then, this class of antennas has been the subject of intensive research and development. There are several thousand papers published on the subject, as well as a number of books.

The basic structure of the microstrip patch antenna is shown in Figure 1.2. It consists of an area of metallization supported above a ground plane by a thin dielectric substrate and fed against the ground at an appropriate location. Four feeding methods are shown in Figure 1.4. They are coaxial probe feed, microstrip line feed, aperture coupled feed and proximity feed. Electromagnetic energy is first guided or coupled to the region under the patch, which acts like a resonant cavity with open circuits on the sides. Some of the energy leaks out of the cavity and radiates into space, resulting in an antenna.

3.2.1 Merit and Demerit of Microstrip Patch Antennas

The advantages make microstrip patch antennas much more suitable for aircrafts, spacecrafts, and missiles than conventional antennas as they do not interfere with the aerodynamics of these moving vehicles.

The merits of microstrip patch antennas are:

- Planar, which can also be made conformal to a shaped surface
- Low profile
- Low radar cross-section
- Rugged
- Can be produced by printed circuit technology
- Can be integrated with circuit elements
- Can be designed for dual polarization operations
- Can be designed for dual or multi-frequency operations

Because of the advantages listed above, the microstrip patch antenna has also become the favorite of antenna designers for commercial mobile and wireless communication systems.

There are several demerits associated with microstrip patch antennas.

- In its basic form, the microstrip antenna has a narrow impedance bandwidth, typically less than 5%. However, various bandwidth-widening techniques have been developed. Up to 50% bandwidth has been achieved. It is generally true that wider bandwidth is achieved with the sacrifice of increased antenna physical volume.
- Due to the small separation between the radiating patch and its ground plane, the microstrip antenna can handle relatively low RF power. The average power considered safe is a few tens of watts.
- While a single patch element generally incurs very little loss because it is only about one half waves long, microstrip arrays generally have larger ohmic loss than arrays of other types of antennas of equivalent aperture size. This ohmic loss mostly occurs in the dielectric substrate and the metal conductor of the microstrip line feed network and power dividing circuit.

3.3 Material Consideration

The metallic patch is normally made of thin copper foil. The substrate material provides mechanical support for the radiating patch elements. It also maintains the required spacing between the patch and its ground plane. The substrate thickness for the basic geometry

is in the range of 0.01 to 0.05 free-space wavelength. The dielectric constant ranges from 1 to 10 and can be separated into three categories.

- Those having a relative dielectric constant (relative permittivity) in the range of 1.0 to 2.0. This type of material can be air, polystyrene foam, or dielectric honeycomb.
- Those having a relative dielectric constant in the range of 2.0 to 4.0. This type of material consists mostly of Fiber-glass reinforced Teflon.
- Those with a relative dielectric constant between 4.0 and 10.0. This type of material can be ceramic, quartz, or alumnia.

The most commonly used material is Teflon-based with a relative permittivity between 2 and 3. This material is also called PTFE (Poly Tera Fluoro Ethylene). It has a structure very similar to fiberglass material used for digital circuit boards, but has a much lower loss tangent. Cost, power loss, and performance are trade-off considerations in choosing the substrate material, as illustrated by the following examples. For example, a single patch or an array of a few elements may be fabricated on a low-cost fiberglass material at the L band frequency, while a 20-element array at 30 GHz may have to use higher-cost, but lower loss, Teflon-based material (loss tangent less than 0.005). For a large number of array elements at lower microwave frequencies (below 15 GHz), a dielectric honeycomb or foam panel may be used as a substrate to minimize loss, antenna mass, and material cost while having increased bandwidth performance. There are materials with relative dielectric constant higher than 10. The patch size is smaller for higher dielectric constant. However, higher dielectric constant also reduces bandwidth and radiation efficiency.

3.4 Feeding Techniques

I briefly describe here four feeding techniques for the microstrip patch antenna design.

3.4.1 Coaxial Probe Feed

This is possibly the most common feeding method. The geometry is shown in Figure 1.4(a) in chapter 1. The coaxial probe usually has a characteristic impedance of 50 Ω. As will be shown in a later chapter, the input impedance of the patch antenna varies with the feed location. Thus the location of the probe should be at a 50 Ω point of the patch to achieve impedance matching. There are a number of terms associated with the coaxial probe.

Type N, TNC, or BNC connectors are for VHF, UHF, or lower microwave frequencies. OSM or OSSM connectors can be used throughout the microwave frequencies. OSSM, OS-50 or K-connector is for millimeter-wave frequencies.

3.4.2 Microstrip Line Feed

A microstrip patch can be connected directly to a microstrip transmission line, as shown in Figure 1.4(b) in chapter 1. At the edge of a patch, the impedance is generally much higher than 50 Ω. To avoid impedance mismatch, sections of quarter-wavelength transformers can be used to transform large input impedance to a 50 Ω line. Thus another method of matching the antenna impedance is to extend the microstrip line into the patch. With the microstrip-line feed approach, an array of patch elements and their microstrip power division lines can all be designed and chemically etched on the same substrate with relatively low fabrication cost per element. However, the leakage radiation of the transmission lines may be large enough to raise the side lobe or cross-polarized levels of the array radiation.

3.4.3 Proximity Coupled Microstrip Line Feed

An open-ended microstrip line can also be used to feed a patch antenna through proximity coupling, as shown in Figure 1.4(c) in chapter 1. For example, the open end of a 100 Ω line can be placed underneath the patch at its 100 Ω location. An open-ended microstrip line can also be placed in parallel and very close to the edge of a patch, to achieve excitation through fringe-field coupling. Both these methods avoid any soldering connection, which in some cases, could achieve better mechanical reliability.

3.4.4 Aperture Coupled Feed

An open-ended microstrip line can be placed on one side of the ground plane to excite a patch antenna situated on the other side through an opening slot in the ground plane, as shown in Figure 1.4(d) in chapter 1. This slot-coupling or aperture coupling technique can be used to avoid soldering connection was well as to avoid leakage radiation of the line to interfere with the patch radiation. In addition, by using a thick substrate, this feed method allows the patch to achieve a wider bandwidth (>10%) compared to the coax probe feed. Still wider bandwidth (about 20%) is obtained if a resonant slot is used. The main disadvantage of this feeding method is the back radiation from the slot.

3.4.5 Summary of Feeding Methods

Table 3.2 summarizes the advantages and disadvantages of the four feeding methods discussed above.

TABLE 3.2 The comparisons between the four common feeding methods for microstrip patch antenna

Feed	Advantages	Disadvantages
Proximity Coupled	• No direct contact between feed and patch • Can have large effective thickness for patch substrate and much thinner feed substrate	• Multilayer fabrication Required
Microstrip Line	• Monolithic • Easy to fabricate • Easy to match by controlling • Insert position	• Spurious radiation from feed line, especially for thick substrate when line width is significant
Coaxial Feed	• Easy to match • Low spurious radiation	• Large inductance for thick substrate • Soldering required
Aperture Coupled	• Use of two substrates avoids deleterious effect of a high-dielectric constant substrate on the bandwidth and efficiency • No direct contact between feed and patch avoiding large probe reactance • No radiation from the feed and active devices since a ground plane separates them from the radiating patch	• Multilayer fabrication required • Higher back lobe Radiation

In the development of the cavity model, the coaxial-line feed is represented by a cylindrical band of electric current flowing from the ground plane to the patch. To simply matters, this is idealized by assuming that it is equivalent to a uniform current of some effective width, centered on the feed axis.

3.5 Feed Modeling

In the development of the cavity model, the coaxial line feed is represented by a cylindrical band of electric current flowing from the ground plane to the patch. To simply matters, this is idealized by assuming that it is equivalent to a uniform current of some effective width (*w*), centered on the feed axis.

$$\vec{J} = \hat{z}\mathrm{J}(\psi)\,\delta(\rho - \mathrm{d})/\mathrm{d} \tag{3.1}$$

where

δ = Dirac delta function and

J = Current density

d = Length of coaxial line

$$J(\psi) = \begin{cases} \mathrm{J}, & \pi - w < \varphi < \pi + w \\ 0, & elsewhere \end{cases} \tag{3.2}$$

The effective annular width *2w* is a parameter chosen so that good agreement between the theoretical and experimental impedances is obtained. Usually, the arc length *2wd* is several times the physical dimension of the inner conductor.

3.6 Losses in Cavity

The losses in the cavity under the patch comprise dielectric loss (P_d), conductor loss (P_c), radiation loss (P_r) and surface-wave loss (P_{sw}). Surface wave loss represents energy leaving the cavity in the form of waves guided along the dielectric. For thin substrates, P_{sw} can be neglected. According to (C. Wood, 1987), it is required that $t/\lambda_o < 0.07$ for $\varepsilon_r = 2.3$ and $t/\lambda_o < 0.023$ for $\varepsilon_r = 9.8$, if the antenna is to launch no more than 25% of the total radiated power as surface waves. For a given thickness (in terms of wavelength), the higher the dielectric constant, the more the surface wave loss.

The dielectric loss (P_d) and the conductor loss (P_c) are calculated from the electric field under the cavity, while the radiation loss (P_r) is calculated from the far-zone electromagnetic field. A good discussion of these can be found in (R. E. Collin, 1992). They are given by

$$Pd = \frac{\omega\varepsilon\delta}{2}\iiint Ez^2 \; dv \tag{3.3}$$

$$Pc = \frac{2Rs}{2}\iiint H^2 \; ds \tag{3.4}$$

$$\Pr = \frac{1}{2}\int_0^{2\pi}\int_0^{\pi}\frac{E^2}{2\eta 0}r^2 sin\theta d\theta d\phi \tag{3.5}$$

The quantity δ in equation 3.3 is the loss tangent of the dielectric and *Rs* in equation 3.4 is the surface resistivity of the conductors. (The loss tangent is also denoted by tan δ).

The radiation efficiency is the ratio of radiated power to input power

$$e\% = \frac{Pr}{Pc + Pd + Pr} \times 100\% \tag{3.6}$$

In an ideal cavity with lossless walls, the loss tangent and the cavity quality factor *Q* are related by

$$\delta = \frac{1}{Q} \tag{3.7}$$

To take into account the radiation loss and the copper loss, the concept of effective loss tangent is defined as (W. F. Richards, 1981)

$$\delta eff = \frac{1}{Qt} \tag{3.8}$$

$$Qt = \frac{\omega Wt}{Pt} \tag{3.9}$$

$$Pt = Pc + Pd + Pr \tag{3.10}$$

In the formula for calculating the cavity field E_z, δ is to be replaced by δ_{eff}. Since the calculation of the power losses depend on E_z, the definition of the effective loss tangent leads to a nonlinear equation for δ_{eff}.

3.7 Input Impedance

The input impedance at the feed of the antenna is given by

$$\mathrm{Z} = \mathrm{R} + \mathrm{jX} = \frac{\mathrm{V}}{\mathrm{I}} = -\frac{\mathrm{E_{avg}\,t}}{\mathrm{I}} \tag{3.11}$$

where

E_{avg} = Average value of the electric field at the feed point

I = Total current

Z = Structure impedance

R = Structure resistance

X = Structure reactance

Unlike the calculations of δ_{eff}, it was found that non-resonant modes must be included in the calculation of input impedance if good agreement between theory and experiment was to be obtained. To keep this term finite at resonance, the permittivity of the dielectric must be considered complex.

If the feed is modeled by equation 3.1, we have

$$\mathrm{E_{avg}} = \frac{1}{2\omega}\int_{\pi-\omega}^{\pi+\omega} Ez(d,\psi)d\psi \tag{3.12}$$

and $$I = -J(2\omega d) \tag{3.13}$$

However, (W. F. Richards, 1981) found that better agreement with experiment was obtained if, instead of the loss tangent of the dielectric, the effective loss tangent is used. There is usually some reactance at the resonant frequency of a mode due to the contributions from the non-resonant modes.

3.8 Qualitative Description of the Cavity Model

It is instructive to describe here the qualitative features which are common to MPAs. These features follow naturally from viewing the MPA as a leaky cavity.

- There are an infinite number of resonant modes, each characterized by a resonant frequency.
- Because of fringing fields at the edge of the patch, the patch behaves as if it has a slightly larger dimension. Semi-empirical factors are usually introduced to obtain these effective dimensions. These factors vary from patch to patch.
- Each resonant mode has its own characteristic radiation pattern. The lowest mode usually radiates strongest in the broadside direction. The pattern of this mode is broad, with half power beam widths of the order of 100°.
- For coaxial-fed antennas, the input impedance is dependent on the feed position. The variation of input resistance at resonance with feed position essentially follows that of the cavity field. For the lowest mode, it is usually large when the feed is near the edge of the patch and decreases as the feed moves inside the patch. Its magnitude can vary from tens to hundreds of ohms. By choosing the feed position properly, an effective match between the antenna and the transmission line can be obtained.
- Since the cavity under the patch is basically a resonator, the total Q and the impedance bandwidth are dependent on the thickness of the substrate t and its permittivity ε_r. For low values of ε_r, the bandwidth generally increases with increasing t and decreases with increasing ε_r. However, detailed analysis shows that the bandwidth and Q are complicated functions of frequency, substrate thickness and permittivity.
- For thin substrates, the impedance bandwidth varies from less than one to several percent.

3.9 Limitations of the Cavity Model Analysis

Let us recap the assumptions and limitations of the cavity model. The basic assumption which renders the calculations of the cavity model relatively simple is that the substrate thickness is assumed to be much smaller than wavelength so that the electric field has only a vertical (z) component which does not vary with z. From this it follows that:

- The fields in the cavity are TM (transverse magnetic).
- The cavity is bounded by magnetic walls ($H_t = 0$) on the sides.
- Surface wave excitation is negligible.
- The current in the coaxial probe is independent of z.

The coaxial probe is modeled by a current ribbon of a certain width, which is a free parameter chosen to fit the experimental data. There are a number of limitations to the cavity model even if the thin substrate condition is satisfied. The magnetic wall boundary condition leads to resonant frequencies which do not agree well with experimental observations, and an ad hoc correction factor has to be introduced to account for the effect of fringing fields. The width of the current ribbon used to model the coaxial probe is another ad hoc parameter. The model cannot handle designs involving parasitic elements, either on the same layer or on another layer. It cannot analyze microstrip antennas with dielectric covers. When the thickness of the substrate exceeds about 2% of the free space wavelength, the cavity model results begin to become inaccurate, due to the breakdown.

Despite the limitations described above, the cavity model has the advantage of being simple and providing physical insight. The basic characteristics and design information for RMPA can be obtained with relative ease, as shown in the next chapter.

CHAPTER 4

Rectangular MSA Design

4.1 Overview

To be able to design microstrip patch antennas to meet the performance specifications, the antenna engineer should possess a combination of certain knowledge and skills. First, I should have an understanding of the principles of operation of the basic microstrip patch antenna structure. This can be obtained from a physical model known as the cavity model, which is based on a number of assumptions applicable to thin substrates. Within its limitations, the theory provides an understanding of the physical principles and can predict the parametric dependence of a number of antenna characteristics.

In practice, it is rare that the performance specifications can be met by the basic microstrip patch antenna structure. Thick substrates and additional features, such as parasitic patches, shorting pins, or slots in the patch, have to be added. Unfortunately, once the structure departs from the basic geometry, it is not amendable to analysis via a simple model. Maxwell's equations must be solved and boundary conditions satisfied, a procedure known as full wave analysis. Such analysis, while not providing much physical insight, does yield numerical results predicting the performance of the antenna structure.

Throughout the 1980's to the mid 1990's, the patch antenna designer often had to perform full wave analysis for specific designs and developed his own computer code to obtain numerical results for the characteristics of a design, which can be validated by comparison with experiment. Through the efforts of many researchers, a wealth of knowledge has been accumulated for sophisticated structures. This knowledge should be at the disposal of the designer. Beginning in the mid 1990's, electromagnetic simulation softwares capable for

solving general planar microstrip structures became commercially available at moderate costs. Table 4.1 shows a number of commercial electromagnetic simulation softwares.

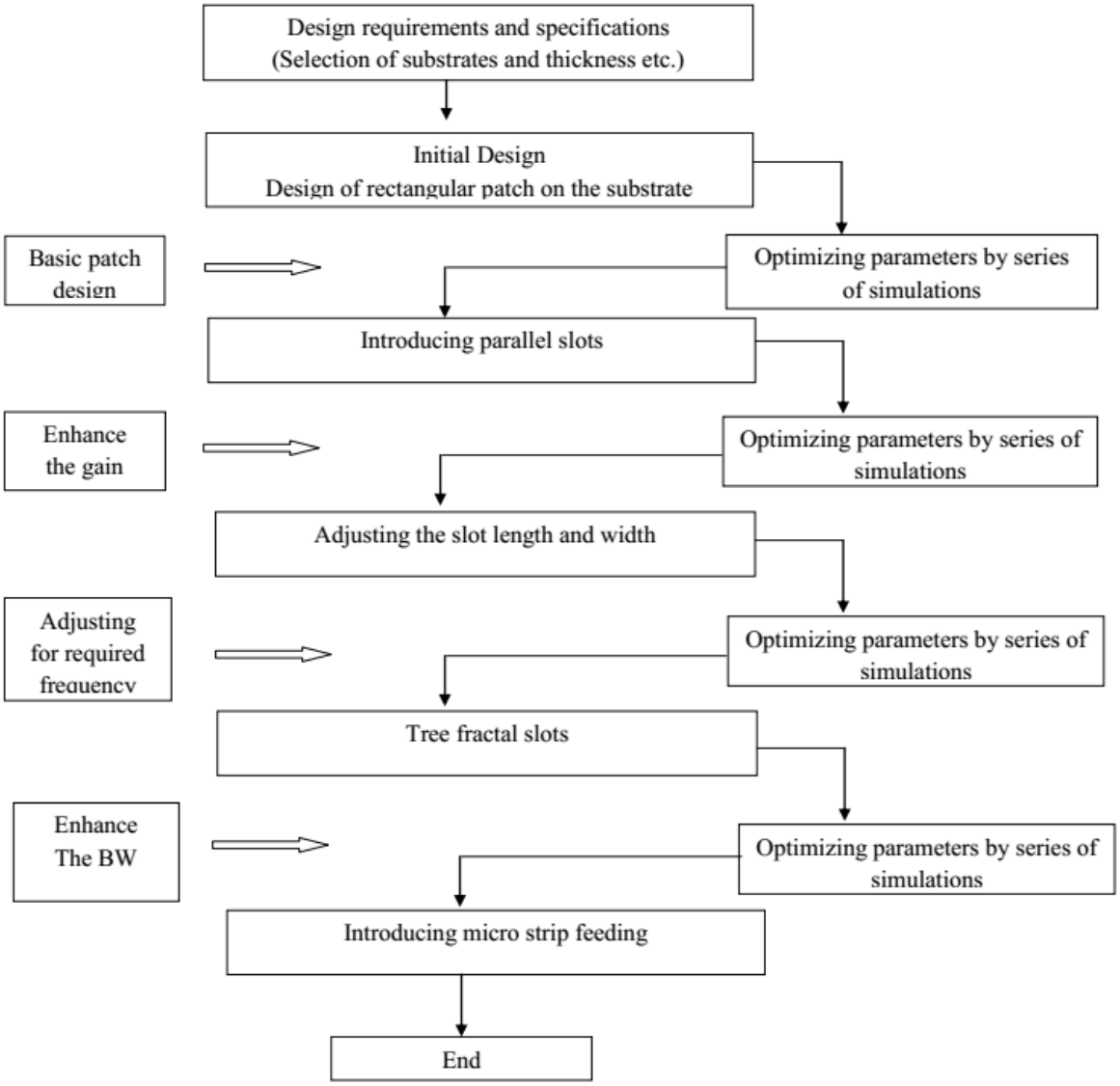

FIGURE 4.1 Antenna design flow chart

One class uses the method of moments (MoM) in the numerical analysis, while another uses the finite difference time domain method (FDTD). HFSS is based on the finite element method and PCAAD is based on the cavity model. The segmentation method used in Micro patch is a variation of the cavity model. Figure 4.1 illustrates the design process, adapted from the concept and also discussed in chapter 2.

TABLE 4.1 List of commercial electromagnetic simulation softwares (John Wiley & Sons, 2008)

Software Name	Theoretical model	Company
Ensemble	Moment method	Ansoft
PCAAD	Cavity model	Antenna Design Associates
Micropatch	Segmentation	Microstrip Design, Inc.
Microwave Studio	FDTD	CST
Fidelity	FDTD	Zeland
HFSS	Finite element	Ansoft

Finally, the antenna designer should have the skills to fabricate the design and verify the predicted performance from measurements.

4.2 Radiation Mechanism

At first glance it might seem surprising that a microstrip antenna can operate very well at all, since it consists of a horizontal electric surface current suspended (via the substrate) a short distance above a ground plane. Basic image theory predicts that such a current will not radiate very well. However, the microstrip patch and the ground plane together form a resonant cavity (filled with the substrate material). The cavity is lossy, due not only to the material (conductor and dielectric) loss, but also to the (desirable) radiation into space. Neglecting material loss, the quality factor *Q* of the antenna is inversely proportional to the substrate thickness h, for a given substrate material, assuming the substrate is thin. Hence the bandwidth is proportional to h. The field level inside the patch cavity at resonance from an impressed current source inside the cavity (e.g., a fixed probe current) is proportional to Q. This means that the surface current on the patch (which is mainly on the lower surface of the patch) is inversely proportional to *h*. This increase in the amplitude of the surface current at resonance as the substrate gets thinner exactly balances the image effect, which causes the radiation level to be reduced by a factor proportional to h (relative to the patch current radiating without the ground plane). From another point of view, the voltage at the edges of the patch (the electric field times h) for a resonant patch remains approximately independent of h as the substrate gets thinner. Hence, both the electric and magnetic current models (discussed later) predict that the

radiation from the patch remains approximately independent of h as the substrate thickness decreases.

Therefore, without material losses, the patch remains a good radiator even for very small substrate thicknesses, and it is possible to obtain a good impedance match even for a very thin substrate. In the lossless case the lower limit on the substrate thickness would only be determined by the bandwidth one is willing to accept. In actuality, the *Q* is limited by the material losses, so for sufficiently thin substrates it becomes difficult to obtain a good impedance match (in this region the radiation efficiency will also be poor). However, even for substrates as thin as $0.005\lambda_0$ a good match may be obtained with a reasonable efficiency of around 65 percent for a typical Teflon substrate and copper conductors.

For the rectangular patch, the TMm_n mode has a normalized electric field that is given by

$$E_z^{mn}(x,y) = cos\left(\frac{m\pi x}{L}\right) cos\left(\frac{n\pi y}{W}\right) \tag{4.1}$$

The usual mode of operation for a broadside pattern is the TM_{10} mode, which has no y variation and has a length *L* that is approximately one half wavelengths in the dielectric. In this mode the patch essentially acts as a wide microstrip line of width *W* that forms a transmission line resonator of length *L*. The width W is usually larger than the length L in order to increase the bandwidth. A ratio $W/L = 1.5$ is typical.

For the circular patch, the TM_{np} mode has a normalized electric field that is given by

$$E_z(\rho,\phi) = \cos(n\phi)\frac{\left(J_n\frac{x_{np}\rho}{a}\right)}{J_n(x_{np})} \tag{4.2}$$

where

E = Electric field intensity

$J_n(x)$.= Bessel function

x_{np} = The p^{th} root of the Bessel function $J_n(x)$.

The usual mode of operation is the TM_{11} mode with x_{11}=1.8418. This mode has the lowest resonance frequency and has a broadside pattern.

4.3 CAD Model for Input Impedance

The patch cavity resonator is modeled as a parallel RLC circuit (tank circuit), and the inductance due to the coaxial feed probe is modeled as the series inductor *Lp*. A justification for this model comes from an eigen function analysis of the input impedance (Y. T. Lo, D. Solomon, 1979).

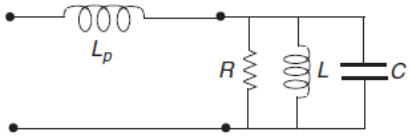

FIGURE 4.2 CAD equivalent tank circuit

From simple circuit theory, the input impedance of the patch is then given by

$$Z_{in} = j\omega L_p + \frac{R}{1 + jQ(f_R - \frac{1}{f_R})} \tag{4.3}$$

where

f_R = Frequency ratio (f / f_0)

f_0 = Resonance frequency

This is not the same as the impedance resonance frequency of the patch (the frequency for which the input reactance is zero), denoted as f_r, due to the presence of the probe inductance. The term R represents the input resistance of the patch at the cavity resonance frequency f_0 (f_R = 1), at which the input resistance is a maximum. At the impedance resonance frequency f_r the input resistance will be slightly lower than the maximum value R according to the approximate formula 4.4.

$$R_{in} = \frac{R}{1 + (\frac{x_p}{R})^2} \tag{4.4}$$

where

$X_p = w_0 L_p$ is the probe reactance.

The probe reactance shifts the impedance resonance up from the cavity resonance by an amount $\Delta f = f_r - f_0$ given by the approximate formula given by equation 4.5.

$$\frac{\Delta f}{f_0} = (BW)\left(\frac{1}{\sqrt{2}}\right)\left(\frac{x_p}{R}\right) \tag{4.5}$$

where

$$BW = \frac{1}{\sqrt{2}Q} \tag{4.6}$$

The input impedance of the tank circuit (the second term on the right-hand side of equation 4.3 along with its real and imaginary parts may be written in a normalized form as

$$\bar{Z}_{RLC} = \frac{1}{1 + jx} \tag{4.7}$$

$$\bar{R}_{RLC} = \frac{1}{1 + x^2} \tag{4.8}$$

$$\bar{X}_{RLC} = \frac{-x}{1 + x^2} \tag{4.9}$$

where

$$x = Q\left(f_R - \frac{1}{f_R}\right) \approx 2Q(f_R - 1) \tag{4.10}$$

is a normalized frequency term, and the bars over the impedance symbols denote that they have been normalized by dividing the impedances by *R*.

The equations in equation 4.7 to 4.9 predict that the input resistance reaches a maximum of $R_{in} = R$ at the frequency f_0 ($x=0$), while the magnitude of the reactance is maximum at $x = \pm 1$, for which $X_{in} = \mp R/2$. At f_0 the input impedance of the patch is simply $Z_{in} = R + jX_p$.

Using the CAD circuit model, the input impedance is plotted versus frequency for a typical rectangular patch using the CAD formulas for the parameters of the circuit model given in the next section. This patch is designed to have an input resistance of $R = 50\ \Omega$

at multiple resonant frequency. The substrate has a relative permittivity of ε_r = 2.2, a loss tangent of 0.001, and a thickness of h = 0.6 mm and an aspect ratio of W/L = 1.5. The ground plane and patch each have a conductivity of 3.0×10^7 S/m. The feed is an SMA coax with a probe radius a = 0.635 mm that is located at x_0 = 1.85 cm and $y_0 = W/2$. Note that the impedance resonance (X_{in} = 0) is shifted to a slightly higher frequency than the cavity resonance (where R is maximum), as expected, and the input reactance of the patch at f_0 is about 10 Ω due to the probe reactance. The difference between the maximum and minimum values of the reactance curve is about the same as the value of R, as expected from equation 4.7 to 4.9. Taking the average of the maximum and minimum reactances provides an easy way to determine the probe reactance.

For this typical substrate thickness (h/λ_0 = 0.008), the simple CAD circuit model, together with the CAD formulas in the next section, works fairly well. For thicker substrates the circuit model will lose accuracy. The model is typically useful in the range $h/\lambda_0 < 0.03$. More sophisticated input impedance models include the transmission line model (A. G. Derneryd, 1976) and the cavity model (Y. T. Lo, D. Solomon, 1979). However, these models are based on the same thin substrate approximation as are the circuit model and the CAD formulas given in the next section, so the improvement in accuracy is questionable. For thicker substrates a full-wave simulator is recommended for maximum accuracy.

4.4 Design Formula for RMPA

This section presents CAD formulas for the rectangular patch shown in Figure 1.1. All of the formulas are independent of the feed except for the input resistance formula, which assumes a coaxial feed. All of these formulas assume that the patch is operating at the resonance of the TM_{10} mode, which is the usual mode of broadside operation (K.F. Lee, 1997).

4.4.1 Resonance Frequency

A fairly simple, yet reasonably accurate formula due to (E. O. Hammerstad, 1975) is

$$f_0 = \frac{c}{2(L + 2\Delta L)\sqrt{\varepsilon_r}} \tag{4.11}$$

Where c is the speed of light in vacuum and the fringing extension added to the resonant (L) dimension is given by

$$\frac{\Delta L}{h} = \frac{0.412(\varepsilon_{eff} + 0.3)\left(\frac{W}{h} + 0.264\right)}{(\varepsilon_{eff} - 0.258)\left(\frac{W}{h} + 0.8\right)} \tag{4.12}$$

with

$$\varepsilon_{eff} = \frac{\varepsilon_r + 1}{2} + \frac{(\varepsilon_r - 1)\left(1 + 10\frac{h}{W}\right)^{-\frac{1}{2}}}{2} \tag{4.13}$$

In some references ε_{eff} is used instead of ε_r in equation 4.11, but according to the discussion in (K. F. Lee (ed.), 1997) using ε_r usually gives more accurate results.

4.4.2 Quality Factor

For a resonant type of antenna such as the microstrip antenna, it is common to express the physical parameters of interest in terms of the quality factor, or *Q*, of the antenna. The *Q* factor is defined as

$$Q = \omega_0 \left(\frac{U_s}{P_{in}}\right) \tag{4.14}$$

where $\omega_0 = 2\pi f_0$ is the resonance frequency in radian/s, *Us* is the energy stored inside the patch cavity, and *Pin* is the average power going into the antenna, which is equal to the average power being radiated plus dissipated. A microstrip antenna has both dielectric and conductor losses, and possibly surface-wave loss as well.

The surface-wave loss depends on the environment surrounding the patch. If there is a substrate that surrounds the patch and the surface-wave power launched by the antenna is gradually dissipated by an absorber, then the power launched into the surface wave by the patch is a loss. On the other hand, if the substrate is truncated so that there is no substrate beyond the perimeter of the patch, then there will be no surface-wave loss. If the substrate extends beyond the patch but then ends at some distance away, the propagating surface wave will diffract at the edge of the substrate and convert into a radiation field.

In this case the surface wave power is not actually a loss, but the diffracted fields will typically result in pattern degradation.

The total quality factor is related to the component quality factors as

$$\frac{1}{Q} = \frac{1}{Q_{sp}} + \frac{1}{Q_{sw}} + \frac{1}{Q_d} + \frac{1}{Q_c} \tag{4.15}$$

where

$$Q_i = \omega_0 \left(\frac{U_s}{P_i}\right) \tag{4.16}$$

The Q_{sp} , Q_{sw}, Q_d, and Q_c denote the space-wave, surface-wave, dielectric, and conductor quality factors corresponding to the powers radiated into space, launched into the fundamental TM_0 surface-wave, dissipated by dielectric loss, and dissipated by conductor loss, respectively.

$$Q_d = \frac{1}{tan\delta} \tag{4.17}$$

If the ground plane and patch metal have surface resistances R_{sg} and R_{sp} denotes the average of the two, then the conductor Q factor is given by

$$Q_c = \mu_r \left(\frac{\eta_0}{2}\right)\left(\frac{k_0 h}{R_s^{ave}}\right) \tag{4.18}$$

The surface resistance is related to the conductivity of the metal σ and the skin depth δ as

$$R_s = \frac{1}{\sigma\delta} \tag{4.19}$$

with

$$\delta = \sqrt{\frac{2}{\omega\mu_0\sigma}} \tag{4.20}$$

Space wave *Q* factor that accounts for the (desired) radiation into space is given as

$$Q_{sp} = \frac{3}{16}\left(\frac{\varepsilon_r}{p_1 c_1}\right)\left(\frac{L_e}{W_e}\right)\left(\frac{1}{h/\lambda_0}\right) \tag{4.21}$$

Where $L_e = L + 2\Delta L$ and $W_e = W + 2\Delta W$ are the effective lengths and widths of the patch, accounting for fringing. The fringing length is given by equation 4.12, while the fringing width is given approximately by (H. A. Wheeler, 1965)

$$\Delta W = h\left(\frac{ln4}{\pi}\right) \tag{4.22}$$

The terms p_r and c_1 are geometry terms given by (K. F. Lee (ed.), 1997)

$$p_r = 1 + \frac{a_2}{10}(k_0 W_e)^2 + (a_2^2 + 2a_4)\left(\frac{3}{560}\right)(k_0 W_e)^4 + c_2\left(\frac{1}{5}\right)(k_0 L_e)^2 + c_2 a_2\left(\frac{1}{70}\right)(k_0 W_e)^2 (k_0 L_e)^2 \tag{4.23}$$

$$c_1 = 1 - \frac{1}{n_1^2} + \frac{2/5}{n_1^4} \tag{4.24}$$

Where

$n_1 = \sqrt{\varepsilon_r \mu_r}$ is the index of refraction of the substrate.

The other constants are

a_2 = - 016605

a_4 = 0.00761

c_2 = - 0.0914153

Assuming that the substrate is infinite (or that there is an absorber to absorb the surface wave), so that surface-wave power is a loss from the antenna radiation point of view, the surface wave excitation represents a loss mechanism, and the *Q* for this loss is given by

$$Q_{sw} = Q_{sp}\left(\frac{e_r^{sw}}{1 - e_r^{sw}}\right) \tag{4.25}$$

Where, e_r^{sw} denotes the radiation efficiency of the patch when accounting for only surface wave loss, and not dielectric or conductor loss.

$$e_r^{sw} = \frac{P_{sp}}{P_{sp} + P_{sw}} \tag{4.26}$$

Where P_{sp} is the power radiated into space and P_{sw} is the power launched into the surface wave. This efficiency is well approximated by that of a unit amplitude infinitesimal horizontal electric dipole (hed) on the substrate. (Unit amplitude means *Il* = 1, with the current amplitude expressed using peak phasor notation, not rms, and the length *l* of the small dipole measured in meters.) Therefore this efficiency is given by

$$e_r^{sw} = e_r^{hed} = \frac{P_{sp}^{hed}}{P_{sp}^{hed} + P_{sw}^{hed}} \tag{4.27}$$

A calculation that is accurate for thin substrates reveals that

$$P_{sp}^{hed} = \frac{1}{\lambda_0^2}(k_0 h)^2 (80\pi^2 \mu_r^2 c_1) \tag{4.28}$$

and

$$P_{sw}^{hed} = \frac{1}{\lambda_0^2}(k_0 h)^3 \left[60\pi^3 \mu_r^3 \left(1 - \frac{1}{n_1^2}\right)^3\right] \tag{4.39}$$

which, results in the expression

$$e_r^{sw} = \ e_r^{hed} = \frac{1}{1 + (k_0 h)\left(\frac{3\pi}{4}\right)\mu_r \frac{1}{c_1}\left(1 - \frac{1}{n_1^2}\right)^3} \tag{4.30}$$

$$P_{sw}^{hed} = \frac{\eta_0 k_0^2}{4} \frac{\varepsilon_r (x_0^2 - 1)^{\frac{3}{2}}}{\varepsilon_r [1 + x_1] + (k_0 h)\sqrt{x_0^2 - 1}[1 + \varepsilon_r^2 x_1]} \tag{4.31}$$

where

$$x_1 = \frac{x_0^2 - 1}{\varepsilon_r - x_0^2} \tag{4.32}$$

$$x_0 = 1 + \frac{-\varepsilon_r^2 + \alpha_0 \alpha_1 + \varepsilon_r \sqrt{\varepsilon_r^2 - 2\alpha_0 \alpha_1 + \alpha_0^2}}{(\varepsilon_r^2 - \alpha_1^2)} \tag{4.33}$$

For nonmagnetic substrates, a more accurate expression that has been found by (D. M. Pozar, 1990) for the surface wave power of the unit amplitude dipole is shown above equations.

with

$$\alpha_0 = s\tan[(k_0 h)s] \tag{4.34}$$

$$\alpha_1 = -\frac{1}{s}\left[\tan(k_0 h)s + \frac{(k_0 h)s}{\cos[(k_0 h)s]^2}\right] \tag{4.35}$$

and

$$s = \sqrt{\varepsilon_r - 1} \tag{4.36}$$

The result is more accurate using equation 4.31 and 4.28 in equation 4.26 than equation 4.30, especially for thicker substrates.

4.4.3 Bandwidth and Radiation Efficiency

The bandwidth of the patch may be defined from the frequency limits at which the standing wave ratio (SWR) reaches a maximum threshold, assuming that the feeding transmission line that connects to the patch is perfectly matched at the resonance frequency (i.e., $Z_0 = R$, if we neglect the effects of the probe inductance). The bandwidth is thus defined as

$$BW = \frac{f_2 - f_1}{f_r} \tag{4.37}$$

where

f_r = The impedance resonance frequency of the patch

f_1 = Low frequency on either side of the resonance frequency at $SWR = S$

f_2 = High frequency on either side of the resonance frequency at $SWR = S$

The bandwidth is then

$$BW = \frac{S-1}{\sqrt{S}Q} \tag{4.38}$$

For the commonly used definition $S = 2$, we have

$$BW = \frac{1}{\sqrt{2}Q} \tag{4.39}$$

The radiation efficiency is the ratio of power radiated into space to the total power input to the antenna. That is,

$$e_r = \frac{P_{sp}}{P_{in}} \tag{4.40}$$

where

$$P_{in} = P_{sp} + P_{sw} + P_d + P_c \tag{4.41}$$

In terms of the Q factors,

$$e_r = \frac{Q}{Q_{sp}} \tag{4.42}$$

4.4.4 Input Resistance and Probe Inductance

The resistance R in the circuit model of Figure 4.2 represents the input resistance of the patch at the cavity resonance frequency f_0 where the input resistance is a maximum. An approximate expression for R is

$$R = R_{edge} \cos\left(\frac{\pi x_0^e}{L_e}\right)^2 \tag{4.43}$$

Where the input resistance when fed at the edge ($x_0 = 0$) is

$$R_{edge} = \eta_0 \mu_r \left(\frac{4}{\pi}\right)\left(\frac{L_e}{W_e}\right)\left(\frac{h}{\lambda_0} Q\right) \tag{4.44}$$

The effective feed location at, $x_0^e = x_0 + \Delta L, y_0^e = y_0 + \Delta W$, accounts for fringing.

A simple yet reasonably accurate formula for the probe inductance L_p in the circuit model of Figure 4.2 may be found by assuming that the coaxial probe feeds an infinite parallel plate waveguide (H. Xu, D. R. Jackson, and J. T. Williams, 2005). A calculation then reveals that the probe reactance is given by

$$X_p = \omega L_p = \eta_0 \mu_r \left(\frac{h}{\lambda_0}\right)\left[-\gamma + \ln\left(\frac{2}{\sqrt{\mu_r \varepsilon_r} k_0 a}\right)\right] \tag{4.45}$$

Where γ = 0.57722 is Euler's constant. The probe inductance is not independent of frequency, due to the wave number term that appears inside the argument of the natural logarithm function. The probe reactance is directly proportional to the substrate thickness. The probe reactance also increases as the probe radius decreases, but the reactance is not a strong function of the probe radius since the variation is logarithmic. For a typical substrate with ε_r = 2.2 and h = 0.1524 cm and a probe radius of a = 0.635 mm (SMA), the probe reactance X_p at 1.575 GHz is about 11 Ω.

4.4.5 Directivity

The directivity of the rectangular patch (with respect to an isotropic radiator) may be approximated in closed form for thin substrates as

$$D = \left(\frac{\eta_0}{40\pi}\right)\left(\frac{1}{p_r c_1}\right)\left[\frac{\tan c^2(k_0 h n_1)}{1 + \left(\frac{\mu_r}{\varepsilon_r}\right) tan^2(k_0 h n_1)}\right] \tag{4.46}$$

where

$$tanc(x) = \tan(x)/x \tag{4.47}$$

For a moderate permittivity substrate such as ε_r = 2.2, the directivity is about 6.1 (7.8 dB) when the substrate is thin. For a high permittivity substrate such as ε_r = 10.8, the directivity is about 3.5 (5.4 dB) when the substrate is thin.

4.4.6 Bandwidth Improvement

The bandwidth of a microstrip antenna may be improved in several ways. First, the use of a low permittivity substrate is beneficial since bandwidth is inversely proportional to the permittivity according to equation 4.21, at least when the patch is operating in a region where the efficiency is high and the space wave Q is dominant (the smallest). Second, a thicker substrate may be used since the bandwidth is proportional to the substrate thickness in the region where the space wave Q dominates, as equation 4.21 again shows.

For a coaxial feed, the bandwidth is limited by the fact that the probe inductance increases with increasing substrate thickness, as seen from equation 4.43. As mentioned in the "Introduction," this limits the substrate thickness to a maximum value, beyond which the coaxially fed patch will not be resonant (i.e., the input impedance will remain inductive). According to equation 4.7 to 4.10 and the discussion immediately afterward, the input reactance of the patch cavity reaches a negative minimum of $X_{RLC} = -R/2$, where R is the value of the maximum input resistance, which occurs at the cavity resonance frequency f_0. Hence if the probe reactance exceeds $R/2$, no resonance frequency f_r can be found for which the input impedance will be real.

Various methods may be used to overcome this limitation due to the probe reactance. A capacitive element may be inserted into the coaxial feed to compensate for the probe reactance. For example, one can use a capacitive annular slot on the patch that surrounds the contact point where the probe meets the patch (P. S. Hall, 1987).

Alternatively, other feed methods may be used that avoid the probe reactance problem. For example, the aperture-coupled feed allows for the patch cavity to be excited without introducing a probe reactance, and hence a thicker substrate is possible.

Other techniques to increase bandwidth include introducing multiple resonances into the structure. This may take the form of stacked patches, coplanar parasitic patches, or patches that have novel shapes such as the U-shaped patch (G. Kumar and K. P. Ray, 2002 and K.L. Wong, 2003). Using special feed networks or feeding techniques to compensate for the natural impedance variation of the patch is another method.

4.4.7 Efficiency Improvement

Surface-wave excitation increases as the permittivity of the substrate increases and as the thickness of the substrate increases (unless the substrate is air). On the other hand, if the substrate is made too thin, the radiation efficiency suffers due to increased conductor and dielectric losses, since the conductor and dielectric *Q* factors will become dominant (smaller than the other ones) as the substrate becomes thin, as seen from equation 4.17 and 4.18. One way to overcome this trade off is to use a low-permittivity substrate material such as foam. The foam substrate may be made thick to minimize conductor and dielectric losses, without suffering from surface-wave excitation. This has the added advantage of increasing the bandwidth. If the application allows it, the substrate may also be removed from the area outside the patch, to avoid surface-wave excitation.

Other alternatives have been developed for minimizing surface-wave excitation. The ground plane may be patterned to form a periodic structure, or a periodic structure may be printed on the substrate surrounding the patch, to form an electromagnetic band gap (EBG) structure (H. Y. D. Yang, R. Kim, and D. R. Jackson, 2000). Being a periodic structure, the EBG structure has pass bands and stop bands, for which modal surface wave propagation on the structure is allowed or prohibited. In the stopband region the surface wave on the structure cannot propagate. Care must be exercised to design the EBG structure so that the stopband is omnidirectional, meaning that the surface wave propagation is prohibited in all directions.

4.4.8 Frequency and Impedance Scaling of RMSA

Whether one designs an RMSA using simple design equations or using any sophisticated software, the experimental results do not always perfectly match with the theoretical results.

There could be several reasons:

- Theoretical modeling is not 100% accurate.
- There could be a fabrication error in the dimensions and the probe position.
- There could be tolerance in ε_r and h of the substrate.

These would result in frequency deviation and mismatch in the input impedance. The deviation in the frequency can be taken care of by either using the frequency tuning methods described in Chapter 3 or by fabricating another RMSA. For fabricating another RMSA, its required length can be calculated by simply using the frequency scaling concept which is given bellow as

$$L_{required} = \frac{L_{measured} \times f_{measured}}{f_{required}} \tag{4.48}$$

Similarly, width can be scaled. If the measured input impedance Z_{in} is not matched, then the probe position x is to be changed. The new position x_{new} for the required input impedance Zrequired can be obtained as

$$Z_e = \frac{Z_{in}}{sin^2(\beta x)} \tag{4.49}$$

$$Z_{required} = Z_e sin^2(\beta x_{new}) \tag{4.50}$$

This simplified to

$$x_{new} = (1|\beta)\sin^{-1}\sqrt{(Z_{required}|Z_{in})sin^2(\beta x)} \tag{4.51}$$

where

$$\beta = \frac{2\pi}{\lambda} \tag{4.52}$$

By fabricating another antenna with dimensions obtained using equation 4.46 and 4.47, the measured values should match with the desired resonance frequency and input impedance values.

4.4.9 Result and Discussion

The aim of this RMPA structure is to design the microstrip patch antennas (which are commonly used for satellite, cellular and almost every wireless communications

application due to their small size, low cost and effective other properties) using the HFSS simulator as per following design consideration.

- Frequency of Operation (f_r)
- Selection of Dielectric material (ε_r)
- Substrate height (h), width (W) and length (L)
- Structure

TABLE 4.2 RMPA design parameters

Frequency f_r (GHz)	**ε_{reff}**	**Height h (mm)**	**Width W (mm)**	**ΔL (mm)**	**Length L (mm)**
2.0	2.03	1.6	60.24	0.85	2.56
2.5	2.02	1.6	48.19	0.85	3.62
3.0	2.00	1.6	40.16	0.85	4.66
3.5	1.99	1.6	34.42	0.85	5.71
4.0	1.98	1.6	30.12	0.85	6.74
4.5	1.97	1.6	26.77	0.85	7.78
5.0	1.96	1.6	24.10	0.85	8.81
5.5	1.95	1.6	21.91	0.84	9.84
6.0	1.94	1.6	20.08	0.84	10.86
6.5	1.94	1.6	18.54	0.84	11.88
7.0	1.93	1.6	17.21	0.84	12.90
7.5	1.92	1.6	16.06	0.84	13.92
8.0	1.91	1.6	15.06	0.83	14.93
8.5	1.91	1.6	14.17	0.83	15.95
9.0	1.90	1.6	13.39	0.85	12.51

The input parameters are calculated according to equations 4.11 to 4.13 and resonant frequency based on specific application.

Substrate height is in the range of $0.002\lambda_0 \leq h \leq 0.05\lambda_0$ (minimum, medium and maximum) and as per formula. Finally selection of width, length and height of substrate as per bellow Table 4.2 and structure design consideration shown in Figure 4.3.

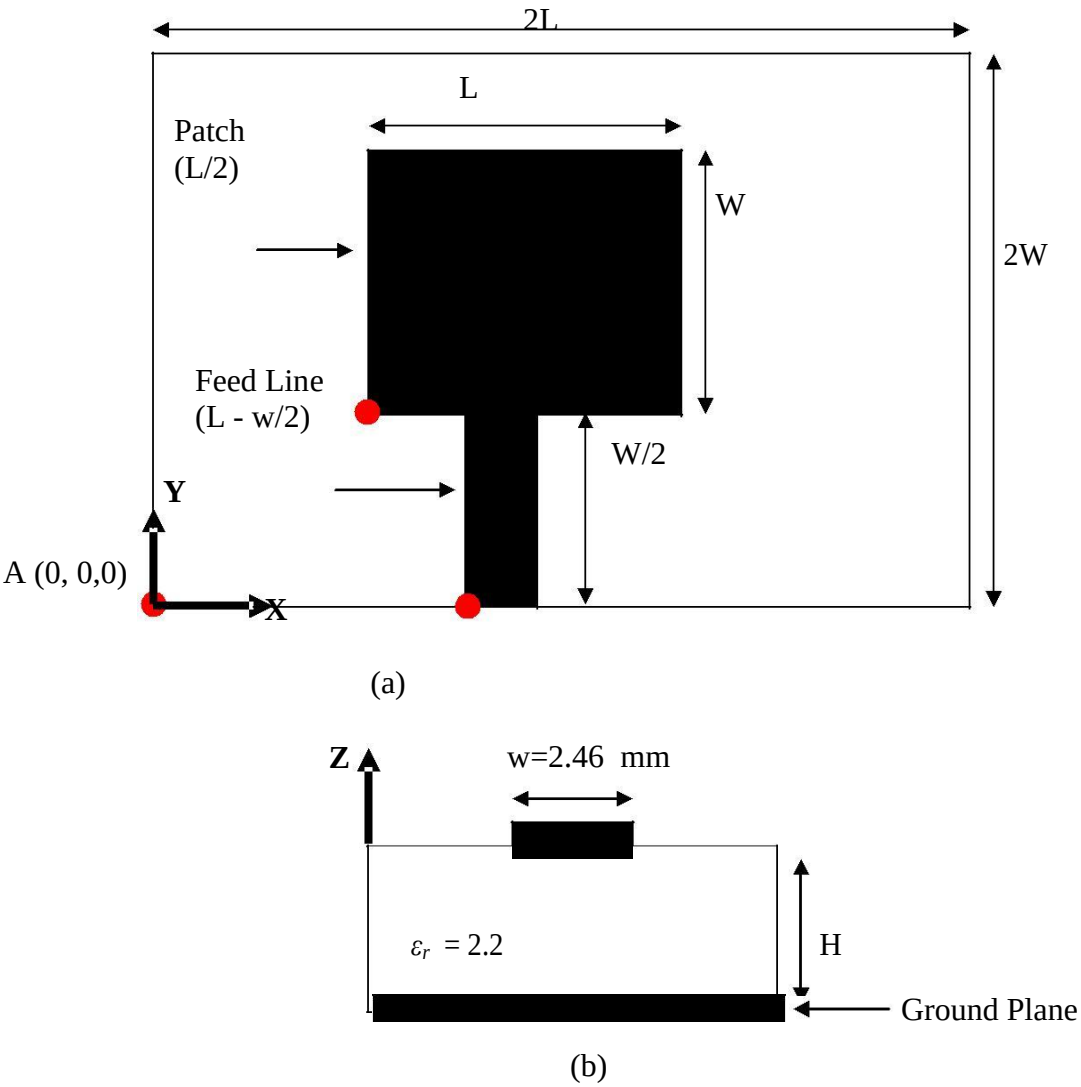

FIGURE 4.3 RMPA design structure (a) Top view and (b) Cross view

TABLE 4.3 RMPA design geometry

Block	Substrate	Feed line	Patch	Ground plane	Boundary
Position	0,0,0	L-(w/2),0,0	L/2,W/2,0	0,0,-h	-5,-5,-5-h
X	2L	W	L	2L	≥2L
Y	2W	W/2	W	2W	≥2W
Z	-h	0.05	0.05	-0.05	10+h

Dimension of substrate, feed line, patch, ground plane and boundary as per geometrical parameter listed in Table 4.3. Result of 25×30 mm RMPA are compare according to design flow shown Figure 4.1 in term of feeding methods and materials effect. The minor different in results of VSWR (0.034), BW (1.3%) and Return loss (1.64 dB) of RMPA design using Teflon material instead of FR4 but gain is 4.2 dB higher which is shown in Figure 4.4 to 4.6 and listed in Table 4.4.

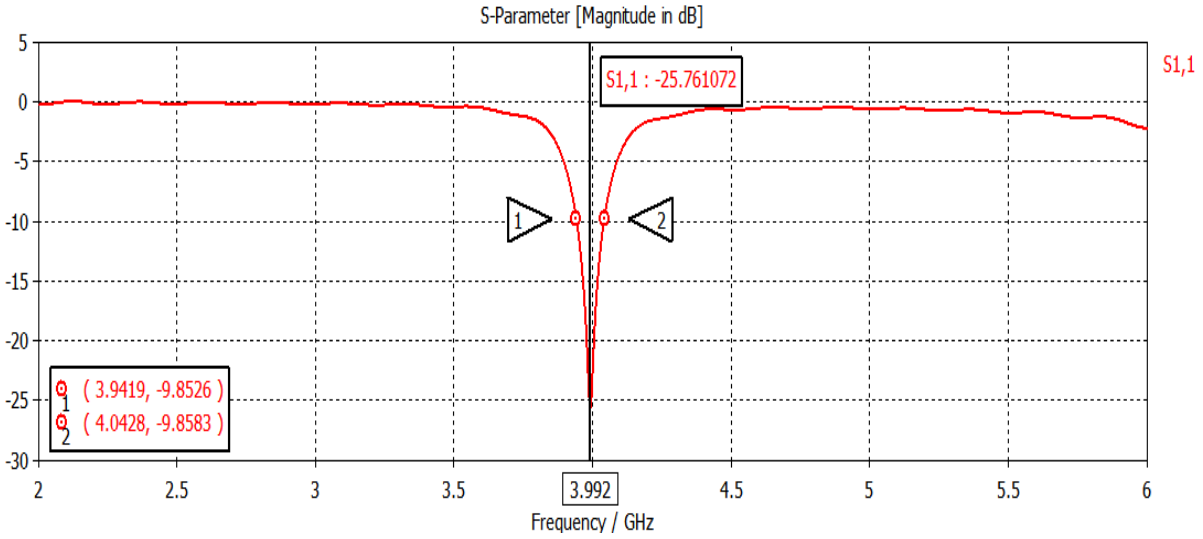

(a)

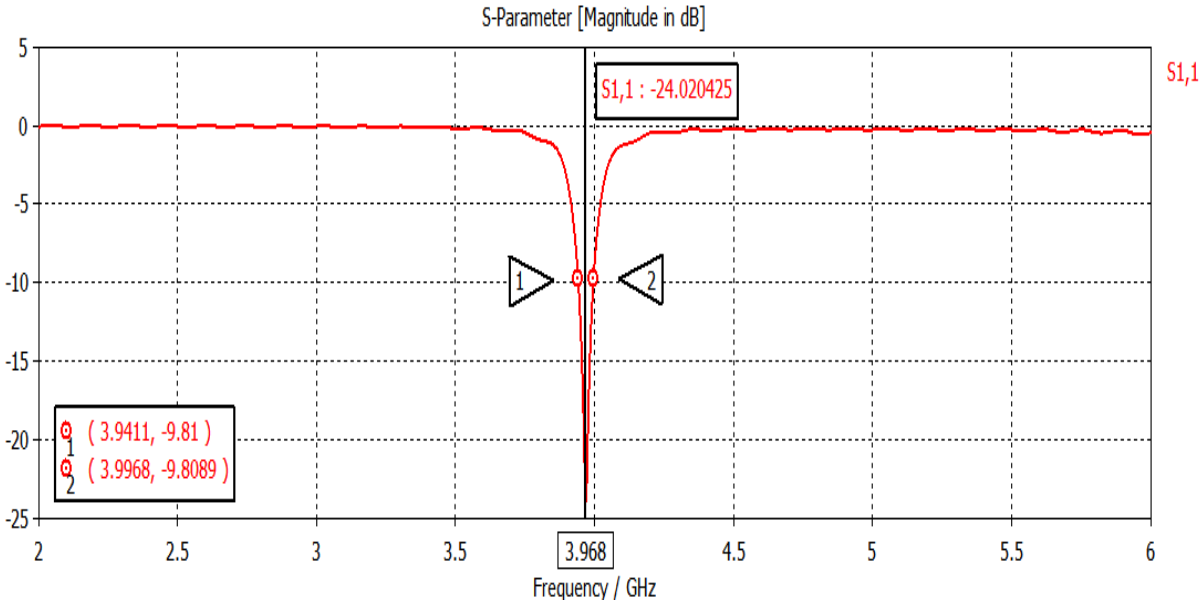

(b)

FIGURE 4.4 Return loss and bandwidth plot with ground plane (a) FR4 (b) Teflon

TABLE 4.4 Parameters comparison of FR4 and Teflon materials for RMPA

Material	Return Loss(dB)	VSWR	Bandwidth (MHz)	Bandwidth (%)	Gain (dB)
FR4	-25.7610	1.1086	0.1009	2.52	3.3
Teflon(PTFE)	-24.0204	1.1343	0.0557	1.39	7.5

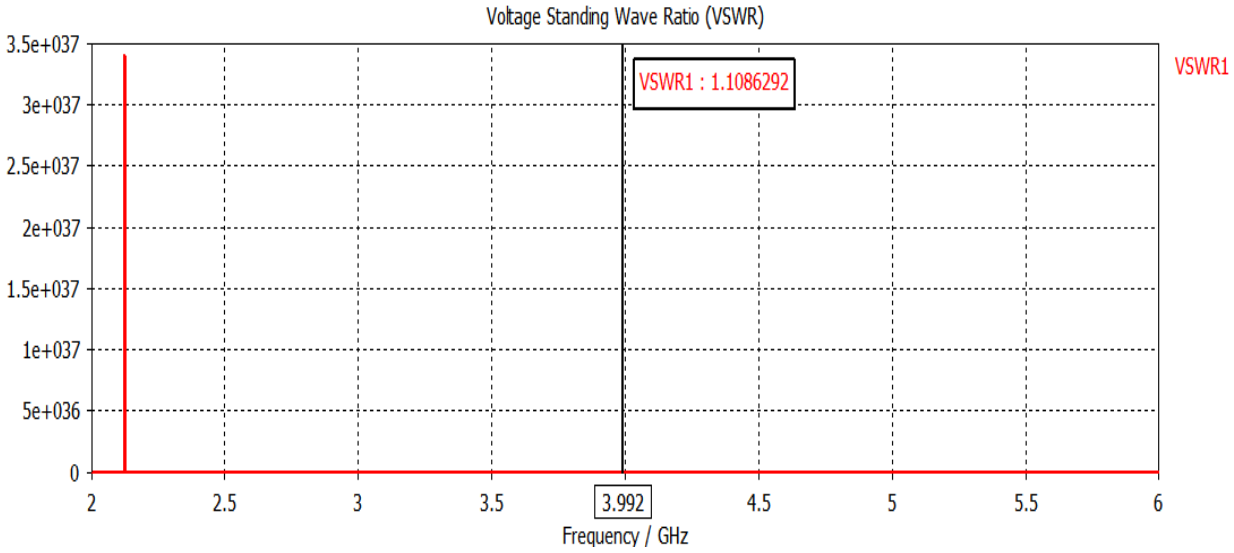

(a)

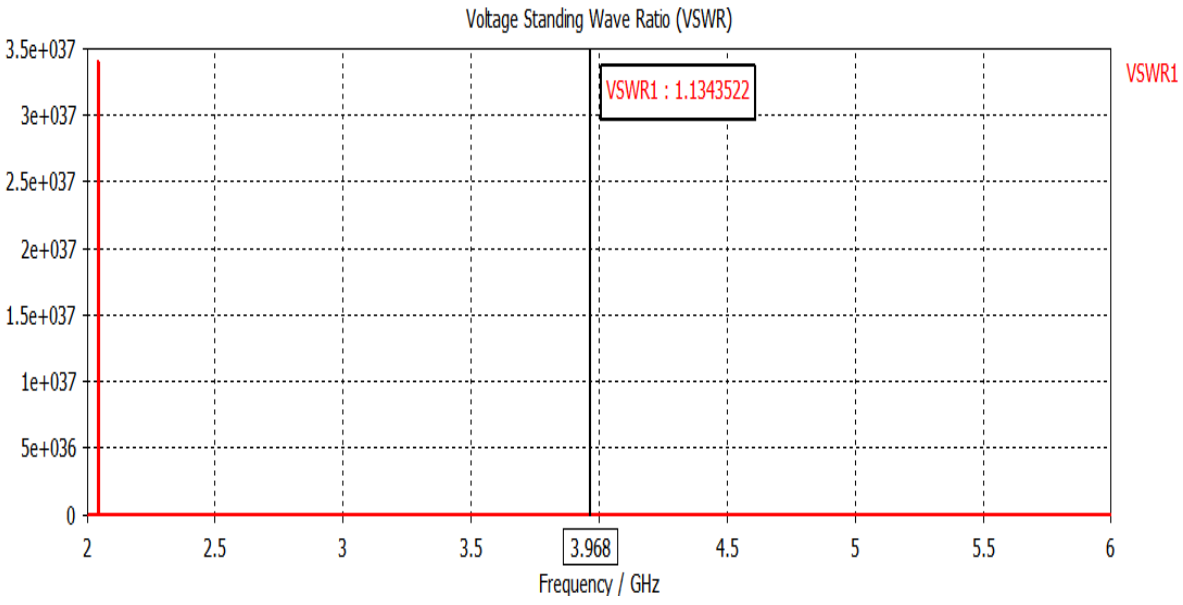

(b)

FIGURE 4.5 VSWR plot with ground plane (a) FR4 (b) Teflon

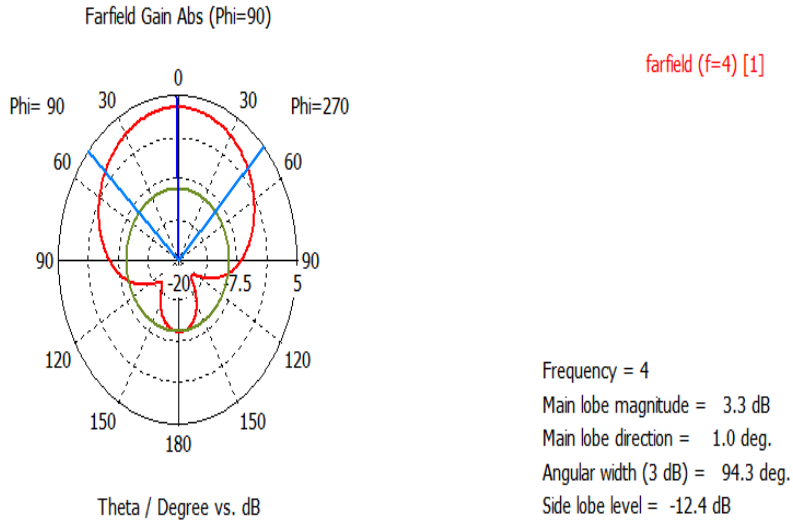

(a)

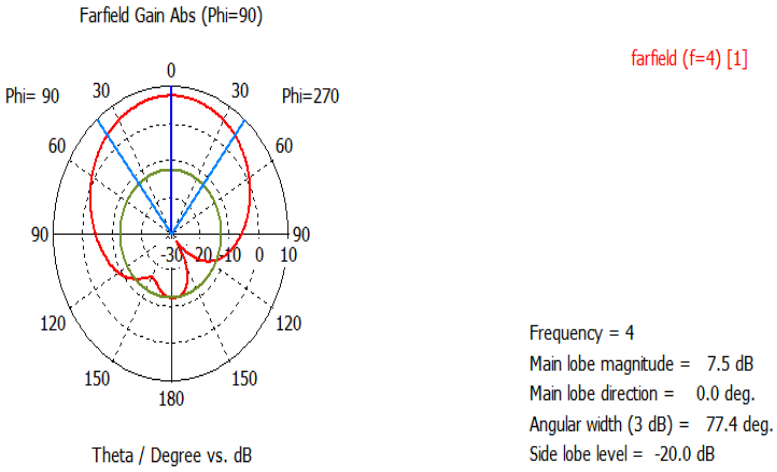

(b)

FIGURE 4.6 Gain plot with ground plane (a) FR4 (b) Teflon

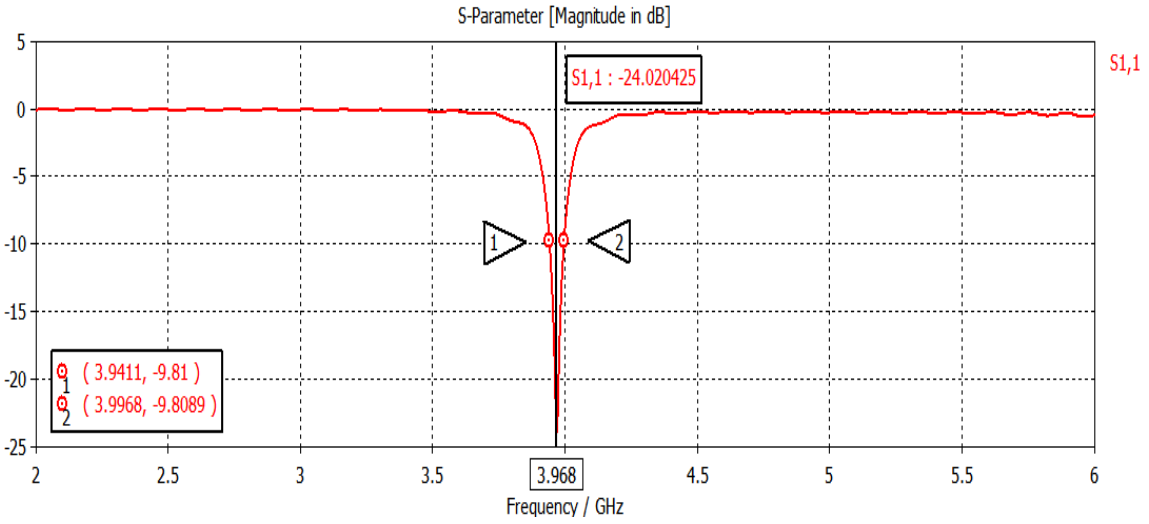

(a)

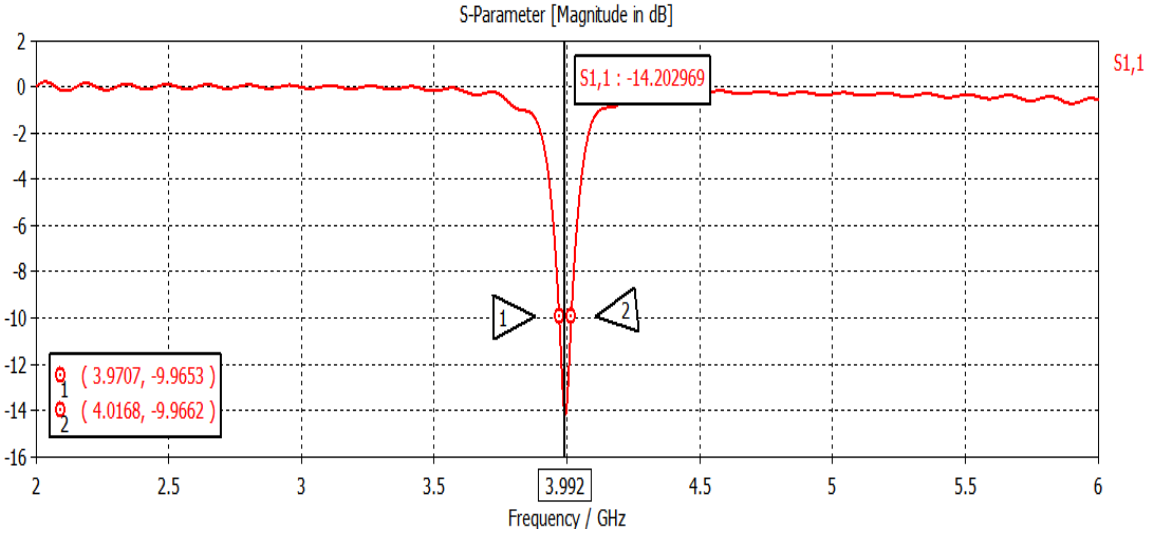

(b)

FIGURE 4.7 Return loss and BW plot (a) Coaxial feed and (b) Microstrip line feed

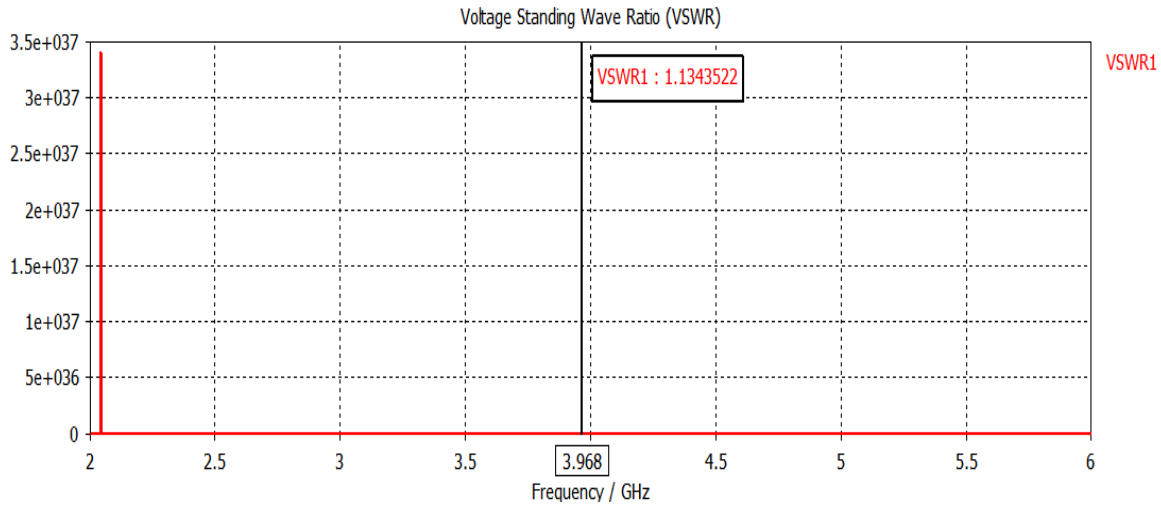

(a)

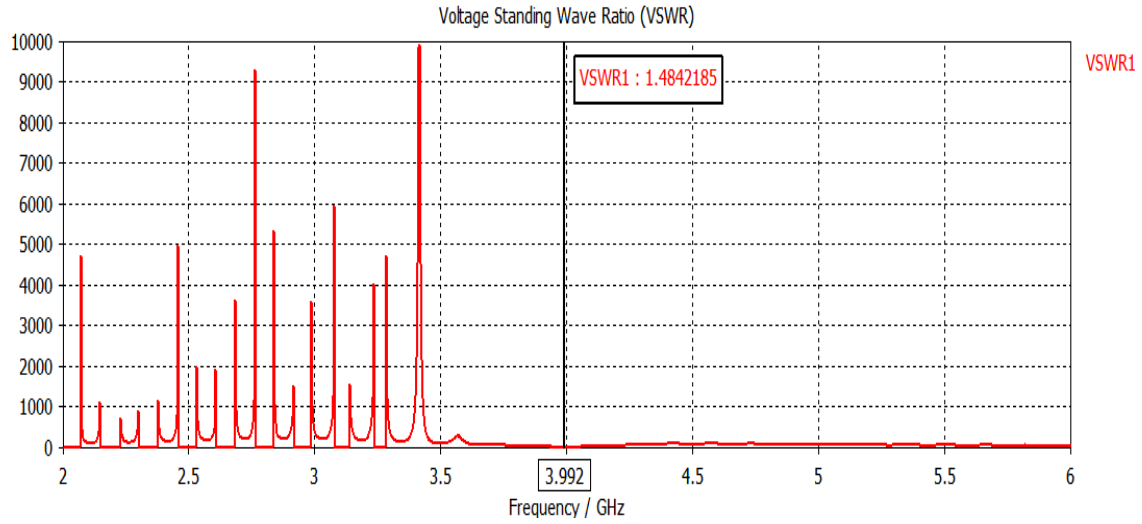

(b)

FIGURE 4.8 VSWR plot (a) Coaxial feed and (b) Microstrip line feed

The minor different in results of VSWR (0.35), BW (0.24%) and Gain (0.5 dB) of RMPA design using Coaxial feed instead of Microstrip feed line but Return loss is 9.82 dB higher which is shown in Figure 4.7 to 4.9 and listed in Table 4.5.

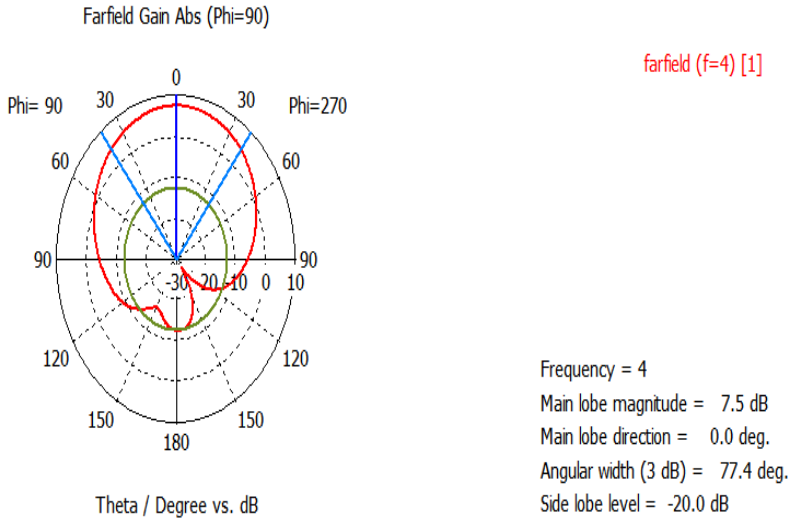

(a)

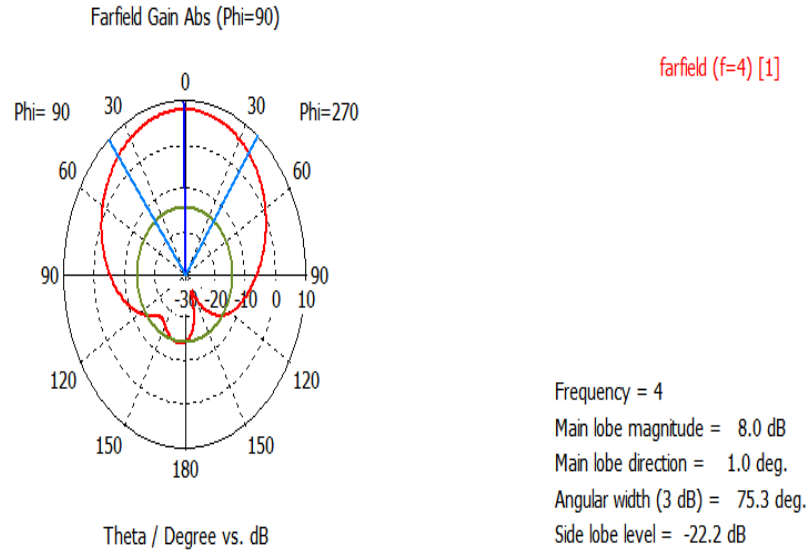

(b)

FIGURE 4.9 Gain plot (a) Coaxial feed and (b) Microstrip line feed

After over all comparison of substrate materials and feeding techniques, it is observed that RMPA design with coaxial feed and FR4 materials give better results in improvement of Return loss and Gain but following parameters are also affect the result

- The length of the antenna is responsible for determining the resonant frequency and the inductance of the antenna increases as the length increases.
- The width of the strip effects on the anti-resonance and increase the bandwidth.

- Similarly, the feed position from the short strip also affects the resonance frequency and bandwidth of the antenna
- Meandering can be made by slitting in patch's edges, or slotting the patch, or truncating patch's angles, and so on.

TABLE 4.5 Parameters comparison of Coaxial and Microstrip feed line for RMPA

Feeding techniques	Return Loss(dB)	VSWR	Bandwidth (MHz)	Bandwidth (%)	Gain (dB)
Coaxial feed	-24.0204	1.1343	0.0557	1.39	7.5
Microstrip feed line	-14.2029	1.4842	0.0461	1.152	8.0

It was found suitable to select a thin dielectric substrate with low dielectric constant permits to reduce the size and also spurious radiation as surface wave, and low dielectric constant for higher bandwidth, better efficiency and low power loss but mutual impedance is also play major roll in impedance mismatch. It was also found antenna design structure dimensions and Feed positions are playing the important role to enhance the Bandwidth and improve the antenna efficiency.

Therefore, meandering can be made by slitting in patch's edges, or slotting the patch, or truncating patch's angles, and so on is extremely crucial to efficient MPA design introducing slit/slot which is shown in Figure 4.10.

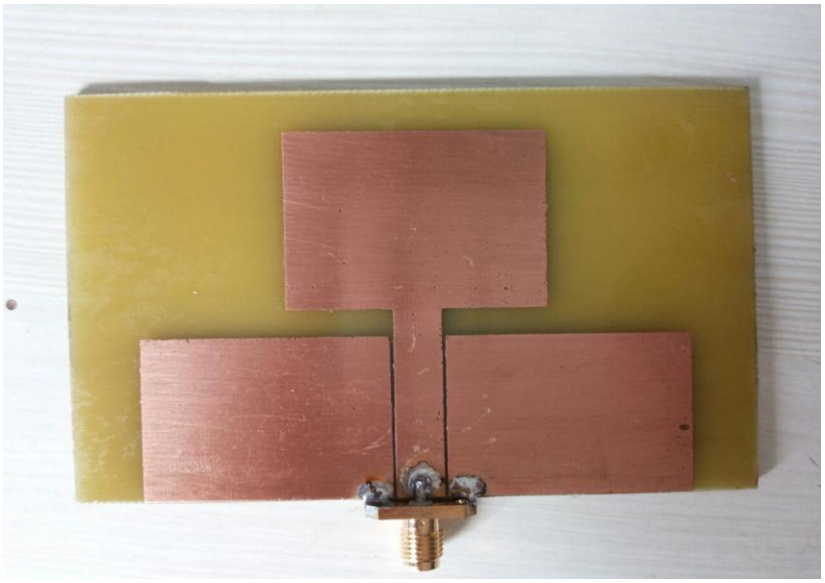

FIGURE 4.10 RMPA design with slit

BW and VSWR results are improve by applying concept of introducing slit and it has also multiband frequency operation. Dual band operation is used for multiple frequency operation in WLAN and WiMAX application which shown in Figure 4.11 and 4.12 and also results are listed in Table 4.6.

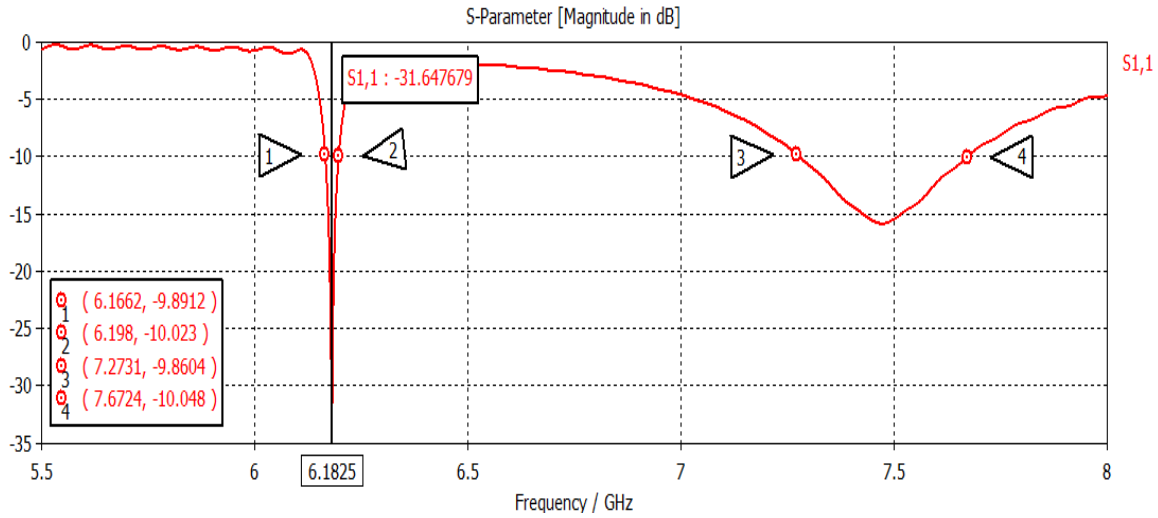

FIGURE 4.11 Return loss and bandwidth plot of RMPA with slit

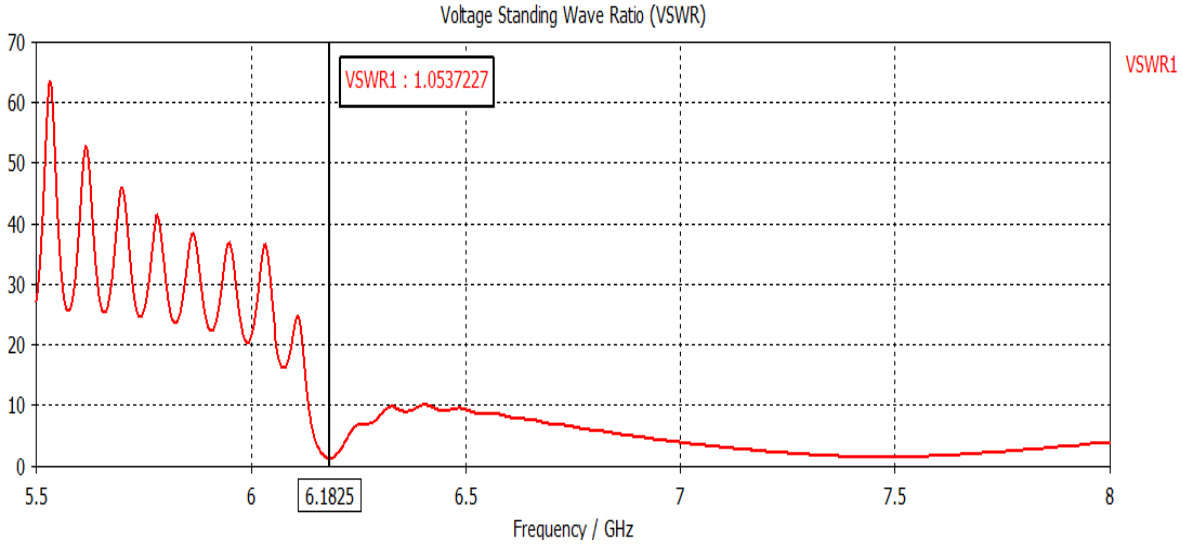

FIGURE 4.12 VSWR plot of RMPA with slit

The design perspective considered suitable value of W/L ratio is 1.5 and height is 0.02λ. Impedance matching is most important issue in antenna feeding and it can do it using scaling according to equation 4.43 to 4.46.

TABLE 4.6 Result comparison of RMPA and RMPA with primary slits

Parameters	Without slit	With slit
Return loss (dB)	-24.0204	-31.6476
VSWR	1.1343	1.053
Bandwidth (%)	2.52	5.3
Gain (dB)	7.5	6.0

Microstrip patch antennas are developing into a fundamental factor in many emerging industries and operation of these antennas in such devices is expected to several interesting properties.

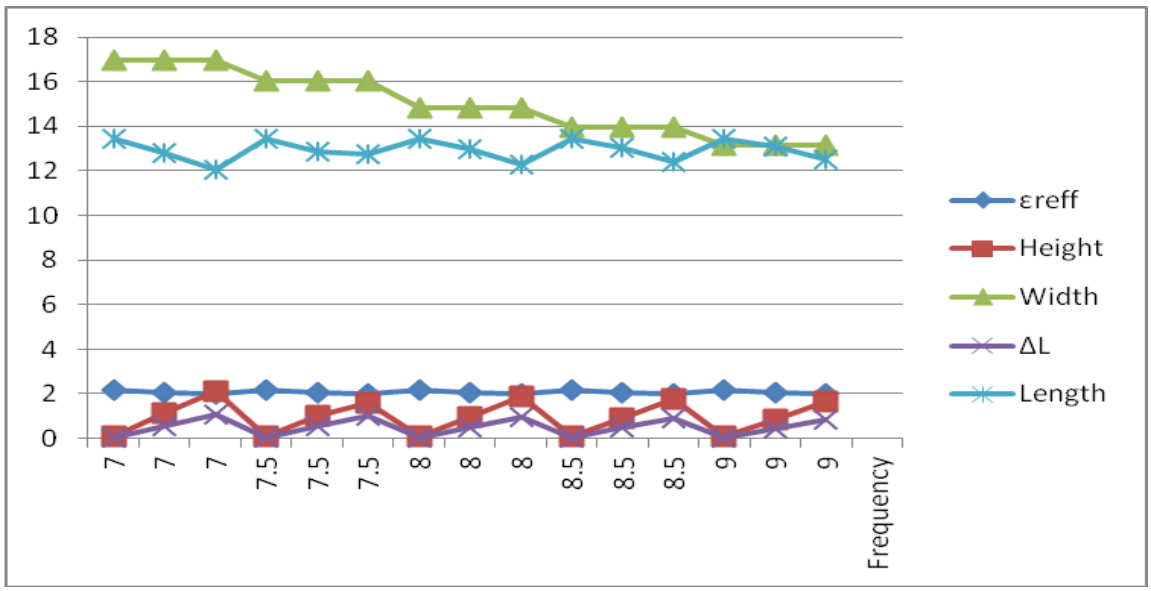

FIGURE 4.13 Design parameters at different frequency

The value of design input parameters (Dimensions of primary structure) shown in Figure 4.13 for 7 – 9 GHz frequency range. Variation dielectric constants of various dielectric materials are shown in Figure 4.14. By selection of appropriate center frequency we can easily chose suitable dimension of primary structure according to Figure 4.13 and it is calculate according to design footprint equation 4.11 to 4.13 and equation 4.43 to 4.46 is used for frequency and impedance scaling after choosing suitable feed location.

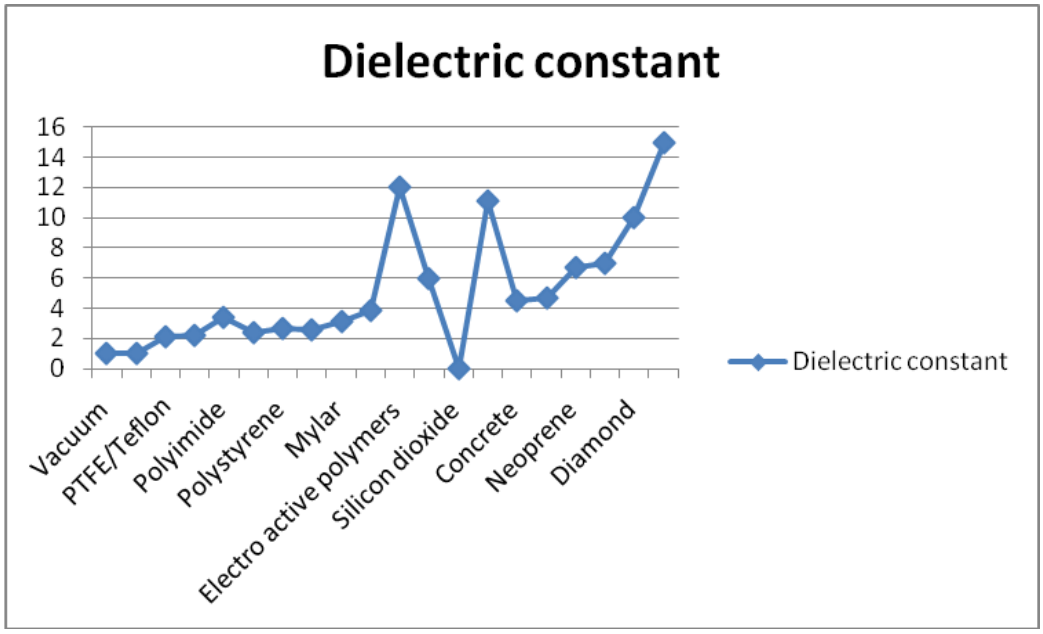

FIGURE 4.14 Dielectric constants for different materials

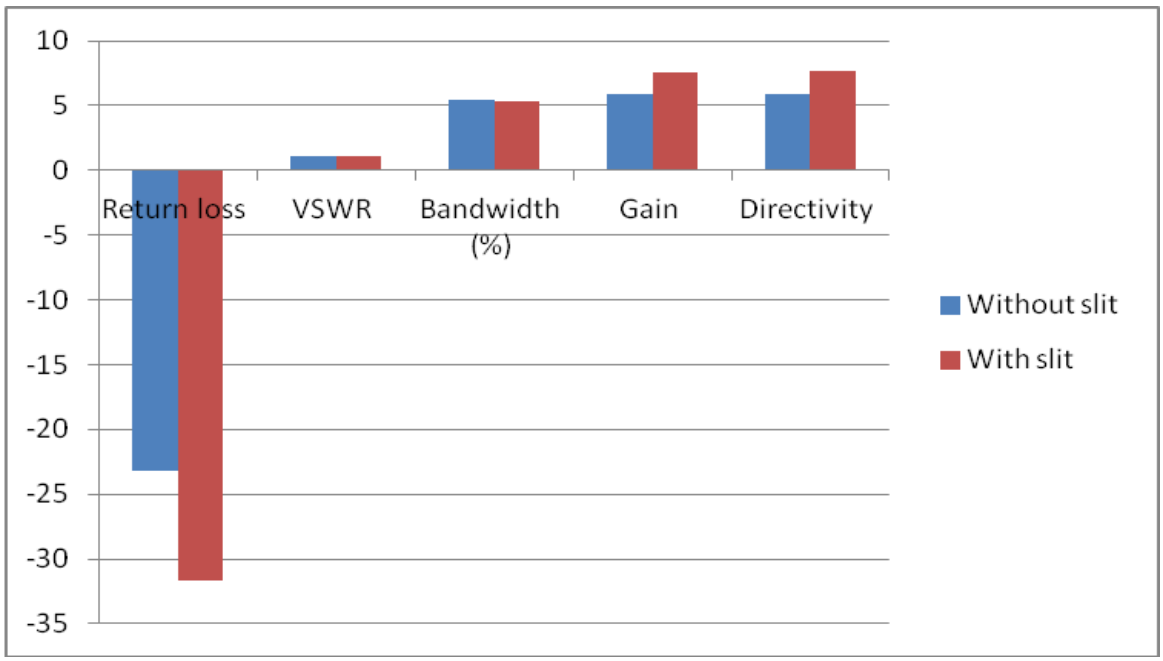

FIGURE 4.15 Parameter comparison of RMPA with slit and without slit

4.5 Summary

Analysis and synthesis of primary RMPA design results including selection of substrate materials and feeding techniques, it is observed that RMPA design with coaxial feed and FR4 materials are suitable for primary design which gives better results, return loss and gain are improved by 9 dB and 4 dB respectively.

The prospective design structured slots to operate at multiple frequency bands. Slots are design on the rectangular patch and fed by a microstrip feeder line. It is also observed that RMPA design including primary slits gives better results compare to primary RMPA design. These designs enhance the BW by 2.5% , return loss by additional 7.5 dB and VSWR by 0.13 but gain is reduced by 1.5 dB but reduction of gain is only due to improper feed location hence impedance mismatch shown in Figure 4.15. RMPA design including slots/slits in different shape will give better improvement in results and also suitable for multiple frequency band in 6 GHz to 15 GHz range. Impedance matching and effect of overall capacitive and inductive reactance are resolve by applying concept of slits in shape tree fractal.

The combinations of the proposed design discuss in next chapter in details which allow the antenna to operate at multiple frequencies for most of the satellite applications. It shows that three different operating frequency bands have VSWR ≤ 2 which is an acceptable range for short to medium range wireless communication.

CHAPTER 5

Tree Fractal Rectangular MSA Design

5.1 Overview

In multichannel applications, the antenna is required to operate over a broad BW to cover all the channels. However, at any given time, it requires a small BW to cover a single channel. In this case, a tunable MSA is required. If the antenna is designed to operate at two far away frequencies, then a dual and triple band MSA could be used. Various techniques have been described to tune the resonance frequency of the MSA. The tuning of the resonance frequency around the 15 to 20% range is achieved by loading the MSA with external reactive components such as stubs, shorting posts, and varactor and PIN diodes. The frequency is also tuned by varying the thickness of the air gap between the patch substrate and the ground plane. This tunable configuration is useful if the increased thickness of the antenna is acceptable.

Selection of appropriate materials and feeding methods are presented in previous chapter and also introduced number of slots/slits in primary design enhance improve the BW and VSWR and also dual and triple band characteristics are achieved. In this chapter finally discussed the multiband characteristics of RMPA including concept of tree fractal with appropriate iterations. Dimensions of novel design are selected base on survey for appropriate band and applications and details given bellow research survey.

With the opening of ultra-wideband (UWB) communication system to civilian areas, UWB starts coming into people's view. The UWB system has been developed rapidly in the field of wireless communication with its advantages of high speed, high resolution, low power consumption and low interference. UWB antenna as an important component of UWB system which requires a very wide bandwidth (3.1 - 10.6 GHz) with good radiation characteristics and time domain characteristics has become a research hotspot.

The classic UWB antennas have Vivaldi antenna (Steven, R. B., 2003, Comisso, M., 2009, Sengupta, K. and K. J. Vinoy, 2006 and Werner, D. H. and S. Ganguly, 2003) and log periodic antenna (Mahatthanajatuphat, C., P. Akkaraekthalin, S. Saleekaw, and M. Krairiksh, 2009), etc. Vivaldi curve has a continuous gradient structure which can obtain a larger bandwidth, but it always needs a large size to achieve good performance. Literature (Werner, D. H. and S. Ganguly, 2003) improved the design of an antipodal Vivaldi antenna which can cover a wideband from 3 GHz to 15.1 GHz, but it still has a size of 41×48 mm^2. Some special shape monopole antennas used an appropriate feeding way can also obtain a large bandwidth, such as circular monopole antennas (Dhar, S., K. Patra, R. Ghatak, B. Gupta, and D. R. Poddar, 2015 and Choukiker, Y. K. and S. K. Behera, 2014), hexagonal monopole antennas (Zhao, X. Y., H. G. Zang, and G. L. Zhang, 2015), etc.

Fractal theory is a novel method for antenna design. Literature (H. A. Wheeler, 1965) summarized that fractals had highly convoluted shapes and could enhance performance when being used in antenna designs. With increasing fractal iteration there is a corresponding increase in total wire length, and a lower resonant frequency will be obtained. Lacunarity is another method to describe a fractal set. The influence of average lacunarity on antenna performance is discussed in literature (C. P. Hartwig, D. Massé, R. A. Pucel, 1968 and J. D. Welch, H. J. Pratt, 1966), and with increasing fractal iteration, the lacunarity and resonant frequency are gradually reduced.

This analysis approach is also more practical for the non fractal antennas. In a word, the complexity of fractal leads to a better performance for antenna, and this complexity can be summarized as self-similarity and space filling. Lacunarity is also a characterization of space filling. The fractal antenna can obtain multiple resonant frequencies even a super wide bandwidth because of its self-similarity. The space filling can reduce the size of the antenna (F. Assadourian, E. Rimai, 1952, J. M. C. Dukes, 1956, T. M. Hyltin, 1965, S. Ramo, J. R. Whinnery, 1944 and E. Gaál, 1962), and these features are not available in other general geometries.

However, there are other narrowband communication systems as WiMAX (3.4 - 3.7 GHz) and WLAN (5.15 - 5.85 GHz) in the band of UWB. In order to avoid the interferences of the UWB system, an effective method is proposed to design a UWB antenna with notch characteristics. UWB antennas with notch characteristics can be achieved by a variety

of ways such as using parasitic elements on the patch (J. D. Cockcroft, 1929 and M. Caulton, J. J. Hughes, H. Sobol, 1966). Cutting slot (S. Ramo, J. R. Whinnery, 1944 and M. Sucher, J. Fox, 1963) on the patch which can change the surface current is the most common method for generating notch bands. The width of the slot is generally small, and changing the length of the slot can adjust the notch performance. The introduction of filter structures (Wu, J. N., Z. Q. Zhao, Z. Q. Nie, and Q. H. Liu, 2014 and Ma, K., Z. Q. Zhao, J. N. Wu, M. S. Ellis, and Z. P. Nie, 2014) can also effectively suppress the interference band. The UWB antenna with multi notch bands is realized by using stepped impedance resonators (Ma, K., Z. Q. Zhao, J. N. Wu, M. S. Ellis, and Z. P. Nie, 2014), but the design process is more complex and with a larger size.

Fractal's self-similarity and space filling can improve performance when being used in antenna designs. Summing up the experience of UWB antenna design, it generally has a continuous gradient structure. Thus, a novel rectangle tree fractal antenna (RTFA) for UWB (WLAN and Wi Max) applications is presented in this chapter, and the fractal makes the antenna contain multiple resonant frequencies (6 – 15 GHz). The proposed RTFA covers the whole band of UWB due to the DGS ground plane which can improve the impedance characteristics between adjacent resonant frequencies. The proposed antenna with a size of 30 × 23 × 1.6 mm^3 has good radiation characteristics, good time domain characteristics and a stable gain in the operating band.

5.2 Tree Fractal Structure Design Steps

The self-similar characteristic and complexity of fractal structure make the fractal antenna have the characteristics of multi-frequency resonance. And the bandwidth can be broadened by improving the impedance matching characteristics of adjacent resonant frequencies. The proposed rectangle tree fractal structure in this chapter is formed by superposing scaled down graphs on the two top corners of the original graph, as shown in Figure 5.2(a). Fractal structure applied to the antenna design will achieve multi-frequency resonance due to those self similar fine structures with different electric scales. The iterative process is a series of self-affine processes which can be described by an iterated function system (IFS) (F. Assadourian, E. Rimai, 1952).

Selection of dimension parameters is base on the application oriented frequency band and also taken care about impedance matching and reactance effect on radiation. 23×30

square tree fractal patch is design base on primary dimension as per listed in Table 5.1 and selected as per RTFA design flow shown in Figure 5.2(a) according to footprint equations.

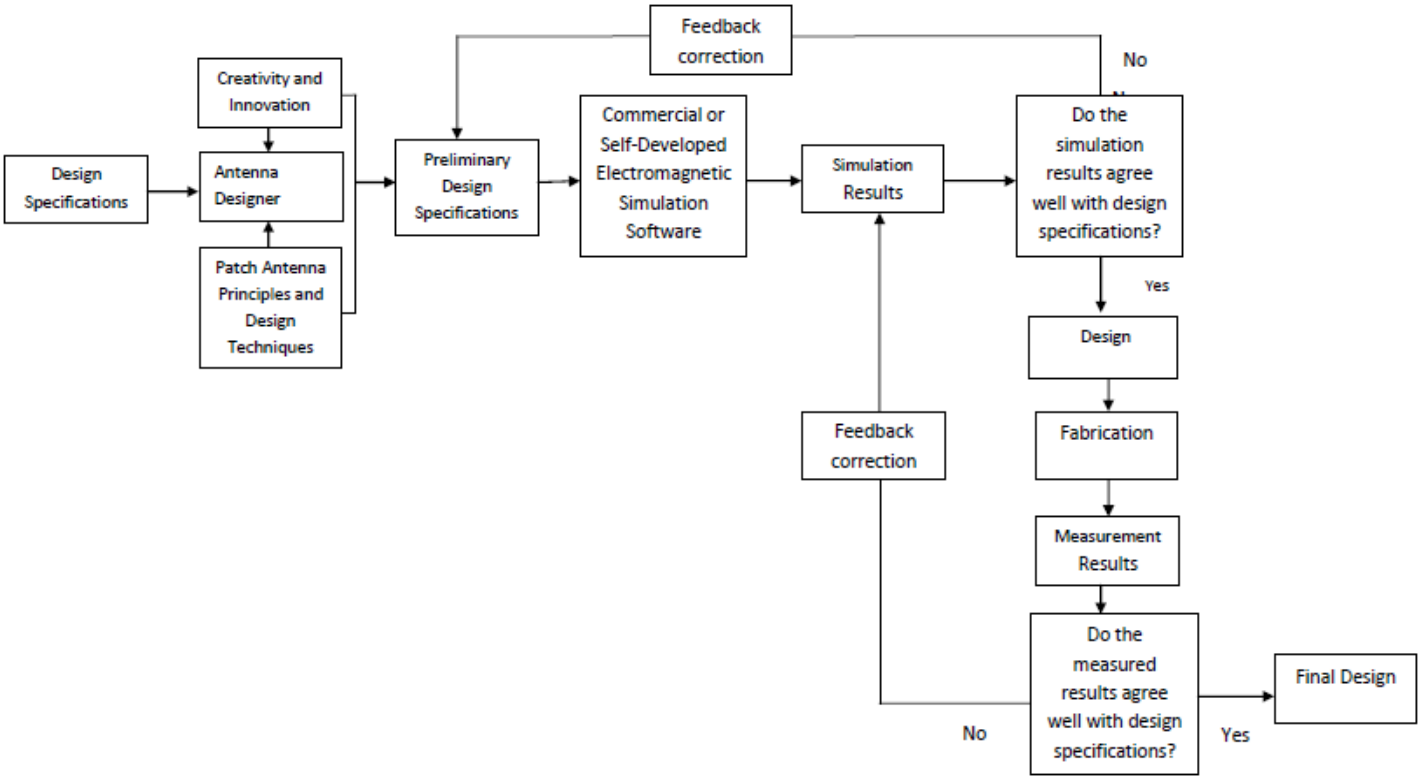

FIGURE 5.1 RTFA design flow

Impedance matching is most important issue in antenna feeding and it can do it using scaling according to equation 4.43 and 4.45 and selection of dimension as per bellow steps.

- Square structure width (W) and length (L)
- Feed length (L_s) and width (W_s)
- U slot air gap (t_s)
- U slot outer length (c) and inner length (L_2) for 1st iteration
- U slot outer width (d) and inner width (L_1) for 1st iteration
- U slot length (L_4) and width (L_3) for 2nd iteration
- DGS corner width (L_{g1}) and triangular width (L_{g2})
- DGS feed point length (W_{g1})
- Scaling factor length (L_f) and width (W_f)

Dimensions are scale according to increment of iterations and all parameters are modified with respect to modification of L_f and W_f. Selection of final dimension of proposed design by series of simulation and analysis of output results according to different range of parameters as per RTFA design flow shown in Figure 5.1. Different range of dimensions is 7.5 mm to 8.5 mm L_2, 5 mm to 6 mm L_4, 0.1 mm to 0.2 mm t_s, 2.5 mm to 3 mm W_s and 4 mm to 6 mm L_s respectively based on multiband operation with suitable application and final selected dimensions of novel RTFA are shown in Table 5.1.

The fundamental structure of the RTFA for UWB operation with multiband characteristics is shown in Figure 5.2. After simulation optimization, the specific parameters are shown in Table 5.1. In addition, the scaling factor $a = 0.7$, $b = 0.5$. The third order fractal structure is printed on a standard FR4 substrate ($W \times L$) with relative permittivity (ε_r) = 4.4, loss tangent (δ) = 0.02 and thickness (h) = 1.6 mm. A microstrip transmission line with a strip width W_f and length L_f is used to feed the antenna. In order to improve the impedance matching characteristics in the operating band, the ground plane with a DGS structure is adopted.

TABLE 5.1 23×30×1.6 mm^3 novel RTFA design dimensions

W (mm)	**L** (mm)	**H** (mm)	**W_f** (mm)	**L_f** (mm)	**c** (mm)	**d** (mm)	**t_s** (mm)	**L_1** (mm)	**L_2** (mm)	**L_3** (mm)	**L_4** (mm)	**L_s** (mm)	**W_s** (mm)	**L_{g1}** (mm)	**L_{g2}** (mm)	**W_{g1}** (mm)
23	30	1.6	2.1	9.1	8	12	0.2	8.5	8.5	4.5	5.8	5.6	2.7	2.3	4.9	7.4

In addition, the rectangular gap in the DGS ground plane is very important to the performance of the antenna, because the capacitance introduced by the rectangular gap can offset a part of inductive capacitance of antenna and improve the impedance matching in the whole band. In this, the sizes of the rectangular gap are divided into different groups. The values of width W_s and length L_s vary from 0 to 2.7 mm and 0 to 5.6 mm, respectively. The impedance matching of the antenna can be improved with length L_s = 5.6 mm and width W_s = 2.7 mm. From this, we can conclude that the reflection coefficient of the operating bandwidth can be adjusted by changing the value of the rectangular gap. The RTFA has three notch bands after three U shaped slots are introduced. According to the principle of half-wave resonance, the slot length should be $\lambda/2$ of corresponding notch band's operating frequency in the waveguide.

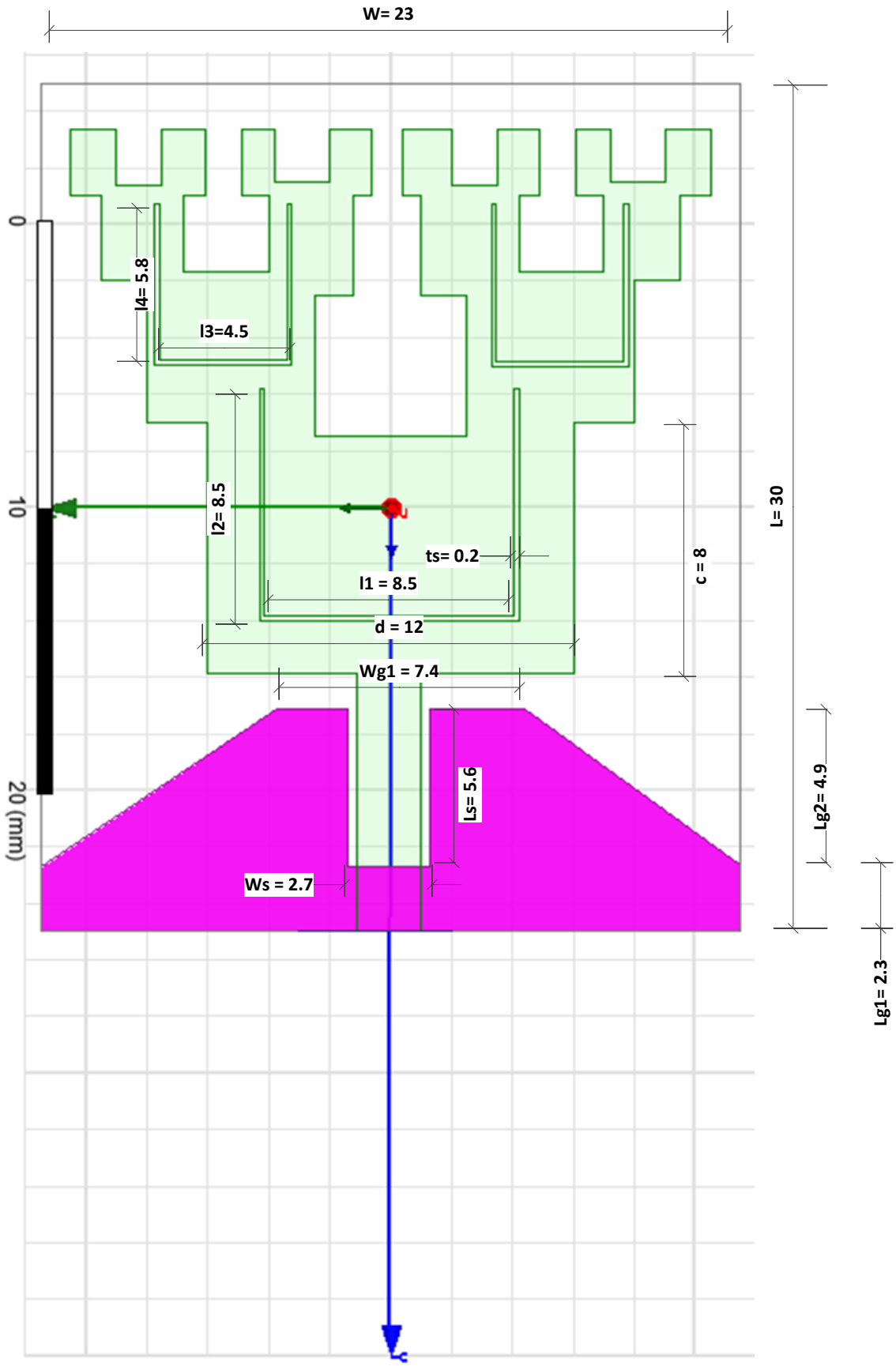

FIGURE 5.2 23×30×1.6 mm^3 tree fractal patch design (a) Dimension layout

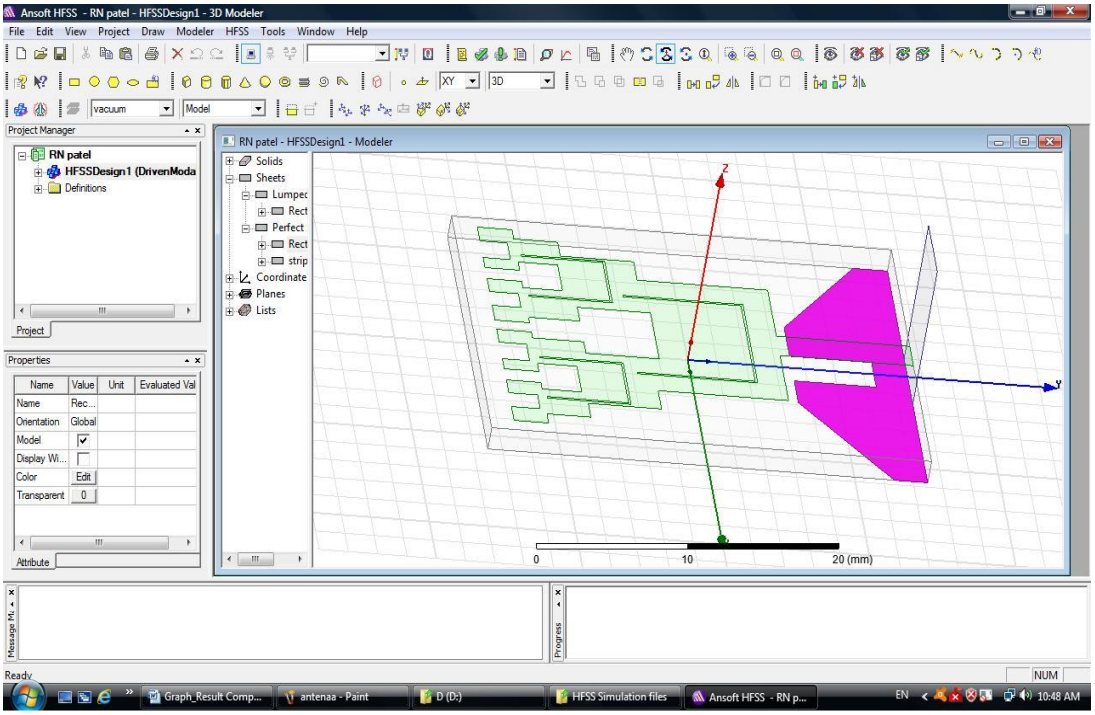

(b)

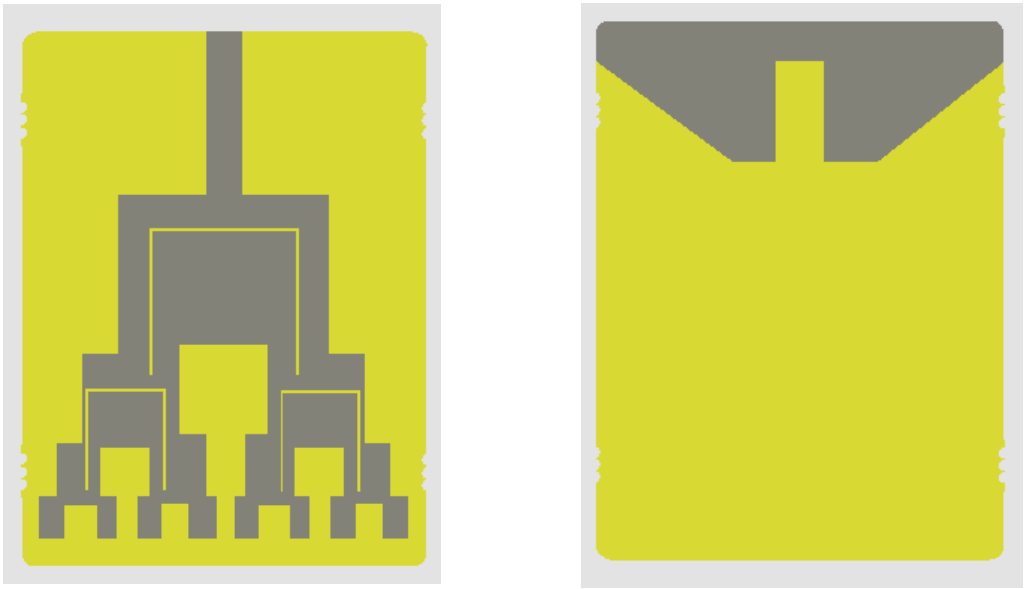

(c)

FIGURE 5.2 23×30×1.6 mm^3 tree fractal patch design (b) Simulation layout (c) Fabrication Layout

The surface current is heavily concentrated near the slot and results in the impedance mismatch when the antenna works in the vicinity of this frequency. The relationship between the operating frequency of the notch band and the length of slot is

$$f_{notch} = \frac{c}{2l\sqrt{\varepsilon_{eff}}} \tag{5.1}$$

$$\varepsilon_{eff} = \frac{\varepsilon_r + 1}{2} \tag{5.2}$$

where

c = The speed of light

l = Total length of the slot

ε_{eff} = Effective permittivity

ε_{eff} = Relative permittivity

5.3 Results and Discussion

The range between 3 GHz – 300 GHz is extremely packed out, with numerous services and applications even occupying the same frequencies in many cases. The DGS ground plane has two symmetrically bevelling corners and a rectangular gap with a size of $L_s \times W_s$ on a rectangular ground plane. Three U shaped slots with air gap of t_s are provided on the tree fractal patch to suppress the interference due to (5.92 - 8.45 GHz) for WiMAX (worldwide interoperability for microwave access) and WiBRO (wireless broadband) in range of Fixed and Mobile satellite applications, (8.5 - 10.55 GHz) for RLAN (Radio location and Aeronautical/Maritine radio navigation) and (12.75 - 14.5 GHz) for LMS (Land mobile satellite and Radio navigation) applications.

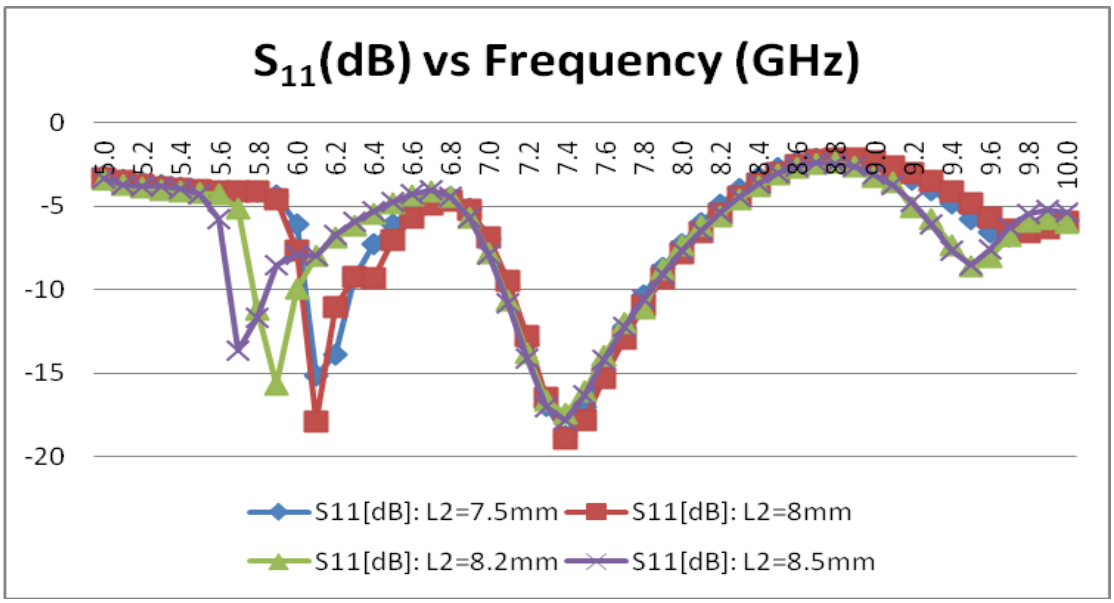

FIGURE 5.3 Return loss characteristics of RTFA with slot variation L_2

The RTFA has only a notch band near 6.2 GHz when there is only $slot_1$, only a notch band near 7.4 GHz when there are only $slot_1$ and $slot_2$, two notch bands near 7.4 GHz and 10.7 GHz when there are $slot_2$ and $slot_3$, three notch bands near 7.4 GHz, 10.7 GHz and 13 GHz when there are $slot_1$, $slot_2$ and $slot_3$, Thus, it can be observed that l_{slot1} ($l_{slot1} = l_1 + 2l_2$) controls the notch near 7.4 GHz, and l_{slot2} ($l_{slot2} = l_{slot3} = l_3 + 2_{l4}$) controls the notch near 10.7 GHz and 13 GHz. Figure 5.3 to 5.18 show the effect on the notch characteristics for part of the slot parameters.

Figure 5.3 shows the simulated reflection coefficient of the RTFA for different values of *slot'* length (L_2) with other parameters remaining fixed. It can be seen from Figure 5.3 that L_2 has an evident effect on resonance frequency of the notch band near 6.2 GHz. It is found that the resonant frequency of the notch band near 6.2 GHz decreases with increasing values of L_2 and has no effect on the notch band near 7.4 GHz.

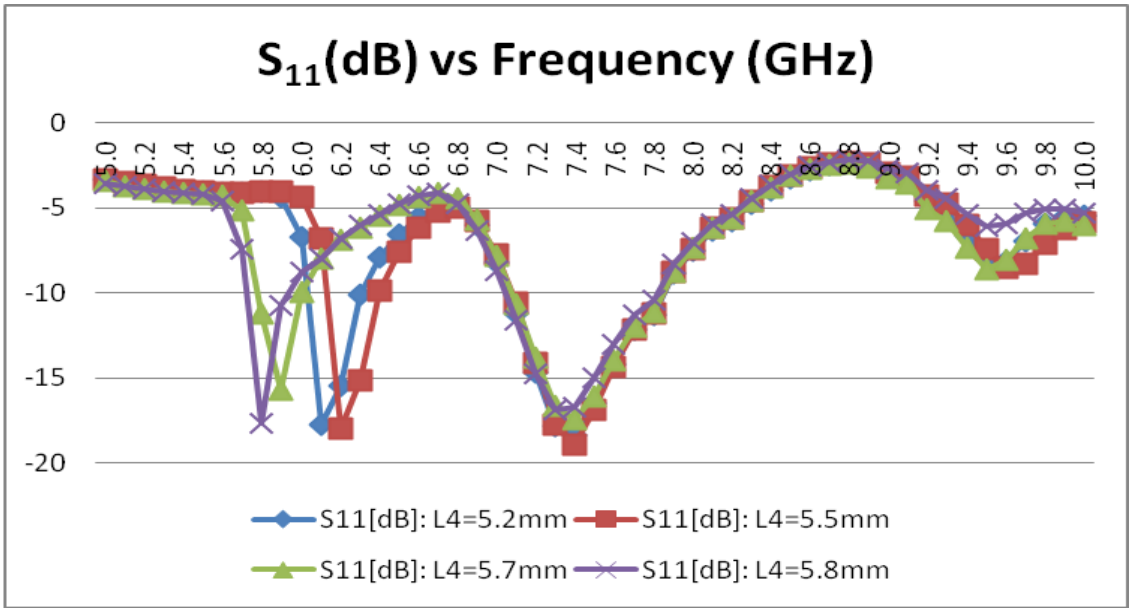

FIGURE 5.4 Return loss characteristics of RTFA with slot variation L_4

Figure 5.4 shows that the resonant frequency of the notch band near 6.2 GHz decreases with increasing values of L_4. It means that the resonant frequency of the notch band decreases with increasing size of the corresponding resonant slot. This is also reliable with formula 5.1.

Figure 5.5 shows the simulated reflection coefficient characteristics for different values of t_s. As *ts* increases from 0.1 to 0.2 mm with other parameters remaining fixed, it can be observed that the notch bandwidth is increased (from the upper band edge).

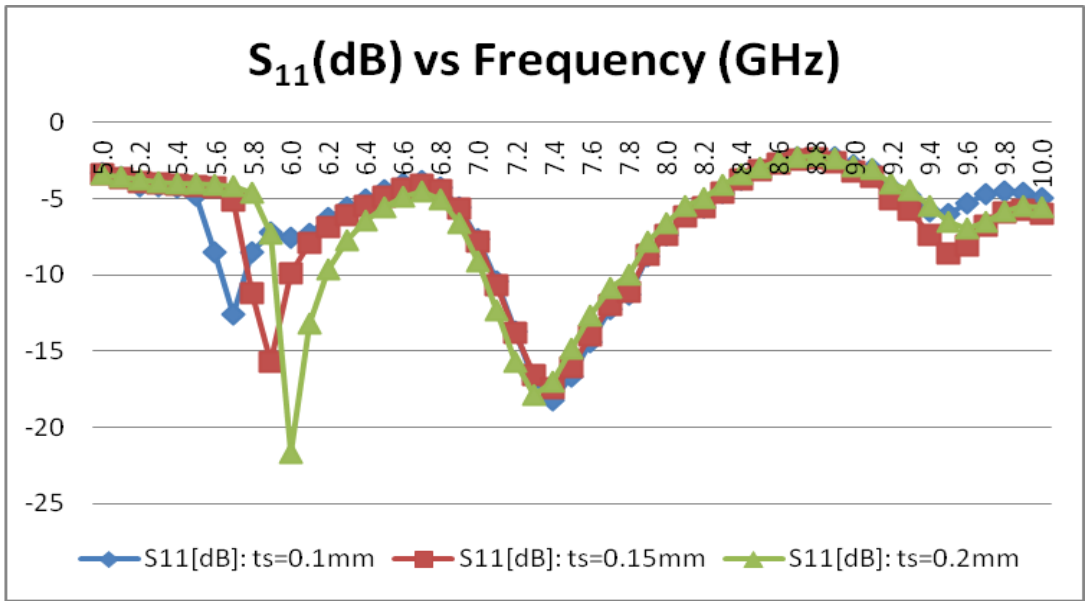

FIGURE 5.5 Return loss characteristics of RTFA with slot variation t_s

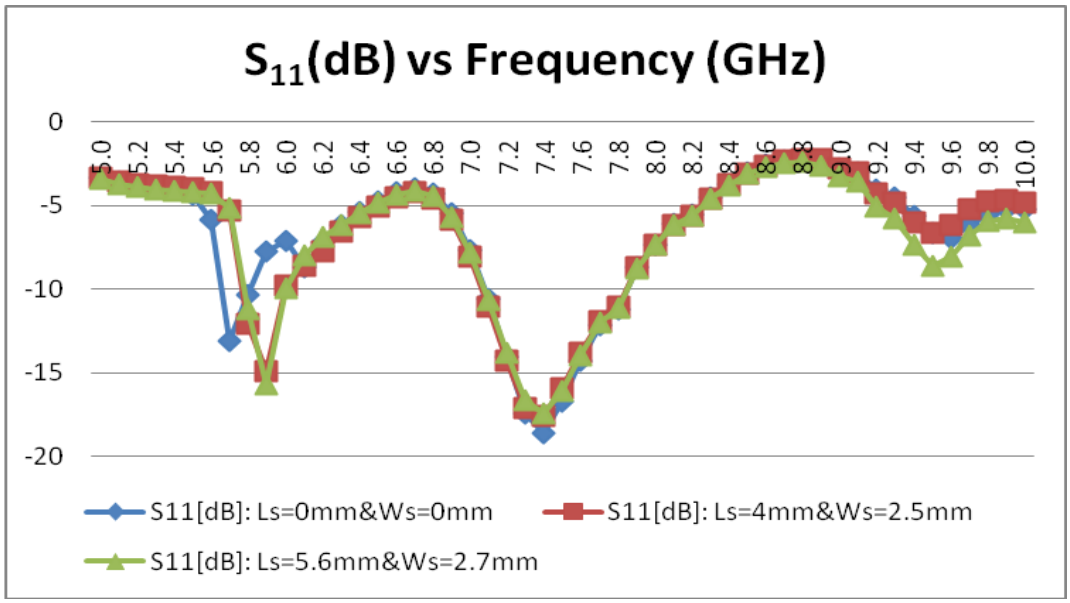

FIGURE 5.6 Return loss characteristics of RTFA with slot variation L_s and W_s

Figure 5.6 shows the simulated reflection coefficient characteristics for different values of L_s and W_s. As L_s and W_s increases from 0 to 5.6 and 2.7 mm respectively with other parameters remaining unchanged, it can be observed that the notch bandwidth is increased

(from the upper band edge). Hence, it can be concluded that the resonant frequency of the notch can be controlled by the length of slots, and the notch bandwidth can be adjusted by the width of the slots.

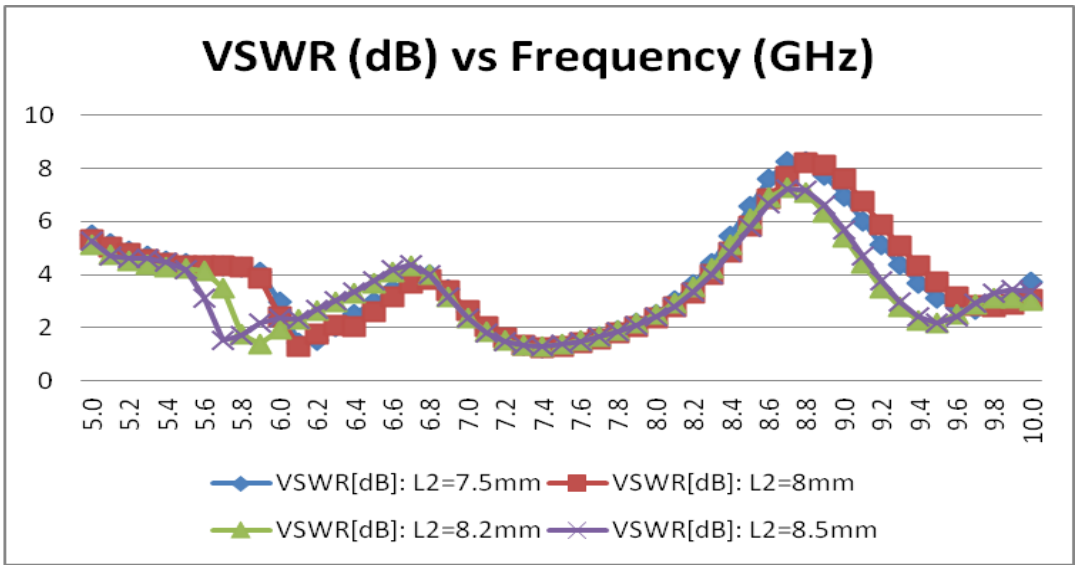

FIGURE 5.7 VSWR characteristics of RTFA with slot variation L_2

Figure 5.7 shows the simulated VSWR of the RTFA for different values of *slot'* length (L_2) with other parameters remaining fixed. It can be seen that L_2 has an evident effect on resonance frequency of the notch band near 6.2 GHz. It is found that the resonant frequency of the notch band near 6.2 GHz decreases with increasing values of L_2 and has no effect on the notch band near 7.4 GHz.

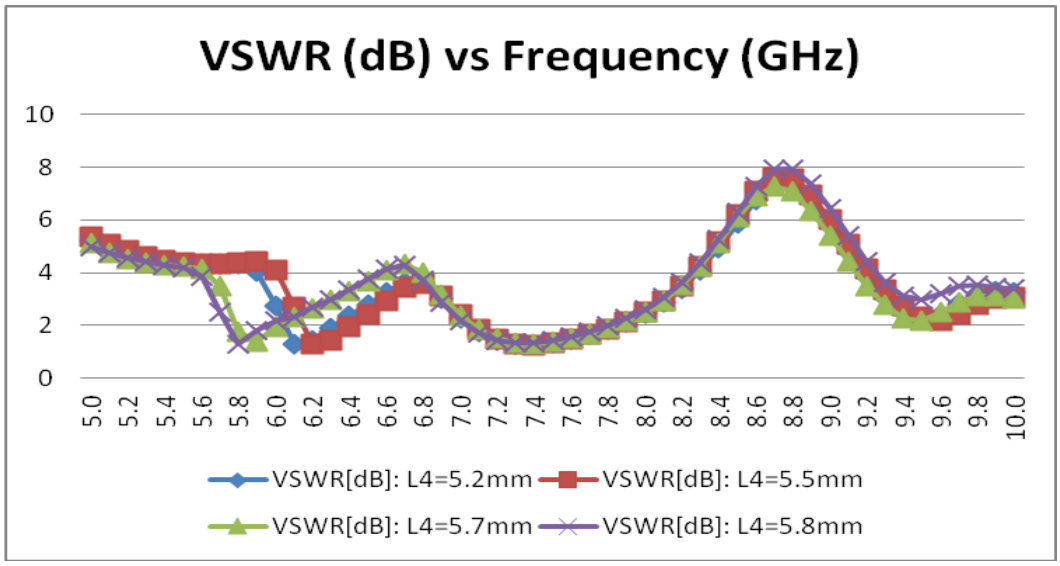

FIGURE 5.8 VSWR characteristics of RTFA with slot variation L_4

Figure 5.8 shows that the resonant frequency of the notch band near 6.2 GHz decreases with increasing values of L_4. It means that the resonant frequency of the notch band decreases with increasing size of the corresponding resonant slot. This is also reliable with formula 5.1.

Figure 5.9 shows the VSWR characteristics for different values of t_s. As *ts* increases from 0.1 to 0.2 mm with other parameters remaining fixed, it can be observed that the notch bandwidth is increased (from the upper band edge).

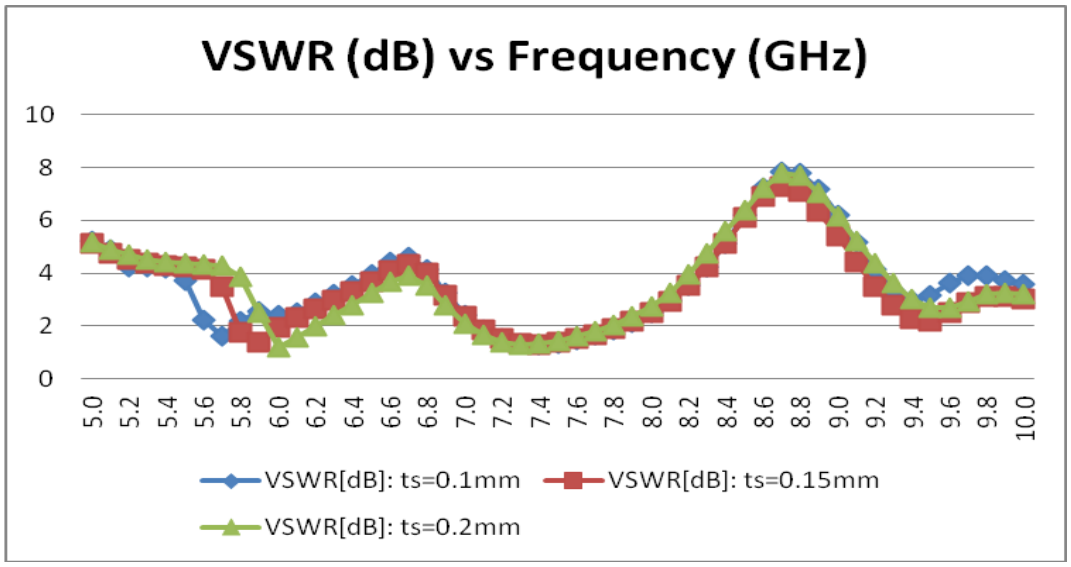

FIGURE 5.9 VSWR characteristics of RTFA with slot variation t_s

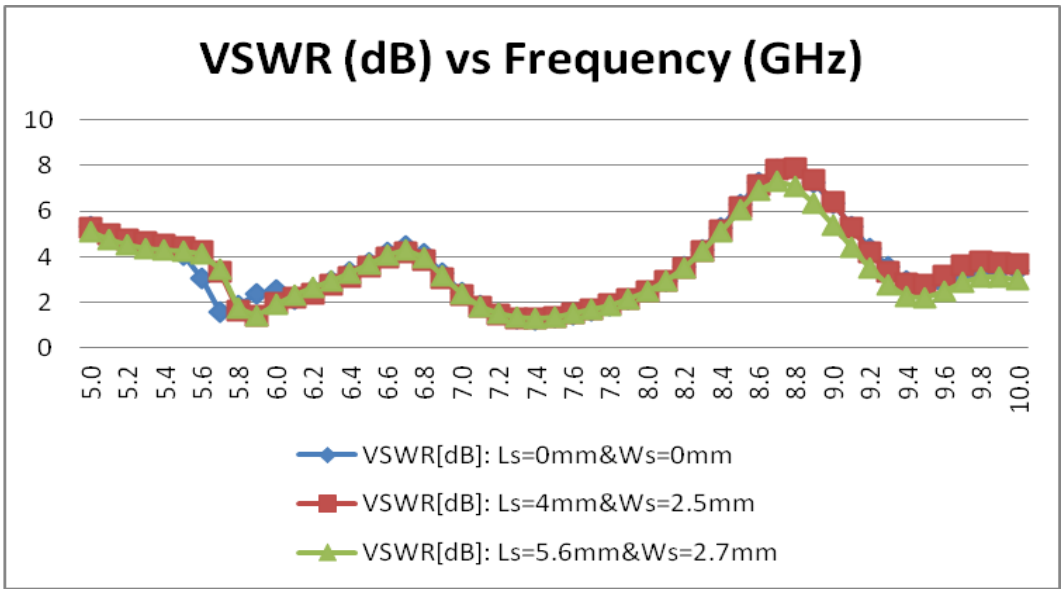

FIGURE 5.10 VSWR characteristics of RTFA with slot variation L_s and W_s

Figure 5.10 shows the simulated VSWR characteristics for different values of L_s and W_s. As L_s and W_s increases from 0 to 5.6 and 2.7 mm respectively with other parameters remaining unchanged, it can be observed that the notch bandwidth is increased (from the upper band edge). Hence, it can be concluded that the resonant frequency of the notch can be controlled by the length of slots, and the notch bandwidth can be adjusted by the width of the slots.

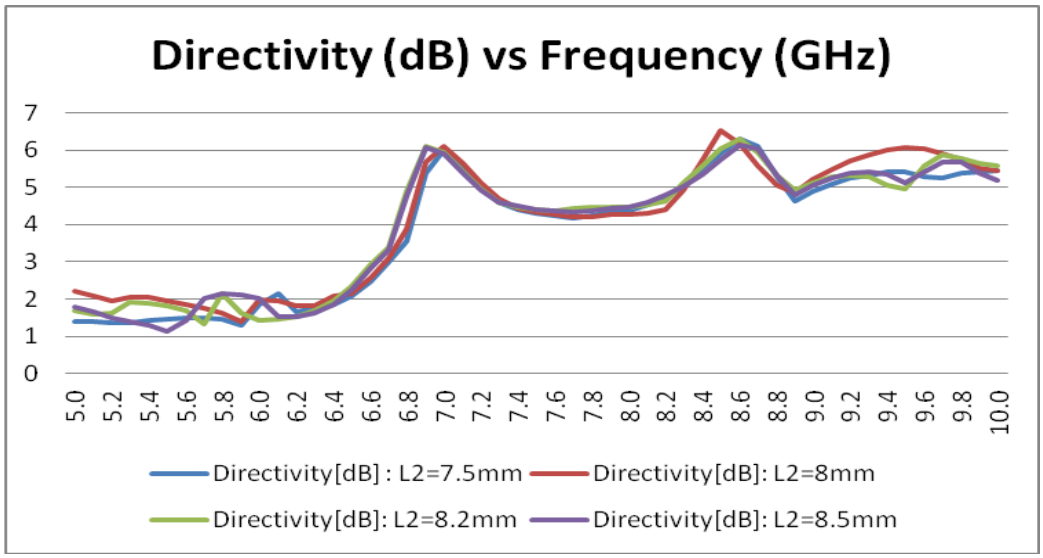

FIGURE 5.11 Directional characteristics of RTFA with slot variation L_2

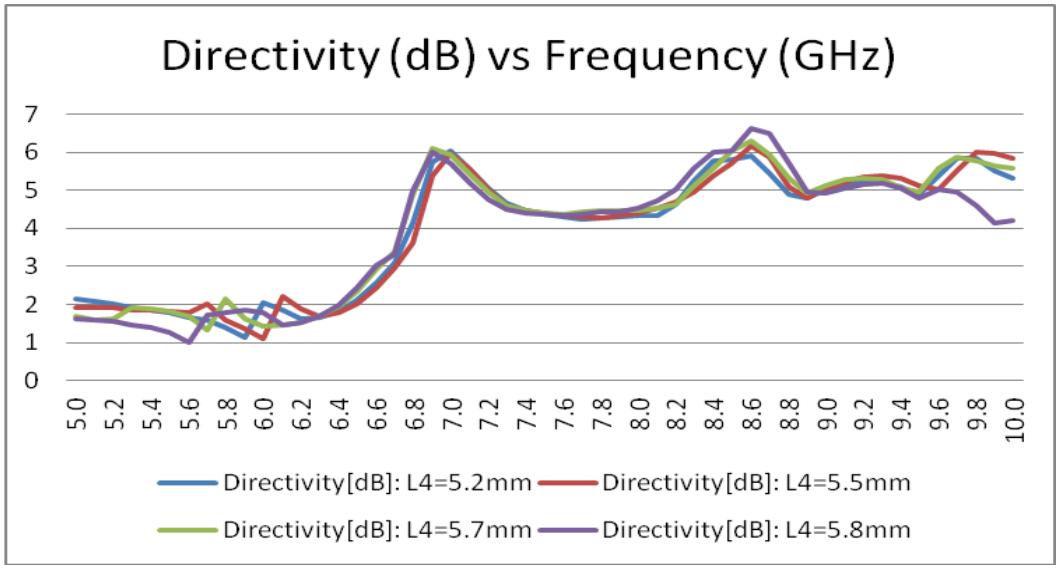

FIGURE 5.12 Directional characteristics of RTFA with slot variation L_4

Figure 5.11 to 5.14 shows the simulated Directional characteristics for different values of L_2, L_4, t_s, L_s and W_s. It can be observed that the directivity is very less at 6.2 GHz band

and it is sufficiently increase after 1st notch band for any range of parameters. Hence, it can be concluded that the resonant frequency of the notch can be selected for 7.4 GHz, 10.7 GHz and 13 GHz triple notch characteristics except 6.2 GHz.

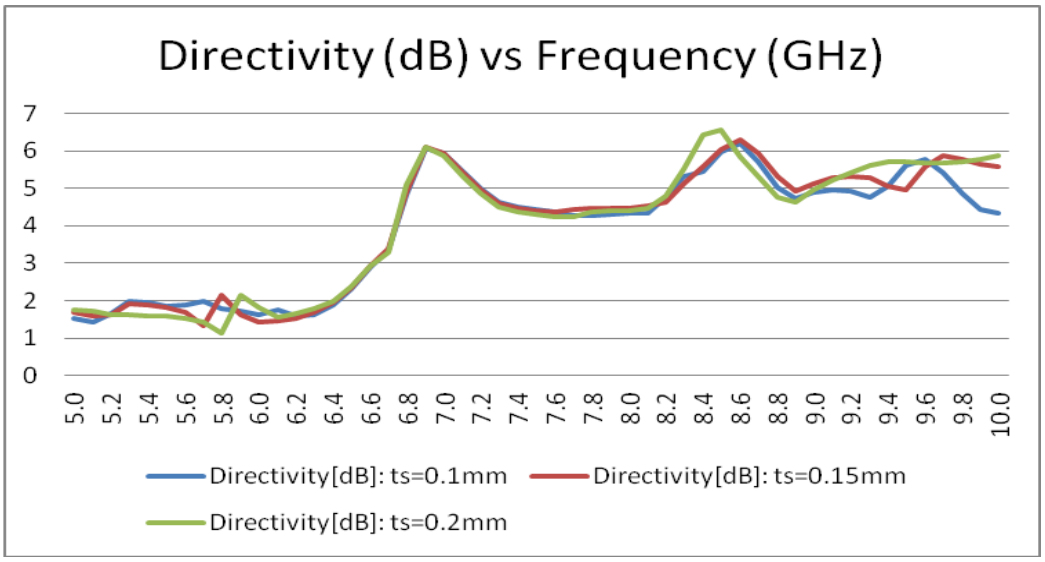

FIGURE 5.13 Directional characteristics of RTFA with slot variation t_s

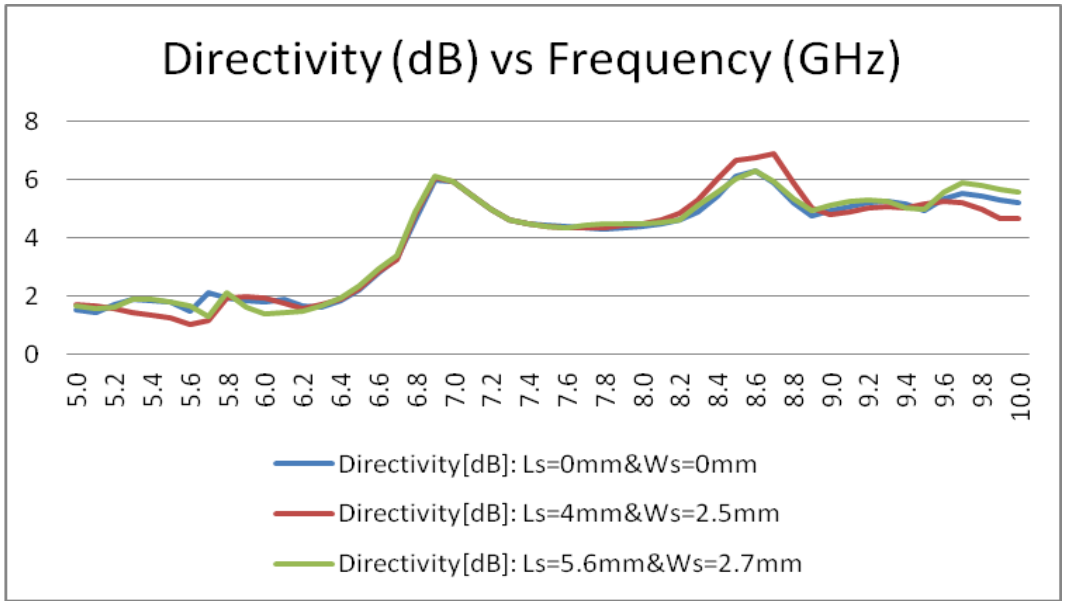

FIGURE 5.14 Directional characteristics of RTFA with slot variation L_s and W_s

Figure 5.15 to 5.18 shows the simulated Bandwidth for different values of L_2, L_4, t_s, L_s and W_s. It can be observed that the *% BW* improved at 9.86% for L_2 = 8.5 mm, 10.27% for L_4 = 5.8 mm, 10.81% for t_s = 0.2 mm and 9.56% for L_s & W_s = 5.6 & 2.7 mm and it is the higher than the other dimension ranges of parameters. Hence, it can be concluded that

the values of L_2, L_4, t_s, L_s and W_s are 8.5 mm, 5.8 mm, 0.2 mm, 5.6 mm and 2.7 mm respectively and resonant frequency of the notch can be selected for 7.4 GHz, 10.7 GHz and 13 GHz triple notch characteristics except 6.2 GHz

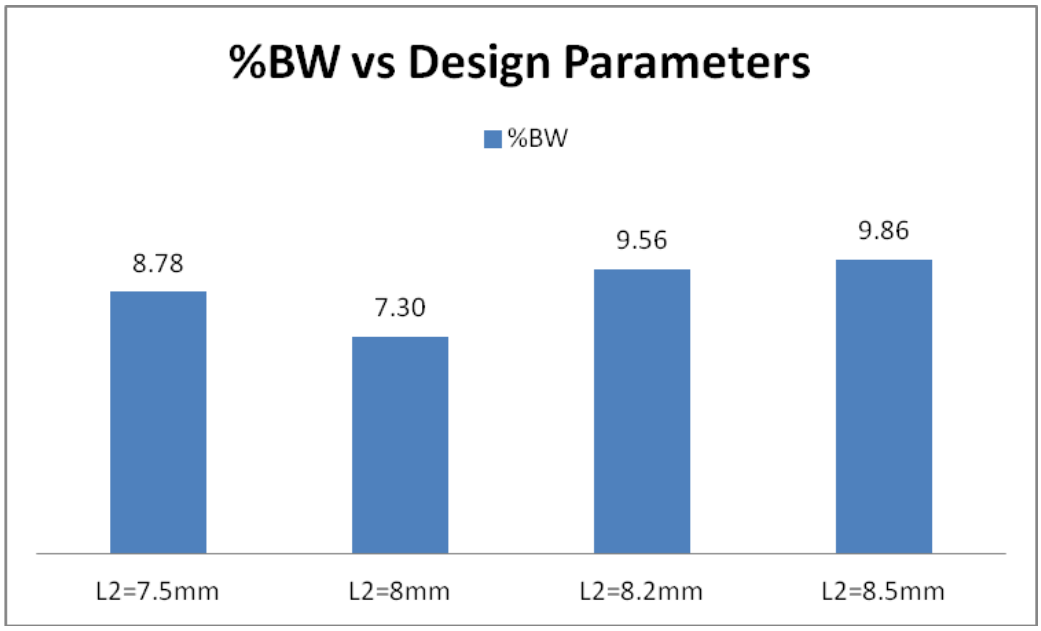

FIGURE 5.15 BW characteristics of RTFA with slot variation L_2

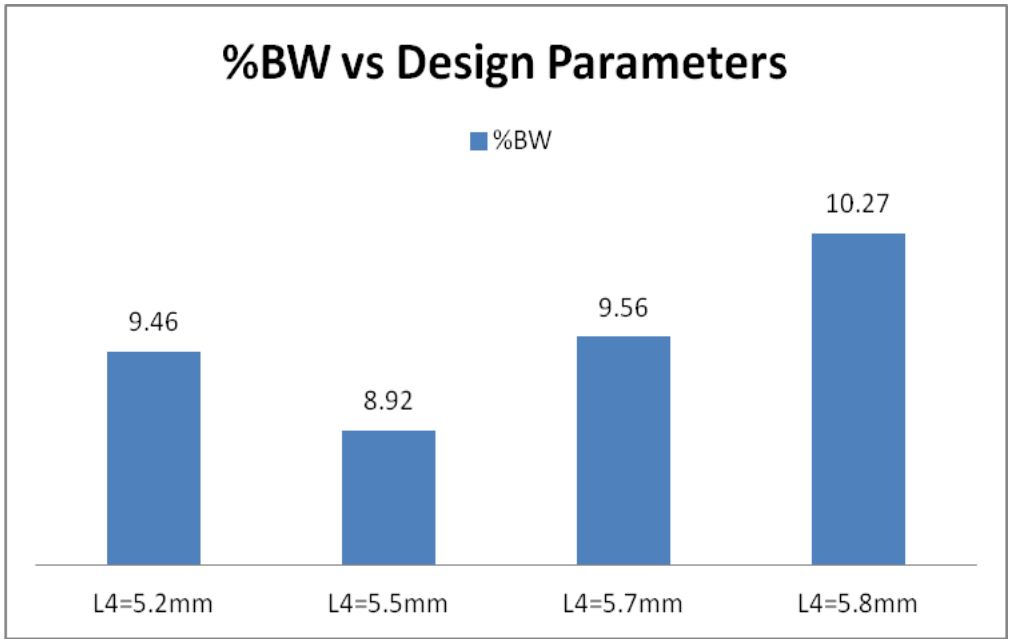

FIGURE 5.16 BW characteristics of RTFA with slot variation L_4

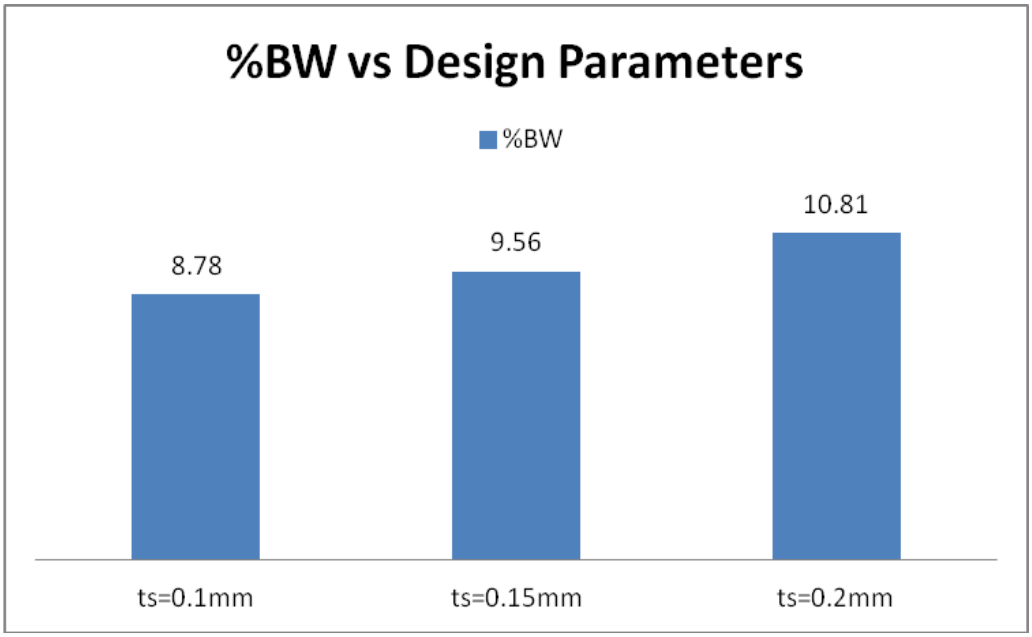

FIGURE 5.17 BW characteristics of RTFA with slot variation t_s

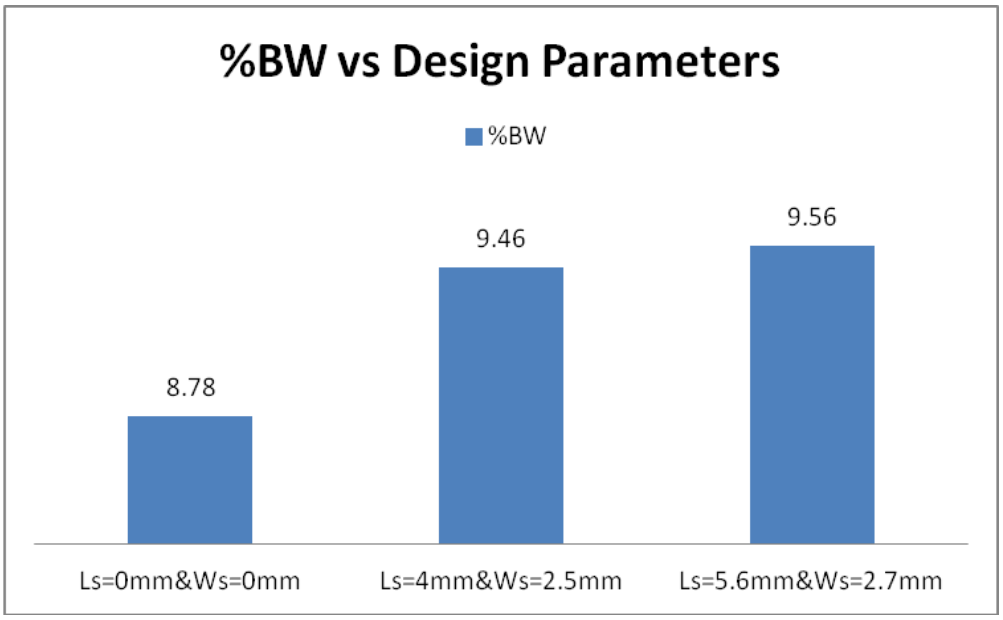

FIGURE 5.18 BW characteristics of RTFA with slot variation L_s and W_s

A patch antenna model with L = 30 mm and W = 23 mm along the patch square yielded a resonant frequency of 7.4 GHz, 10.7 GHz and 13 GHz, as well as an excellent resonant return loss and VSWR is less than 2.0 with different choice of L_2 from 7.5 mm to 8.5 mm as listed in Table 5.2 and shown in Figure 5.19 and Figure 5.20 shows Bandwidth and return loss for triple notch band characteristics for actual RTFA design results.

TABLE 5.2 Parameters comparison base on selection of L_2

Parameter	%BW	VSWR	S_{11}(dB)
l2=7.5 mm	16.2	1.3	-17.62
l2=8.2 mm	15.08	1.22	-19.93
l2=8.5 mm	**18.74**	**1.33**	**-24.12**

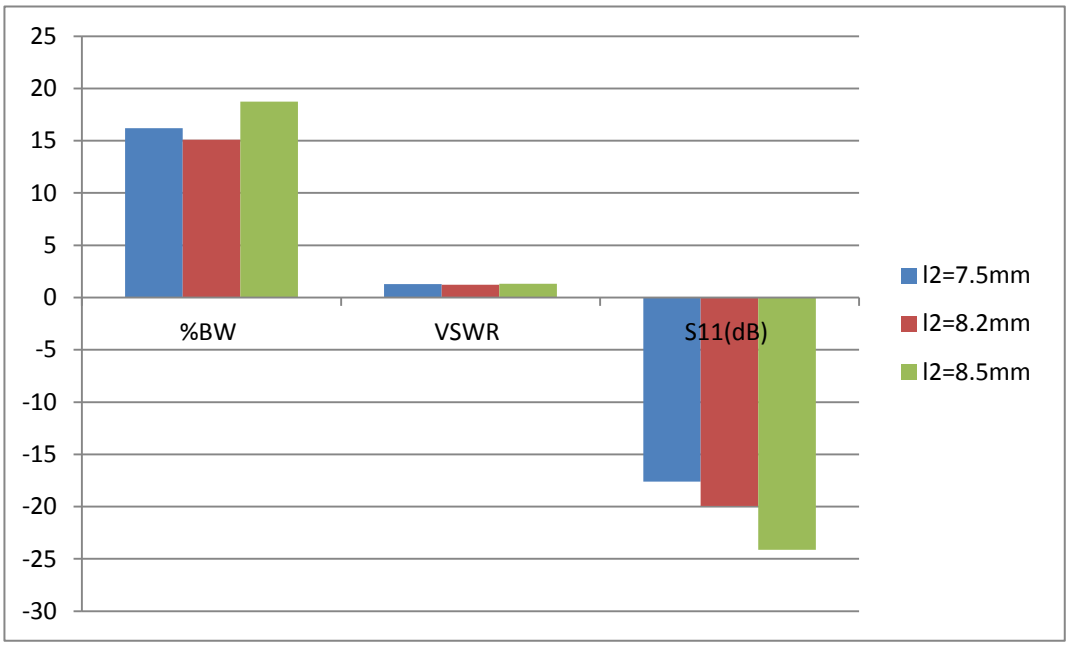

FIGURE 5.19 Parameters comparison base on selection of L_2

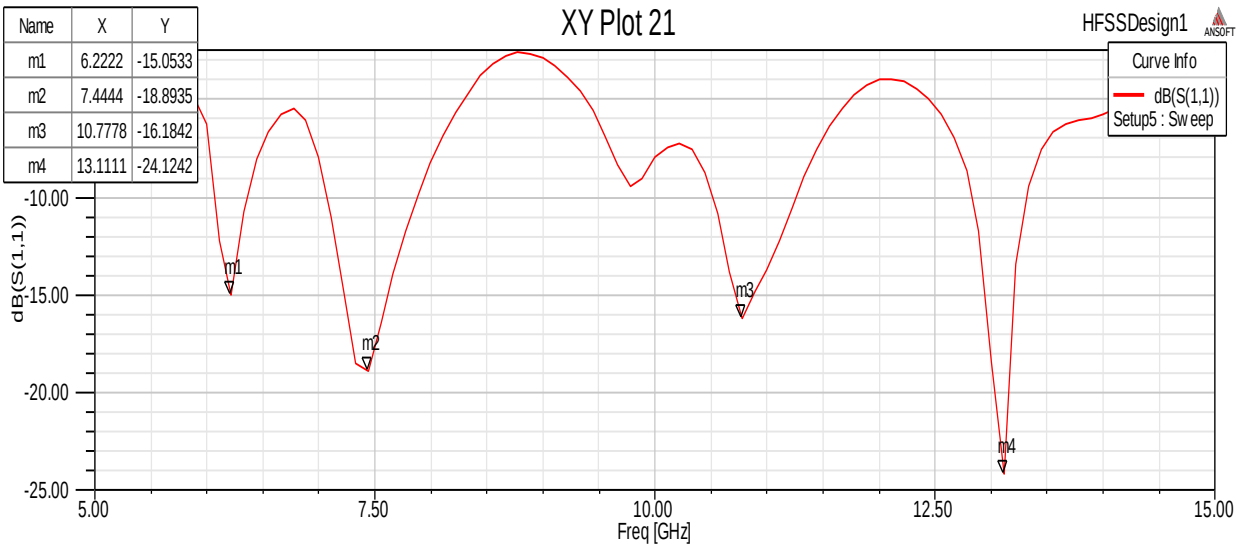

FIGURE 5.20 BW and Return loss base on selection of L_2=8.5 mm

A patch antenna model with L = 30 mm and W = 23 mm along the patch square yielded a resonant frequency of 7.4 GHz, 10.7 GHz and 13 GHz, as well as an excellent resonant return loss and VSWR is less than 2.0 with different choice of L_4 from 5.2 mm to 5.8 mm as listed in Table 5.3 and shown in Figure 5.21 and Figure 5.22 shows Bandwidth and return loss for triple notch band characteristics for actual RTFA design results.

TABLE 5.3 Parameters comparison base on selection of L_4

Parameter	**%BW**	**VSWR**	**S_{11}(dB)**
l4=5.2 mm	15.03	1.24	-19.36
l4=5.5 mm	16.65	1.15	-23
l4=5.8 mm	**19.23**	**1.13**	**-24.37**

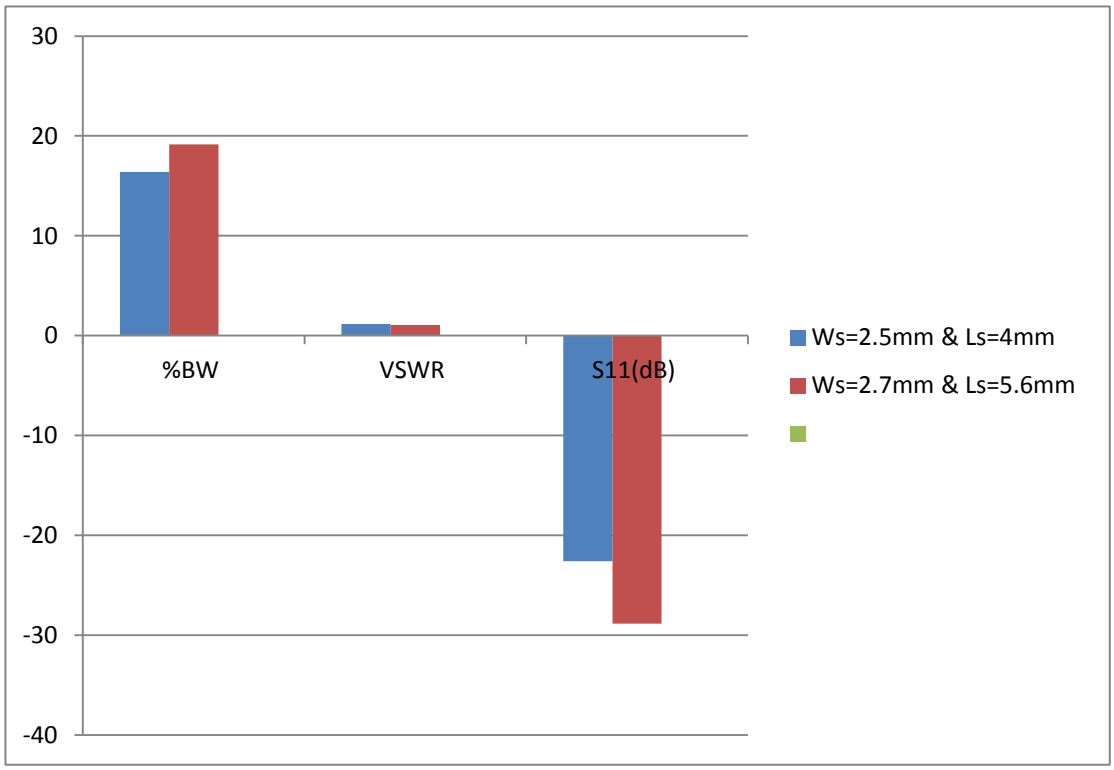

FIGURE 5.21 Parameters comparison base on selection of L_4

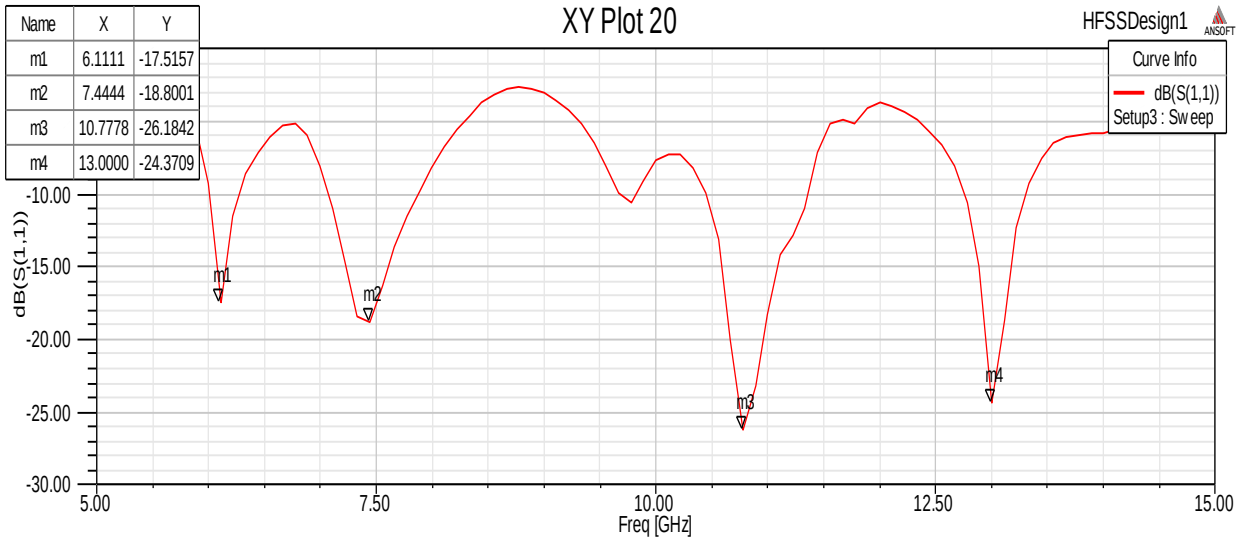

FIGURE 5.22 BW and Return loss base on selection of L_4 = 5.8 mm

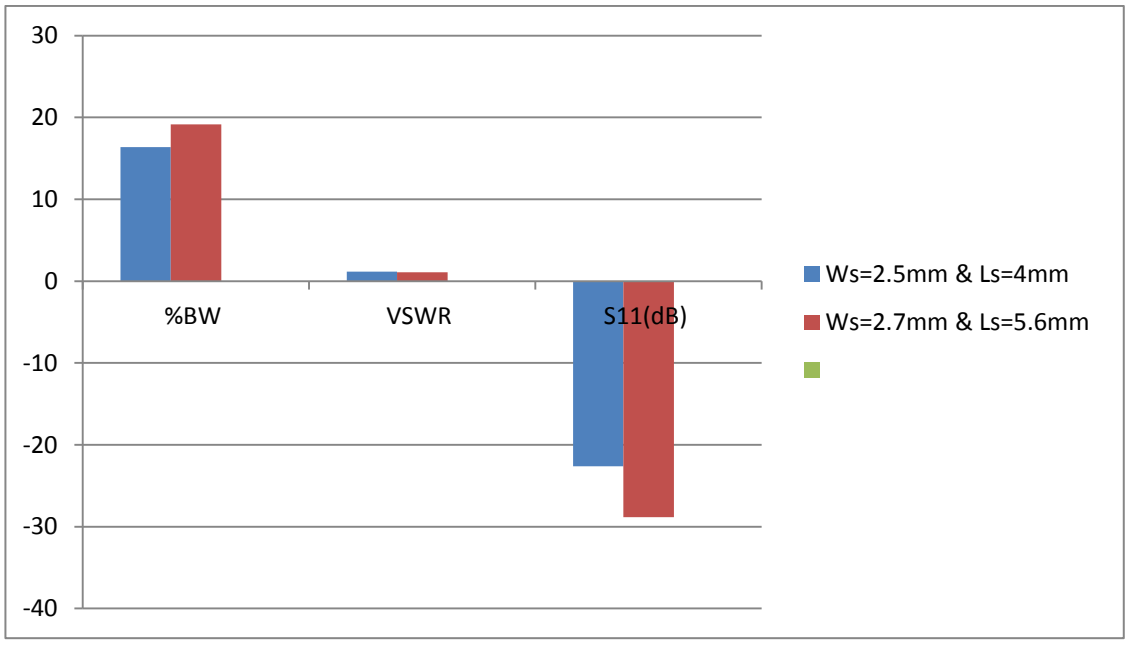

FIGURE 5.23 Parameters comparison base on selection of t_s

A patch antenna model with L = 30 mm and W = 23 mm along the patch square yielded a resonant frequency of 7.4 GHz, 10.7 GHz and 13 GHz, as well as an excellent resonant return loss and VSWR is less than 2.0 with different choice of t_s from 0.1 mm to 0.2 mm as listed in Table 5.4 and shown in Figure 5.23 and Figure 5.24 shows Bandwidth and return loss for triple notch band characteristics for actual RTFA design results.

TABLE 5.4 Parameters comparison base on selection of t_s

Parameter	%BW	VSWR	S_{11}(dB)
ts=0.1	16.03	1.38	-15.9
ts=0.15	16	1.12	-25.15
ts=0.2	**19.23**	**1.1**	**-26.74**

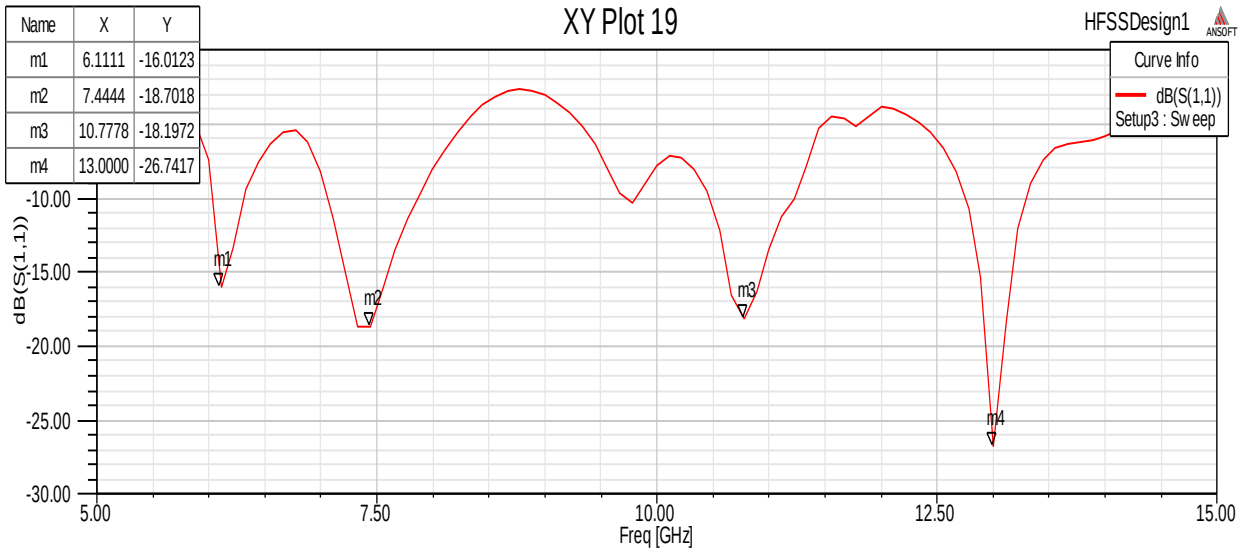

FIGURE 5.24 BW and Return loss base on selection of t_s = 0.2 mm

A patch antenna model with L = 30 mm and W = 23 mm along the patch square yielded a resonant frequency of 7.4 GHz, 10.7 GHz and 13 GHz, as well as an excellent resonant return loss and VSWR is less than 2.0 with different choice of W_s from 2.5 mm to 2.7 mm and L_s from 4 mm to 5.6 mm as listed in Table 5.5 and shown in Figure 5.25 and Figure 5.26 shows Bandwidth and return loss for triple notch band characteristics for actual RTFA design results.

TABLE 5.5 Parameters comparison base on selection of W_s and L_s

Parameter	%BW	VSWR	S_{11}(dB)
W_s=2.5 mm & L_s=4 mm	16.38	1.16	-22.6
W_s=2.7 mm & L_s=5.6 mm	**19.15**	**1.07**	**-28.85**

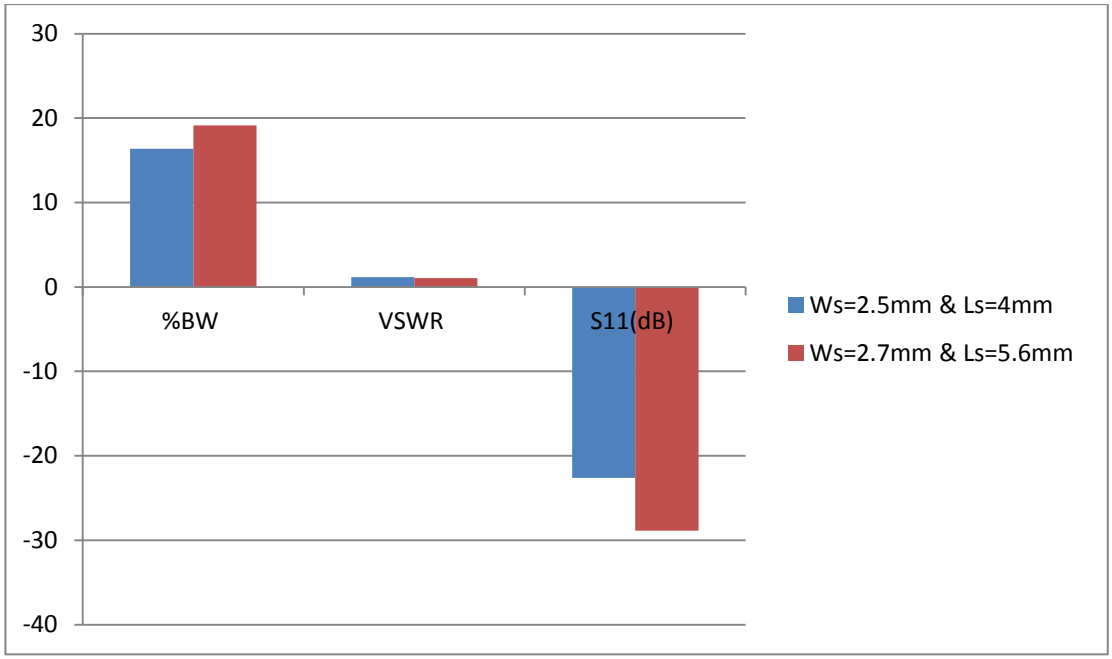

FIGURE 5.25 Parameters comparison base on selection of W_s and L_s

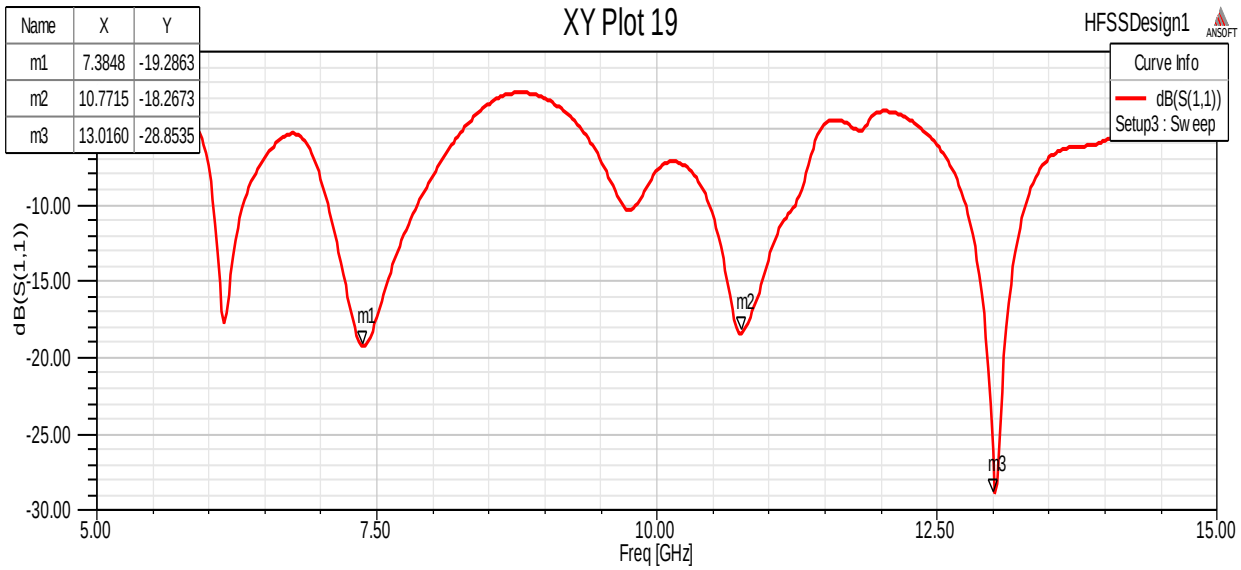

FIGURE 5.26 BW and Return loss base on selection of W_s=2.7 mm and L_s=5.6 mm

An excellent resonant return loss of -28.85 dB, Bandwidth of 19.23% and VSWR of 1.07 with finally preferred exact dimension and gain and directivity of around 6 dB and 7 dB respectively and also it is efficient upto 85% efficiency achieved. A RTFA novel model with L = 30 mm and W = 23 mm along the patch square yielded a triple notch band characteristics at resonant frequency of 7.4 GHz, 10.7 GHz and 13 GHz, as well as an excellent resonant return loss and VSWR and also bandwidth is enhance upto 19.23% shown in Table 5.6.

TABLE 5.6 Actual RTFA design simulation results

Parameters	Simulation Result
S_{11}(dB)	-28.85
VSWR	1.07
Directivity (dB)	7.66
Gain (dB)	6.17
Efficiency (%)	84.78
% BW	19.23

An excellent VSWR around 1.1 achieved by RTFA novel model with L = 30 mm and W = 23 mm along the patch square yielded a triple notch band characteristics at resonant frequency of 7.4 GHz, 10.7 GHz and 13 GHz shown in Figure 5.27 to 5.30.

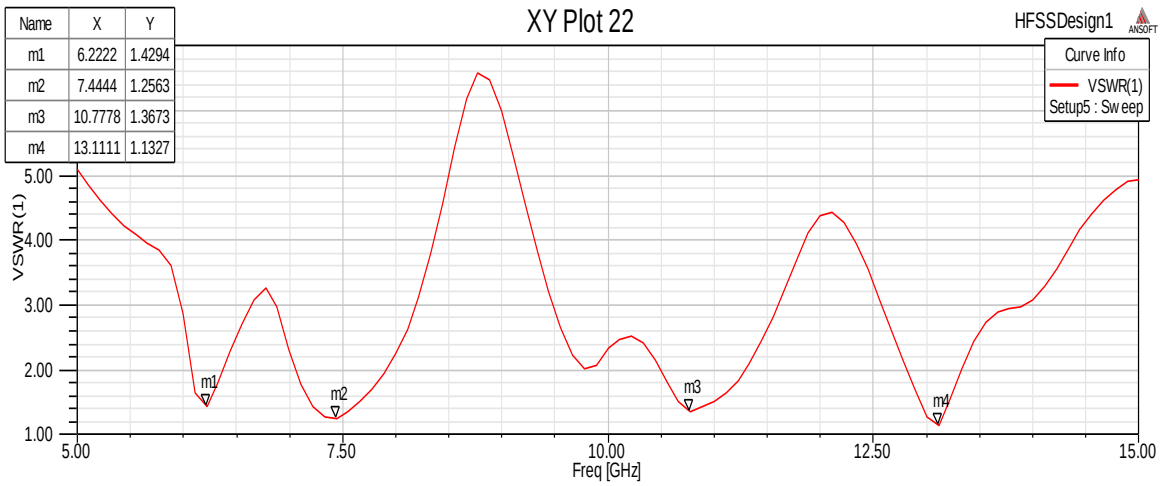

FIGURE 5.27 VSWR base on selection of L_2=8.5 mm

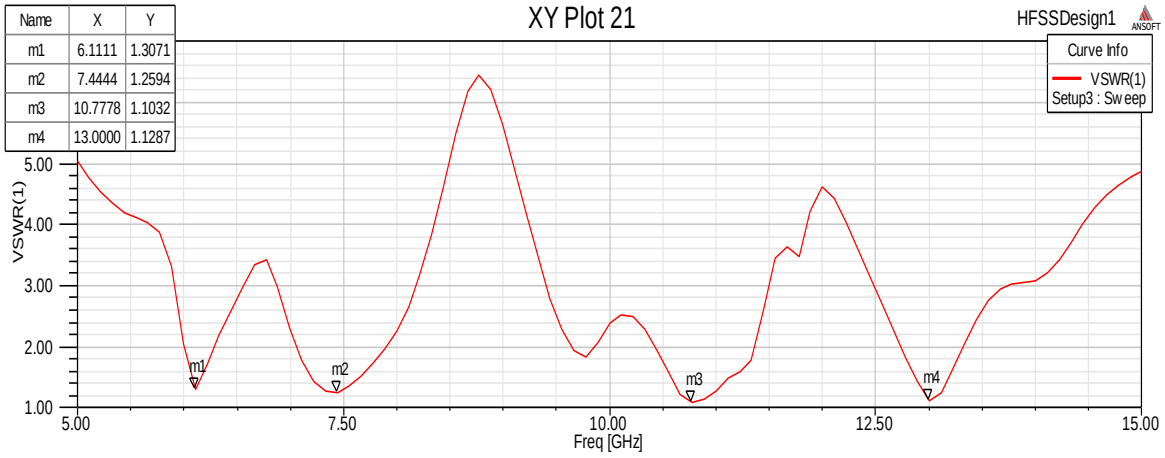

FIGURE 5.28 VSWR base on selection of L_4=5.8 mm

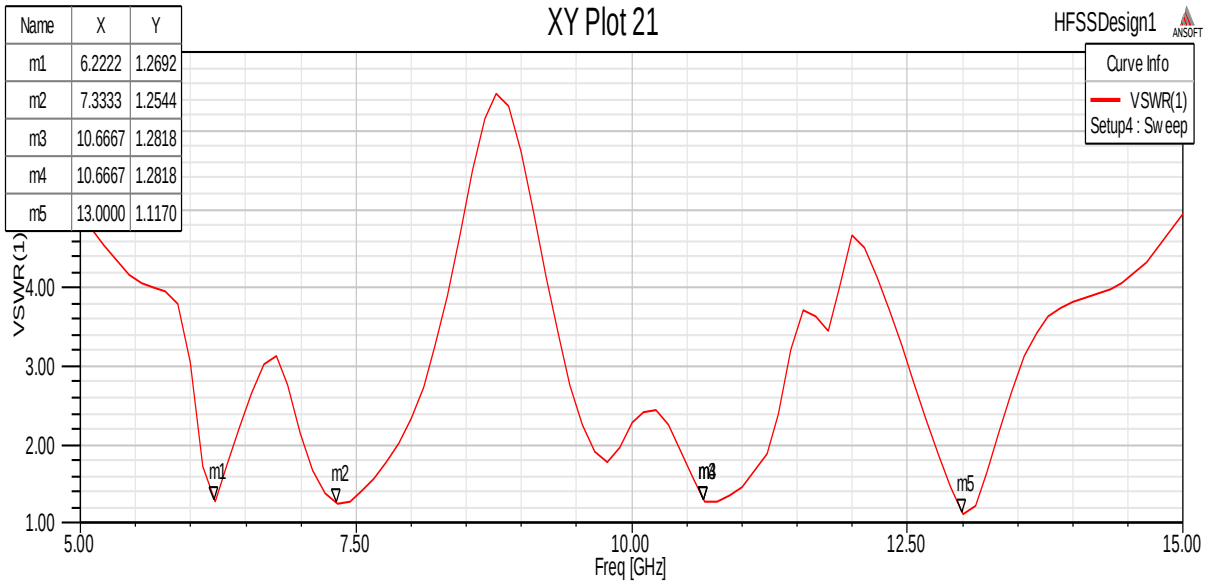

FIGURE 5.29 VSWR base on selection of t_s=0.2 mm

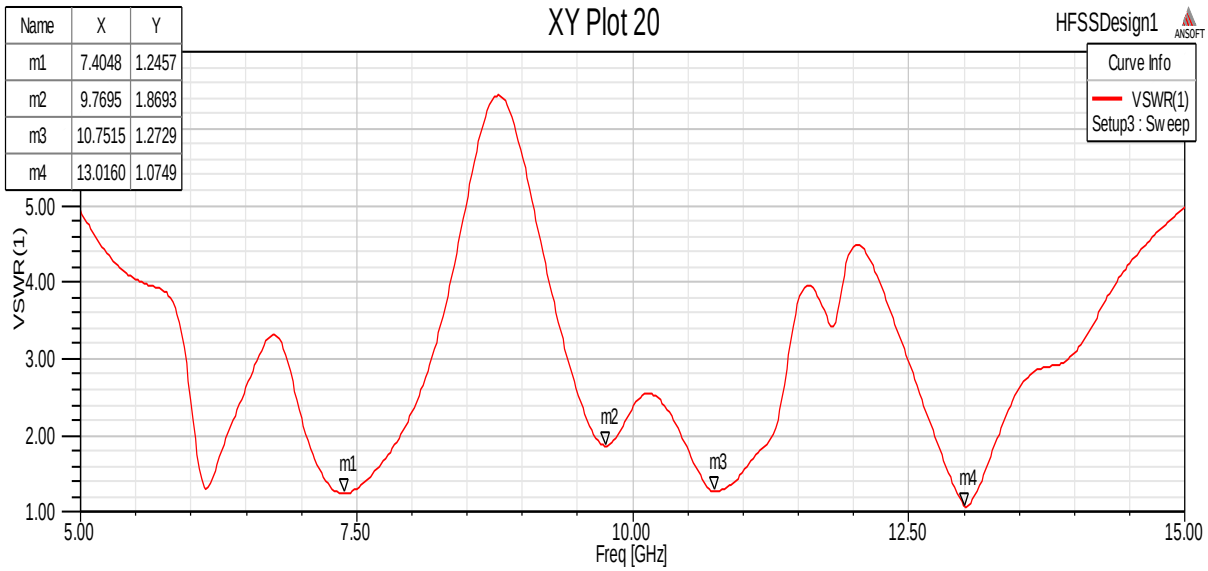

FIGURE 5.30 VSWR base on selection of W_s=2.7 mm and L_s=5.6 mm

Figure 5.31 shows (a) Gerber layout for fabrication and (b) the fabricated RTFA for (5.92 - 8.45 GHz) for WiMAX (worldwide interoperability for microwave access) and WiBRO (wireless broadband) in range of Fixed and Mobile satellite applications, (8.5 - 10.55 GHz) for Radio location and Aeronautical/Maritine radio navigation application and (12.75 - 14.5 GHz) for Land mobile satellite and Radio navigation operation with triple notches, and the overall size of the antenna is 30 × 23 × 1.6 mm^3 with appropriate values of actual novel RTFA design dimensions which shown in Table 5.1.

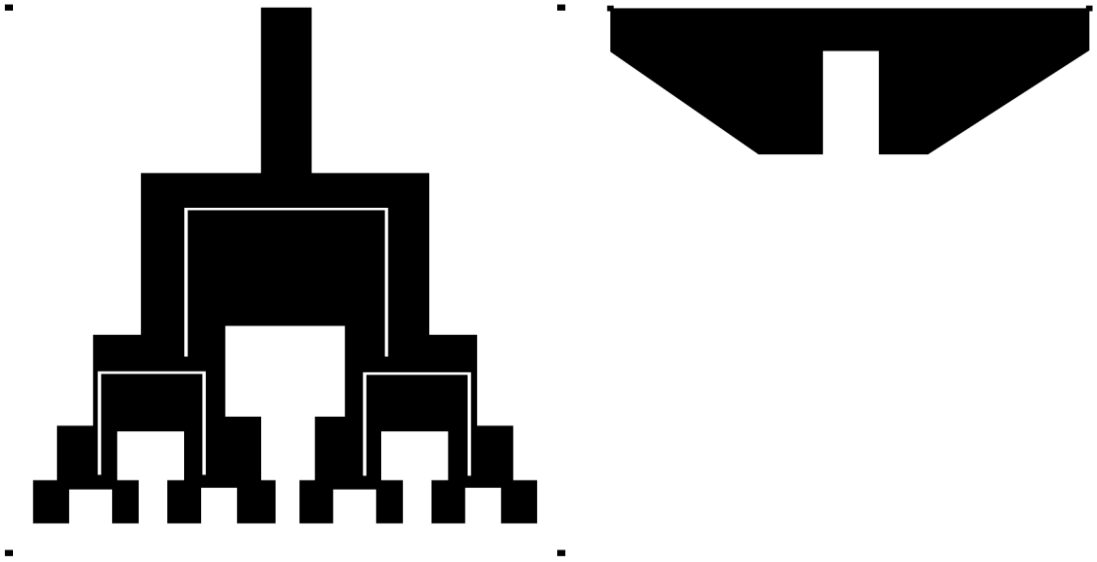

(a)

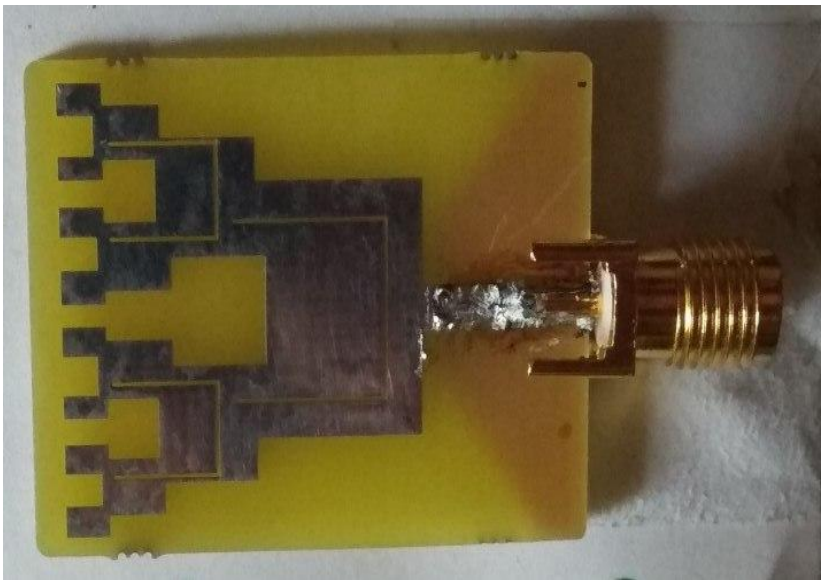

(b)

FIGURE 5.31 23×30×1.6 mm^3 tree fractal patch design (a) Gerber layout for fabrication and (b) the fabricated RTFA

The fabricated antenna is welded on the 50 Ω SMA connector and measured on vector network analyzer. Figure 5.32 shows measurement of RTFA using vector network analyser (VNA) and Figure 5.33(a) and (b) shows measured result of RTFA. Figure 5.34 shows the measured and simulated results of the proposed antenna.

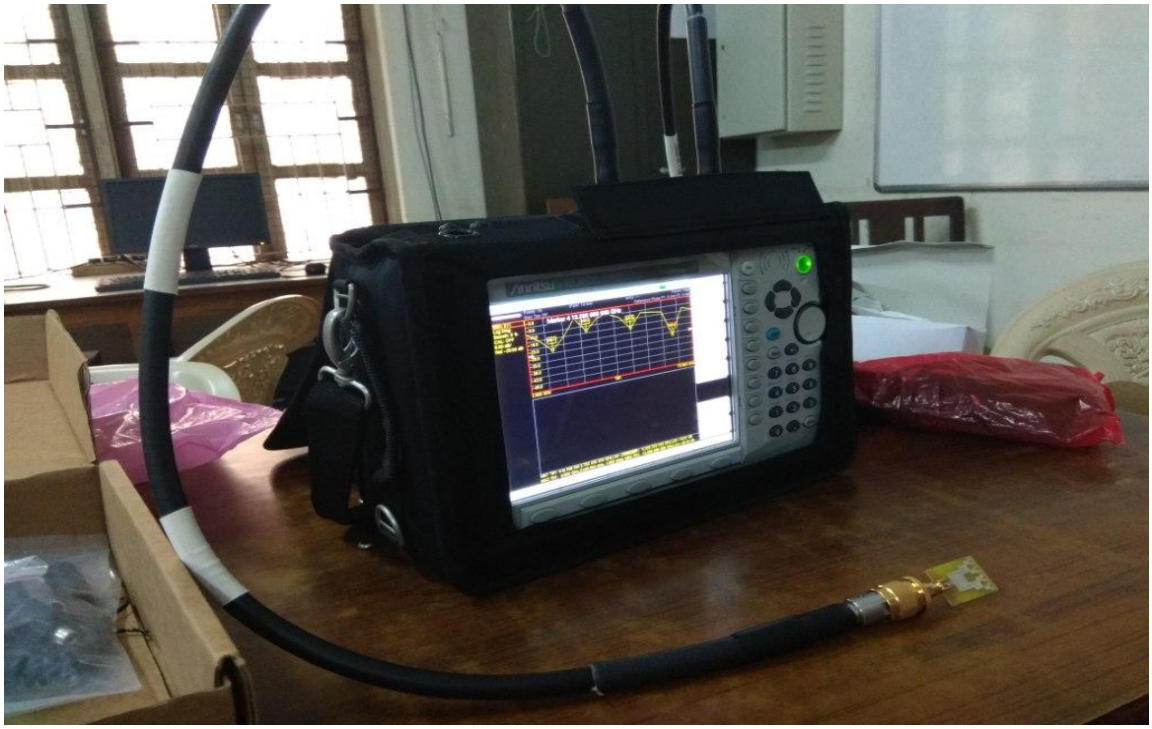

FIGURE 5.32 Measurement of RTFA using VNA

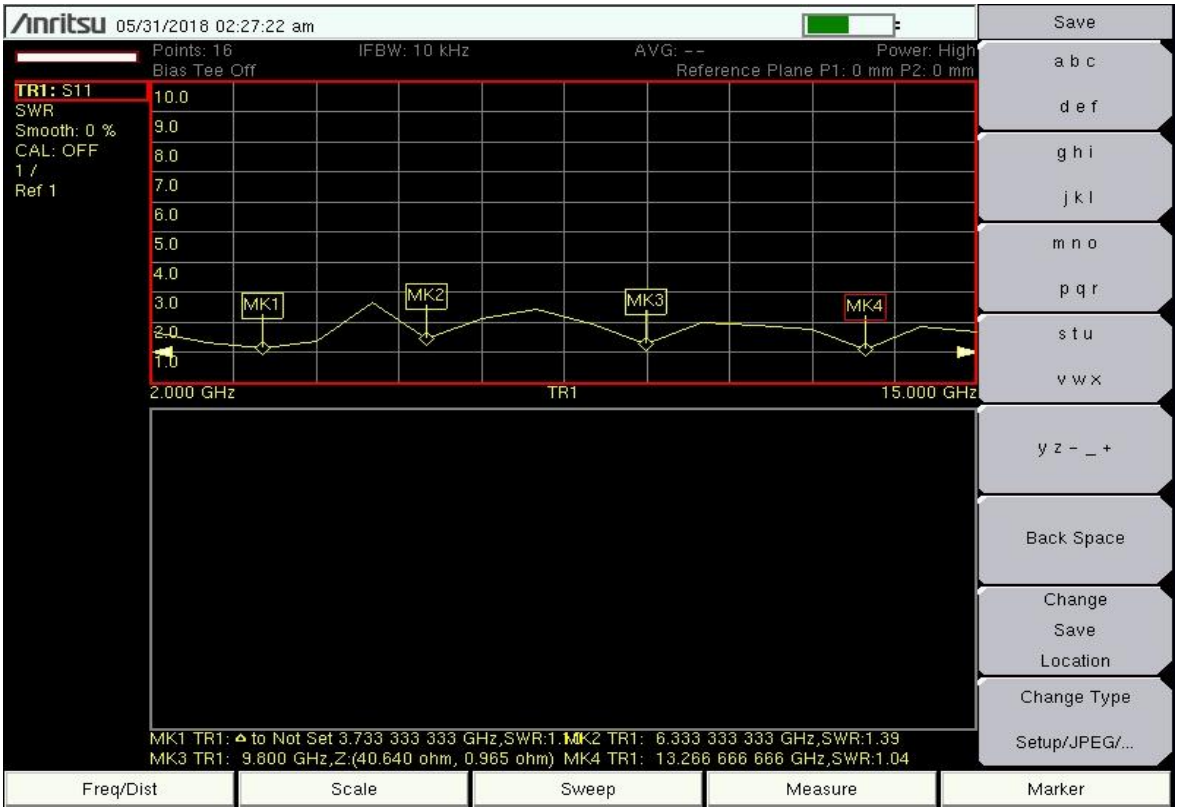

FIGURE 5.33(a) RTFA measurement of VSWR

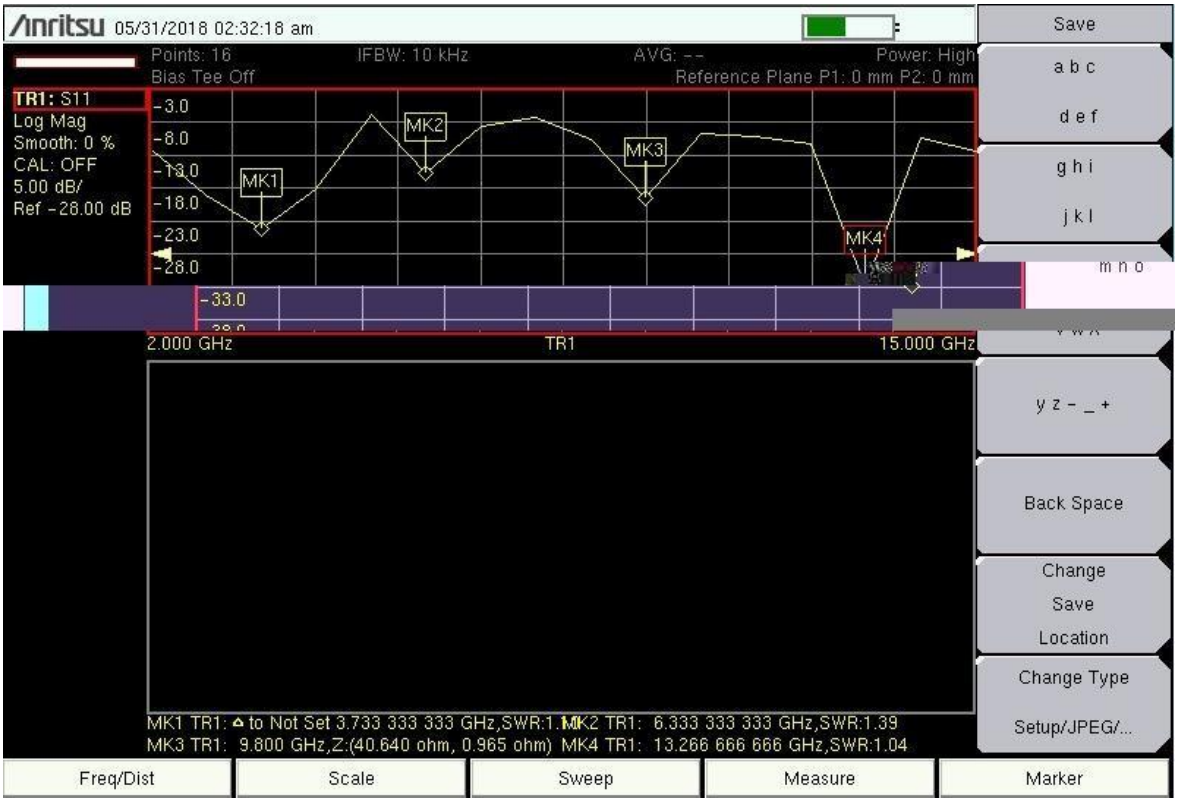

FIGURE 5.33(b) RTFA measurement of Return loss

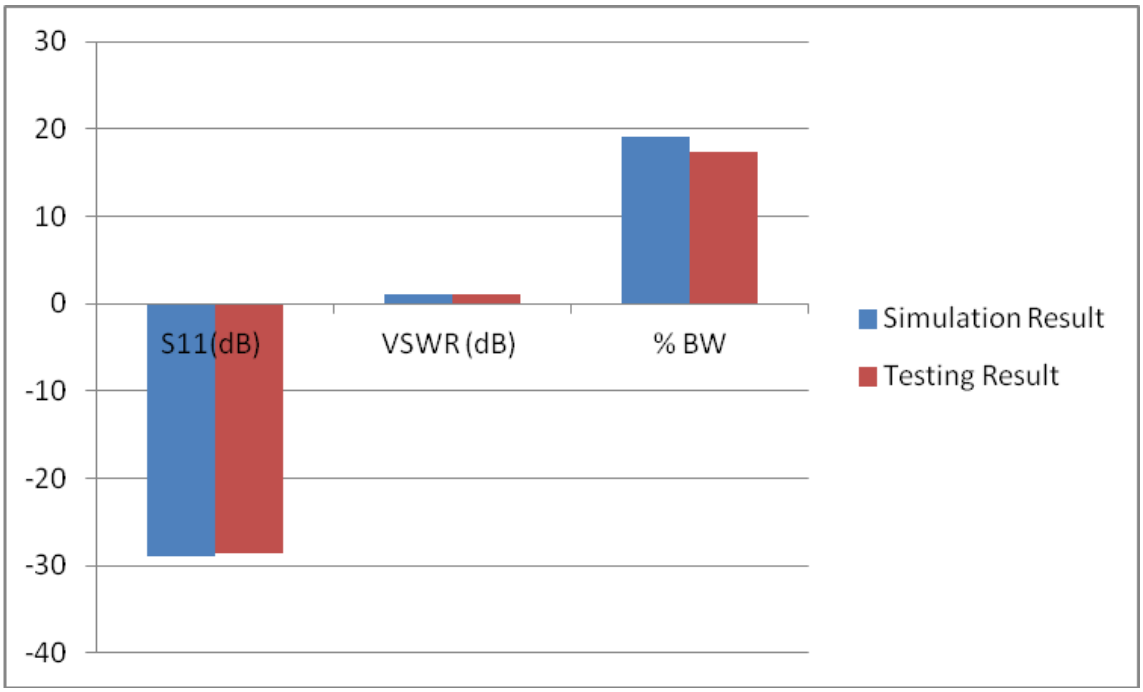

FIGURE 5.34 RTFA measured and simulation result

The experimental results have some deviations compared to the simulation results due to machining error and welding error. The test shows that the operating bandwidth

of the proposed RTFA covers the entire frequency band from 6 to 15 GHz, and including notch bands of (5.92 GHz – 8.45 GHz) for WiMAX, WiBRO, (8.5 GHz – 10.55 GHz) for RLAN and (12.75 GHz – 14.5 GHz) for LMS.

TABLE 5.7 RTFA performance analyses

Reference	**Size (mm^3)**	**Substrate**	**Operating band (GHz)**	**Notch Band (GHz)**
Sengupta, K. and K. J. Vinoy, 2006 [20]	42 × 36 × 1.6	FR4	3.7 – > 18	-
S. Ramo, J. R. Whinnery, 1944 [66]	34 × 34 × 1.6	FR4	3.1 – > 10.6	5GHz to 6GHz
Werner, D. H. and S. Ganguly, 2003 [21]	50 × 50 × 1.57	Taconic	2.3 – > 11	6.2GHz to 6.9GHz
Choukiker, Y. K. and S. K. Behera, 2014 [24]	50 × 50 × 1.6	FR4	5.52 – > 10.7	-
Zhao, X. Y., H. G. Zang, and G. L. Zhang, 2015 [25]	30 × 23 × 1	FR4	2.62 – > 11	3.3GHz to 4.08GHz & 5.04GHz to 6.03GHz
This thesis work (Reference figures: 5.27 to 5.30 and 5.33)	30 × 23 × 1.6	FR4	6 – > 15	5.92GHz to 8.45GHz & 8.5GHz to 10.55GHz & 12.75GHz to 14.5GHz

Table 5.7 compares the proposed novel RFTA antenna characteristic to some other antennas presented in (Sengupta, K. and K. J. Vinoy, 2006 and S. Ramo, J. R. Whinnery, 1944), (Werner, D. H. and S. Ganguly, 2003 and Choukiker, Y. K. and S. K. Behera, 2014) and (Zhao, X. Y., H. G. Zang, and G. L. Zhang, 2015). It is clear that the proposed

RTFA is smaller. Some of the other antennas are large in size, have no notch band or cannot cover the whole band of UWB and also operating upto dual notch band characteristics.

5.4 Summary

A novel rectangle tree fractal antenna (RTFA) for ultra-wideband (UWB) and LMS application with triple band notch characteristics is proposed. The radiating path is the tree fractal structure which is formed by the superposition of a number of rectangular patches, and multi-frequency resonance characteristics are obtained by only increasing the tree fractal iterations. The proposed RTFA covers the entire frequency band from 6 to 15 GHz, and including notch bands of (5.92 GHz – 8.45 GHz) for WiMAX, WiBRO, (8.5 GHz – 10.55 GHz) for RLAN and (12.75 GHz – 14.5 GHz) for LMS is achieved by using defected ground structure (DGS) on the ground plane to improve the impedance characteristics between adjacent resonant frequencies. The triple notch bands characteristics are realized by three U-slots on the tree fractal path and effectively suppress the interferences. The measurement and simulation results have an acceptable agreement, and indicate that the antenna is suitable for WiMAX, WiBRO, RLAN and LMS applications.

In the notch bands, the gain decreases sharply and maintains stable in the working band. The time domain characteristics show that the proposed antenna can maintain a small distortion in the operating band. All these simulations and measurements imply that the antenna can be widely used in various satellite communication systems.

CHAPTER 6

Conclusion and Future work

6.1 Conclusion

The range between 3 GHz to 300 GHz is extremely packed out, with numerous services and applications even occupying the same frequencies in many cases. The DGS ground plane has two symmetrically bevelling corners and a rectangular gap with a size of $L_s \times W_s$ on a rectangular ground plane. Three U shaped slots with air gap of t_s are provided on the tree fractal patch to suppress the interference due to (5.92 GHz – 8.45 GHz) for WiMAX (worldwide interoperability for microwave access) and WiBRO (wireless broadband) in range of Fixed and Mobile satellite applications, (8.5 GHz – 10.55 GHz) for RLAN (Radio location and Aeronautical/Maritine radio navigation) and (12.75 GHz – 14.5 GHz) for LMS (Land mobile satellite and Radio navigation) applications.

Selection of appropriate materials and feeding methods are presented in thesis and also introduced number of slots/slits in primary design enhance improve the BW and VSWR and also triple band characteristics are achieved. Selection of dimension parameters is base on the application oriented frequency band and also taken care about impedance matching and reactance effect on radiation. 23×30 square tree fractal patch is design base on primary dimension

In addition, the rectangular gap in the DGS ground plane is very important to the performance of the antenna, because the capacitance introduced by the rectangular gap can offset a part of inductive capacitance of antenna and improve the impedance matching in the whole band. In this, the sizes of the rectangular gap are divided into different groups.

An excellent resonant return loss of -28.85 dB, Bandwidth of 19.23% and VSWR of 1.07 with finally preferred exact dimension and gain and directivity of around 6 dB and 7 dB

respectively and also it is efficient upto 85% efficiency achieved. A RTFA novel model with L = 30 mm and W = 23 mm along the patch square yielded a triple notch band characteristics at resonant frequency of 7.4 GHz, 10.7 GHz and 13 GHz, as well as an excellent resonant return loss and VSWR and also bandwidth is enhance upto 19.23%.

The experimental results have some deviations compared to the simulation results due to machining error and welding error. The test shows that the operating bandwidth of the proposed RTFA covers the entire frequency band from 6 to 15GHz, and including notch bands of (5.92 GHz – 8.45 GHz) for WiMAX, WiBRO, (8.5 GHz – 10.55 GHz) for RLAN and (12.75 GHz – 14.5 GHz) for LMS.

A novel rectangle tree fractal antenna (RTFA) for ultra-wideband (UWB) and LMS application with triple band notch characteristics is proposed. The radiating path is the tree fractal structure which is formed by the superposition of a number of rectangular patches, and multi-frequency resonance characteristics are obtained by only increasing the tree fractal iterations. The proposed RTFA covers the entire frequency band from 6 to 15 GHz, and including notch bands of (5.92 GHz – 8.45 GHz) for WiMAX, WiBRO, (8.5 GHz – 10.55 GHz) for RLAN and (12.75 GHz – 14.5 GHz) for LMS is achieved by using defected ground structure (DGS) on the ground plane to improve the impedance characteristics between adjacent resonant frequencies. The triple notch bands characteristics are realized by three U-slots on the tree fractal path and effectively suppress the interferences. The measurement and simulation results have an acceptable agreement, and indicate that the antenna is suitable for WiMAX, WiBRO, RLAN and LMS applications.

6.2 Future work

In multichannel applications, the antenna is required to operate over a broad BW to cover all the channels. However, at any given time, it requires a small BW to cover a single channel. In this case, a tunable MSA is required. If the antenna is designed to operate at two far away frequencies, then a dual and triple band MSA could be used. Various techniques have been described to tune the resonance frequency of the MSA. The tuning of the resonance frequency around the 15 to 20% range is achieved by loading the MSA with external reactive components such as stubs, shorting posts, and varactor and PIN diodes. The frequency is also tuned by varying the thickness of the air gap between

the patch substrate and the ground plane. This tunable configuration may be achieved by applying external reactive components. Same configuration may be design by additional concept of tuning characteristic and it is simultaneously applicable for all notch band applications.

References

Research Journal Paper

[1] Munson, R. E., ‘‘Conformal Microstrip Antennas and Microstrip Phased Arrays,’’ IEEE Trans. Antennas Propagation, Vol. AP-22, 1974, pp. 74–78.

[2] Howell, J. Q., ‘‘Microstrip Antennas,’’ IEEE Trans. Antennas Propagation, Vol. AP-23, January 1975, pp. 90–93.

[3] Carver, K. R., and J. W. Mink, ‘‘Microstrip Antenna Technology,’’ IEEE Trans. Antennas Propagation, Vol. AP-29, January 1981, pp. 2–24.

[4] Mailloux, R. J., et al., ‘‘Microstrip Array Technology,’’ IEEE Trans. Antennas Propagation, Vol. AP-29, January 1981, pp. 25–37.

[5] James, J. R., et al., ‘‘Some Recent Development in Microstrip Antenna Design,’’ IEEE Trans. Antennas Propagation, Vol. AP-29, January 1981, pp. 124–128.

[6] Y. T. Lo, D. Solomon and W. F. Richards, “Theory and experiment on microstrip antennas,” IEEE Trans. Antennas Propagat., Vol. AP-27, pp. 137–145, 1979.

[7] W. F. Richards, Y. T. Lo and D. D. Harrison, “An improved theory for microstrip antennas and applications,” IEEE Trans. Antennas Propagat., Vol. AP-29, pp. 38–46, 1981.

[8] C. Wood, “Analysis of microstrip circular patch antennas,” IEE Proc. Vol. 128H, pp. 69–76, 1981.

[9] K. F. Lee and J. S. Dahele, “Characteristics of microstrip patch antennas and some methods of improving frequency agility and bandwidth,” in Handbook of Microstrip Antennas, J. R. James and P. S. Hall (Editors), Peter Peregrinus, Ltd., London, 1989.

[10] Wu, J. N., Z. Q. Zhao, Z. Q. Nie, and Q. H. Liu “A printed UWB vivaldi antenna using stepped connection structure between slotline and tapered patches,” IEEE Antennas and Wireless Propagation Letters, Vol. 11, 698–701, 2014.

[11] Ma, K., Z. Q. Zhao, J. N. Wu, M. S. Ellis, and Z. P. Nie, “A printed vivaldi antenna with improved radiation patterns by using two pairs of eye-shaped slots for UWB applications,” Progress In Electromagnetic Research, Vol. 148, 63–67, 2014.

[12] Nassar, I. T. and T. M. Weller "A novel method for improving antipodal vivaldi antenna performance," IEEE Transactions on Antennas and Propagation, Vol. 63, No. 7, 3321–3324, 2015.

[13] Natarajan, R., J. V. George, M. Kanagasabai, and A. K. Shrivastav, "A compact antipodal Vivaldi antenna for UWB applications," IEEE Antennas and Wireless Propagation Letters, Vol. 14, 1557–1560, 2015.

[14] Amini, A., H. Oraizi, andM. A. C. Zadeh, "Miniaturized UWB log-periodic square fractal antenna,"IEEE Antennas and Wireless Propagation Letters, Vol. 14, 1322–1325, 2014.

[15] Liang, J. X., C. C. Chiau, X. D Chen, and C. G. Parini, "Study of a printed circular disc monopole antenna for UWB systems," IEEE Transactions on Antennas and Propagation, Vol. 53, No. 11, 3500–3504, 2005.

[16] Gong, B., J. L. Li, Q. R. Zheng, Y. Z. Yin, and X. S. Ren, "A compact inductively loaded monopole antenna for future uwb applications," Progress In Electromagnetic Research, Vol. 139, 265–275, 2013.

[17] Dikmen, C. M., S. Cimen, and G. Cakr, "Planar octagonal-shaped UWB antenna with reduced radar cross section," IEEE Transactions on Antennas and Propagation, Vol. 62, No. 6, 2946–2953, Jun. 2014.

[18] Steven, R. B., "A discussion on the significance of geometry in determining the resonant behavior of fractal and other non-euclidean wire antennas,"IEEE Antennas and Propagation Magazine, Vol. 45, No. 3, 9–28, 2003.

[19] Comisso, M., "On the use of dimension and lacunarity for comparing the resonant behavior of convoluted wire antennas," Progress In Electromagnetic Research, Vol. 96, 361–376, 2009.

[20] Sengupta, K. and K. J. Vinoy, "A new measure of lacunarity for generalized fractals and its impact in the electromagnetic behavior of Koch dipole antennas," Fractals, Vol. 14, No. 4, 271–282, 2006.

[21] Werner, D. H. and S. Ganguly, "An overview of fractal antenna engineering research," IEEE Antennas and Propagation Magazine, Vol. 45, No. 1, 38–57, 2003.

[22] Mahatthanajatuphat, C., P. Akkaraekthalin, S. Saleekaw, and M. Krairiksh, "A bidirectional multiband antenna with modified fractal slot fed by CPW," Progress In Electromagnetic Research, Vol. 95, 69–72, 2009.

[23] Dhar, S., K. Patra, R. Ghatak, B. Gupta, and D. R. Poddar, "A dielectric resonator-loaded minkowski fractal-shaped slot loop heptaband antenna," IEEE Transactions on Antennas and Propagation, Vol. 63, No. 4, 1521–1529, Apr. 2015.

[24] Choukiker, Y. K. and S. K. Behera, "Modified Sierpinski square fractal antenna covering ultrawide band application with band notch characteristics," IET Microwaves, Antennas & Propagation, Vol. 8, No. 7, 506–512, 2014.

[25] Zhao, X. Y., H. G. Zang, and G. L. Zhang, "A novel ultra-wideband fractal tree-shape antenna,"Journal of Electronic & Information Technology, Vol. 37, No. 4, 1008–1012, 2015.

[26] Li, T., H. Q. Zhai, and G. H. Li, "Compact UWB band-notched antenna design using interdigital capacitance loading loop resonator," IEEE Antennas and Wireless Propagation Letters, Vol. 11, 724–727, 2012.

[27] Ojaroudi, N. and M. Ojaroudi, "Novel design of dual band-notched monopole antenna with bandwidth enhancement for UWB applications," IEEE Antennas and Wireless Propagation Letters, Vol. 12, 698–701, 2013.

[28] Li, Y. S., W. X. Li, and Q. B Ye, "A CPW-fed circular wide-slot UWB antenna with dual-notch bands by combining slot and parasitic element techniques," Microwave and Optical Technology Letters, Vol. 56, No. 5, 1240–1244, 2014.

[29] Weng, Y. F., S. W. Cheung, and T. I. Yuk, "Design of multiple band-notch using meander lines for compact ultra-wide band antennas," IET Microwaves, Antennas & Propagation Vol. 6, No. 8, 908–914, 2012.

[30] Liu, X. l., Y. Z. Yin, P. G. Liu, J. H. Wang, and B. Xu, "A CPW-fed dual band-notched UWB antenna with a pair of bended dual-L-shape parasitic branches," Progress In Electromagnetic Research, Vol. 136, 623–634, 2013.

[31] Gheethan, A. A. and D. E. Anagnostou, "Dual band-reject UWB antenna with sharp rejection of narrow and closely-spaced bands," IEEE Transactions on Antennas and Propagation, Vol. 60, No. 4, 2071–2076, Apr. 2015.

[32] Wu, Z. H., F. Wei, X. W. Shi, and W. T. Li, "A compact quad band-notched UWB monopole antenna loaded one lateral l-shaped slot," Progress In Electromagnetic Research, Vol. 139, 303–315, 2013.

[33] Gao, P., L. Xiong, J. B. Dai, S. He, and Y. Zheng, "Compact printed wide-slot UWB antenna with 3.5/5.5-GHz dual band-notched characteristics," IEEE Antennas and Wireless Propagation Letters, Vol. 12, 983–986, 2013.

[34] Ma, T. G. and J. W. Tsai, "Band-rejected ultra wideband planar monopole antenna with high frequency selectivity and controllable bandwidth using inductively coupled resonator pairs," IEEE Transactions on Antennas and Propagation, Vol. 58, No. 8, 2747–2752, Aug. 2010.

[35] Zhang, Y., W. Hong, and C. Yu, "Design and implementation of planar ultra-wideband antennas with multiple notched bands based on stepped impedance resonators," IET Microwaves, Antennas & Propagation, Vol. 3, No. 7, 1051–1059, 2012.

[36] Dong, Y. D., W. Hong, Z. Q. Kuai, C. Yu, Y. Zhang, J. Y. Zhou, and J. X. Chen, "Development of ultrawideband antenna with multiple band-notched characteristics using half mode substrate integrated waveguide cavity technology," IEEE Transactions on Antennas and Propagation, Vol. 56, No. 9, 2894–2901, Sep. 2008.

[37] Siddiqui, J. Y., C. Saha, and Y. M. M. Antar, "Compact dual-srr-loaded UWB monopole antenna with dual frequency and wideband notch characteristics," IEEE Antennas and Wireless Propagation Letters, Vol. 14, 100–103, 2015.

[38] Dhar, S., R. Ghatak, B. Gupta, and D. R. Poddar, "A wideband minkowski fractal dielectric resonator antenna," IEEE Transactions on Antennas and Propagation, Vol. 61, No. 6, 2895–2903, Jun. 2013.

[39] Tian Tiehong, Zhou Zheng, A Novel Multiband Antenna: Fractal Antenna, Proceedings of ICCT, 2003.

[40] Kai da xu, han xu, yanhui liu, jianxing li, and qing huo liu, Microstrip Patch Antennas with Multiple Parasitic Patches and Shorting Vias for Bandwidth Enhancement, IEEE March 16, 2018.

[41] Emre Erdil, Kagan Topalli, Mehmet Unlu, Ozlem Aydin Civi, and Tayfun Akin, Frequency Tunable Microstrip Patch Antenna Using RF MEMS Technology, IEEE transactions on antennas and propagation, vol. 55, no. 4, april 2007.

[42] Sang-Hyuk Wi, Yong-Shik Lee, and Jong-Gwan Yook, Wideband Microstrip Patch Antenna with U-Shaped Parasitic Elements, IEEE transactions on antennas and propagation, vol. 55, no. 4, april 2007.

[43] Yazan al-alem , and ahmed a. Kishk, Low-Profile Low-Cost High Gain 60 GHz Antenna, IEEE March 28, 2018.

[44] Alireza Motevasselian1 , William G. Whittow, Patch size reduction of rectangular microstrip antennas by means of a cuboid ridge, IET Microwaves, Antennas & Propagation, 2nd July 2015.

[45] Intan Helina Hasan, Mohd Nizar Hamidon, Alyani Ismail, YIG Thick Film as Substrate Overlay for Bandwidth Enhancement of Microstrip Patch Antenna, IEEE, 2017.

[46] M. M. Islam, M. T. Islam, M.Samsuzzaman, M. R. I. Faruque, and N. Misran, Omni-directional Microstrip Monopole Antenna For UWB Microwave Imaging System, IEEE, 2015.

[47] L. Hadj Abderrahmane, M. Benyettou, M. N. Sweeting, An S Band Antenna System Used for Communication on Earth Observation Microsatellite, IEEE November 15, 2005.

[48] Pichet Moeikham, Prayoot Akkaraekthalin, A Compact Printed Slot Antenna with High Out-of-band Rejection for WLAN/WiMAX Applications, RADIOENGINEERING, Sep, 2015.

[49] Chatree mahatthanajatuphat, narintra srisoontorn, thanakarn suangun, Prayoot akkaraekthalin, A Wideband Slot Antenna with Folded Parasitic Line for Multiple Band Operation, RADIOENGINEERING, Dec, 2016.

[50] Zhangfang Hu, Yinping Hu, Yuan Luo, and Wei Xin, A Novel Rectangle Tree Fractal UWB Antenna with Dual Band-Notched Characteristics, Electromagnetics Research C, Vol. 68, 21–30, 2016.

[51] Priyanka Kakaria, Rajesh Nema, Review and Survey of Compact and Broadband Microstrip Patch Antenna, IEEE International Conference on Advances in Engineering & Technology Research (ICAETR - 2014), August 01-02, 2014.

[52] Wen-Shan Chen and Chin-Hsin Kao, A study of the broadband printed rectangular slot antenna with a 3D microstrip-line fed, IEEE, 2005.

[53] Chi Sang You and Woonbong Hwang, Gain Enhancement Method of Microstrip Antennas by Dielectric Cover, Considering Bandwidth, IEEE, 2005.

Bappadittya Roy, Ankan Bhattacharya, A.K.Bhattacharjee, S.K.Chowdhury, Effect of Different Slots in a Design of Microstrip Antennas, IEEE sponsored second international conference on electronics and communication

Systems (ICECS ‘2015).

[54] Meriem Harbadji, Amel Boufrioua, Investigation of rectangular multi-band microstrip patch antennas with slots, IEEE, 2014.

[55] J.R. James and G.J. Wilson, Microstrip antennas and arrays. Pt. 1 - Fundamental action and limitations, microwaves, optics and acoustics, vol. 1, no., September 1977.

[56] R A Abd-Alhameed, N J McEwan, P S Excell, M M Ibrahim, Z M Hejazi and M Musa, New Procedure For Design Of Microstrip Patch Antennas Using Method Of Moments, Antennas and Propagation, 14-17 April 1997.

[57] Aditi Mandal, Antara Ghosal, Anurima Majumdar, Analysis of Feeding Techniques of Rectangular Microstrip Antenna, IEEE, 2012.

[58] A. Henderson and Prof. J.R. James, Design of microstrip antenna feeds Part 1: Estimation of radiation loss and design implications, IIEEE PROC, Vol. 128, Pt. H, No. 1, February 1981.

[59] A. G. Derneryd, "Linearly Polarized Microstrip Antennas," IEEE Trans. Antennas Propagat., vol. AP-24, no. 6 (November 1976): 846–850.

[60] H. A. Wheeler, "Transmission-line properties of parallel strips separated by a dielectric sheet",IEEE Trans. Microwave Theory and Techniques, vol. MTT-13, pp. 172-185, March 1965.

[61] C. P. Hartwig, D. Massé, R. A. Pucel, "Frequency dependent behavior of microstrip", G-MTT Internat'l Microwave Symp., 1968-May-20-22.

[62] J. D. Welch, H. J. Pratt, "Losses in microstrip transmission systems for integrated microwave circuits", NEREM Rec., vol. 8, pp. 100-101, 1966.

[63] F. Assadourian, E. Rimai, "Simplified theory of microstrip transmission systems", Proc. IRE, vol. 40, pp. 1651-1657, December 1952

[64] J. M. C. Dukes, "An investigation into some fundamental properties of strip transmission lines with the aid of an electrolytic tank", Proc. IEE, vol. 103, pp. 319-333, 1956

[65] T. M. Hyltin, "Microstrip transmission on semiconductor dielectrics", IEEE Trans. Microwave Theory and Techniques, vol. MTT-13, pp. 777-781, November 1965

[66] S. Ramo, J. R. Whinnery, "8" in Fields and Waves in Modern Radio, New York:Wiley, 1944

[67] E. Gaál, "Current distribution on a strip line", Acta Tech. (Budapest), vol. 38, pp. 387-397, 1962

[68] J. D. Cockcroft, "Skin effect in rectangular conductors at high frequencies", Proc. Roy. Soc. (London), vol. 122, pp. 533-542, 1929

[69] M. Caulton, J. J. Hughes, H. Sobol, "Measurements on the properties of microstrip transmission lines for microwave integrated circuits", RCA Rev., vol. 27, pp. 377-391, 1966

[70] G. D. Vendelin, "High-dielectric substrate for microwave hybrid integrated circuitry", IEEE Trans. Microwave Theory and Techniques (Correspondence), vol. MTT-15, pp. 750-752, December 1967

[71] H. A. Wheeler, "Formulas for the skin effect", Proc. IRE, vol. 30, pp. 412-424, September 1942

[72] C. G. Shafer, Higher mode of the microstrip transmission line, November 1957

[73] M. Sucher, J. Fox, "8" in Handbook of Microwave Measurements, New York:Polytechnic Press, vol. II, pp. 417-495, 1963

[74] Wu, J. N., Z. Q. Zhao, Z. Q. Nie, and Q. H. Liu "A printed UWB vivaldi antenna using stepped connection structure between slotline and tapered patches," IEEE Antennas and Wireless Propagation Letters, Vol. 11, 698–701, 2014

[75] MARKS, R., B.: The IEEE 802.16 Working Group on Broadband Wireless Access Standards, IEEE, Inc., 2007, online: <http://www.ieee802.org/16>

Book

[1] James, J. R., and P. S. Hall, Handbook of Microstrip Antennas, Vol. 1, London: Peter Peregrinus Ltd., 1989.

[2] Girish Kumar, K. P. Ray, Broadband Microstrip Antennas, Artech House antennas and propagation library, ISBN 1-58053-244-6, 2003

[3] David R. Jackson, Antenna Engineering Handbook, Volakis Chapter 7, 147574-5, 2007

[4] R. S. Elliott, Antenna Theory and Design, Prentice Hall, 1981, Chapter 3 and 7.

[5] R. E. Collin, Foundations of Microwave Engineering, Second Edition, McGraw-Hill, Inc. New York, 1992.

[6] D. R. Jackson, J. T. Williams, and D. R. Wilton, "Antennas-II," Handbook of Engineering Electromagnetics, Chapter 9, Rajeev Bansal (ed.) (New York: Marcel Dekker, 2004).

[7] J. D. Kraus, Antennas, 2nd Ed. (New York: McGraw-Hill, 1988).

[8] W. F. Richards, "Microstrip Antennas," Antenna Handbook: Theory, Applications, and Design, Chapter 10, Y. T. Lo and S. W. Lee (eds.) (New York: Van Nostrand Reinhold, 1993).

[9] C. A. Balanis, Antenna Theory: Analysis and Design, 3rd Ed. (New York: John Wiley & Sons, 2005).

Symposium and Patent

[1] Deschamps, G. A., ‘‘Microstrip Microwave Antennas,’’ Proc. 3rd USAF Symposium on Antennas, 1953.

[2] Munson, R. E., ‘‘Single Slot Cavity Antennas Assembly,’’ U.S. Patent No. 3713162, January 23, 1973.

Publications

Journal Paper

- Ratansing N Patel, Dr. Vipul Shah, Jayesh Patel, "*Review and Analytical Survey on RMPA Design*" in International Journal of Advance Research in Science and Engineering, ISSN-2319-8354, Volume 6, Issue 8, August 2017, (page no. 1762-1768), (UGC approved and SCOPUS indexed)
- Ratansing N Patel, Dr. Vipul Shah, "*Rectangular Patch Antenna with Tree Fractal Structure*" in Journal of Applied Science and Computations, ISSN-1076-5131, Volume 5, Issue 12, December 2018, (page no. 882-895), (UGC approved and SCOPUS indexed)
- Ratansing N Patel, Dr. Vipul Shah, "*Rectangular Tree Fractal Patch Antenna with Multi band Notched Characteristics*" in IEEE Transactions on Antennas and Propagation, manuscript ID is AP1812-2321(Under Review)

Conference Paper

- R.N. Patel, Dr. Vipul A. Shah, "*Substrate material effect on MPA design parameter*", 1st International Conference on Advances in Engineering (SITICAiE–2015) on 22nd and 23rd January, 2015 at S.P.B.Patel Engineering College, Linch-Mehsana (1st prize young author winner) collaboration with Indian Journal of Applied Research, Volume 5, Issue 1, Jan Special Issue 2015, ISSN - 2249-555X (page no. 75-77)
- Ratansing N Patel, Vipul Shah, Jayesh Patel, "*Design Investigation and parametric assessment of rectangular microstrip patch antenna*" OWT-2017, IRISWORLD Science & Technology Education and Research Society(Reg. No.247/Jaipur/2016-17) 1st International Conference on Optical and Wireless Technology 2017, Jaipur, India, March 18-19, 2017

Miscellaneous

- Presented work in special session on GUJCOST Sponsored Scholars' Day in Information & Communication Technology department at Dharmsinh University, Nadiad during 19th , September, 2015 organised by IEEE chapter